Exploring the Prox1 SUMO-switch in hepatocytes

Thesis by
Ana Jimena Alfaro Núñez

Dissertation
submitted to the
TUM School of Life Sciences Weihenstephan

TECHNISCHE UNIVERSITÄT MÜNCHEN
Munich, Germany

2020
Defended : March 19 2021

TUM School of Life Sciences

Exploring the Prox1 SUMO-switch in hepatocytes

Ana Jimena Alfaro Nunez

Vollständiger Abdruck der von der TUM School of Life Sciences der Technischen Universität München zur Erlangung des akademischen Grades eines Doktors der Naturwissenschaften genehmigten Dissertation.

Vorsitzende: Prof. Dr. Corinna Dawid

Prüfende/-r der Dissertation:

1. Prof. Dr. Ilona Grunwald Kadow

2. Prof. Dr. Stephan Herzig

Die Dissertation wurde am 20.07.2020 bei der Technischen Universität München eingereicht und durch die TUM School of Life Sciences am 28.01.2021 angenommen.

The work presented in this thesis was carried out at the Institute for Diabetes and Cancer (IDC) at the Helmholtz Center Munich.

First referee: Prof. Dr. Ilona Grunwald Kadow

Second referee: Prof. Dr. Stephan Herzig

Declaration:
I herewith declare that the presented research project was carried out autonomously; no other resources and aids besides the ones recited in this thesis were used.

Ana Jimena Alfaro Núñez

Date of submission: July 2020

ABSTRACT

The temporal organization of nutrient intake and utilization is essential to maintain energy homeostasis. The circadian regulation of hepatic metabolism in response to nutrient availability is modulated for the most part by nuclear receptors. There is strong evidence demonstrating that post-translational modification by the Small Ubiquitin-related Modifier (SUMO) can influence the activity of nuclear receptors and their co-regulators.

We have previously analyzed the SUMO proteome in the mouse liver during fasted and re fed conditions and identified the Prospero homeobox protein 1 (Prox1) as a nutrition-dependent SUMO target. Prox1 has been described as a co-regulator of nuclear receptors controlling energy homeostasis in the liver. Moreover, recent studies have shown that hepatic Prox1 is required for a proper lipid metabolism.

Follow-up *in vivo* studies presented in this work demonstrate that Prox1 is highly modified by SUMOylation in the mouse liver. The conjugation of Prox1 with SUMO is inhibited by food deprivation but promoted by food intake. In addition, the conjugation of Prox1 with SUMO appears to be influenced by a diurnal component. The responsiveness of the Prox1 SUMO-switch to nutrient availability is blunted during the light/rest phase of the mice.

Experiments in polarized primary hepatocytes suggest that the SUMO-switch on Prox1 could be regulated by 5' AMP-activated protein kinase (AMPK) and by chenodeoxycholic acid, which is a primary component of the bile acid pool.

As key part of this work, a conditional SUMO-deficient (K556R) Prox1 knock-in mouse model was characterized. With this model the conjugation of Prox1 with SUMO was blocked specifically in hepatocytes and after liver development. The metabolic function of the Prox1 SUMO-switch was investigated in young male and female mice. Blocking the conjugation of Prox1 with SUMO had no effects on systemic glucose or lipid metabolism. In line, blocking Prox1 SUMOylation in hepatocytes had very subtle impacts on the liver transcriptome.

We also gather data showing that the conjugation of Prox1 with SUMO is inhibited in mouse modes of liver fibrosis linking the Prox1 SUMO-switch with a state of liver damage or regeneration.

With this work, it has been demonstrated that Prox1 is a highly efficient SUMO target in hepatocytes. Prox1 is conjugated to a single SUMO moiety on lysine residue 556 within a SUMO consensus motif. The Prox1 SUMO-switch is regulated by metabolic and diurnal cues in the mouse liver. The function of this metabolic switch in the maintenance of energy homeostasis remains to be elucidated.

Zusammenfassung

Der zeitliche Ablauf der Nährstoffaufnahme und -verwertung spielt eine zentrale Rolle bei der Aufrechterhaltung der Energiehomöostase. Die zirkadiane Regulation des Leberstoffwechsels als Reaktion auf die Nährstoffverfügbarkeit wird dabei zum größten Teil durch nukleäre Rezeptoren moduliert. Vieles deutet darauf hin, dass die posttranslationale Modifikation durch Small Ubiquitin-related Modifier (SUMO) ein zentraler Mechanismus in der Regulation nukleärer Rezeptoren und ihrer Co-Regulatoren ist.

Wir haben bereits in der Vergangenheit das SUMO-Proteom in Mäuselebern im gefasteten und gefütterten Zustand analysiert und dabei Prospero homeobox protein 1 (Prox1) als ein ernährungsabhängiges Ziel für SUMO identifiziert. Es ist bekannt, dass Prox1 ein transkriptioneller Co-Regulator von einer Reihe von nukleären Rezeptoren ist, die die Energiehomöostase in der Leber kontrollieren. Darüber hinaus wurde Prox1 bereits von uns und anderen als ein Schlüsselregulator des hepatischen Lipidstoffwechsels beschrieben.

Die in dieser Arbeit vorgestellten *in vivo* Folgestudien zeigen, dass Prox1 in der Leber von Mäusen stark modifiziert wird. Die Konjugation von Prox1 mit SUMO wird dabei durch die Nahrungsaufnahme gefördert, während sie beim Fasten blockiert wird. Darüber hinaus scheint die Konjugation von Prox1 mit SUMO durch eine tageszeitliche Komponente beeinflusst zu sein. Die Reaktionsfähigkeit des Prox1-SUMO-Schalters auf Nährstoffverfügbarkeit ist während der Licht/Ruhephase der Mäuse vermindert.

Des Weiteren legen Experimente in polarisierten primären Hepatozyten nahe, dass der Prox1-SUMO-Schalter durch 5' AMP-activated protein kinase (AMPK) und Chenodeoxycholsäure, eine zentrale Komponente des Gallensäurepools, reguliert werden könnte.

Als Kernbestandteil dieser Arbeit wurde ein konditionales SUMO- defizientes (K556R) Prox1 Mausmodell charakterisiert. Mit diesem Modell war es uns möglich, die SUMO-Konjugation von Prox1 in Hepatozyten spezifisch zu blockieren. Dadurch konnte die metabolische Funktion des hepatischen Prox1-SUMO-Schalters untersucht werden. Junge männliche und weibliche Mäuse wiesen keine Veränderungen des systemischen Glukose- und Lipidstoffwechsels auf. In Einklang damit hatte die Blockierung der Prox1-SUMOylierung in Hepatozyten keine Auswirkungen auf das Lebertranskriptom.

Abschließend präsentiere ich Daten, die darauf hindeuten, dass die Konjugation von Prox1 mit SUMO in Mausmodellen der Leberfibrose gehemmt ist. Daher vermute ich, dass die SUMOylierung von Prox1 entweder an der Beschädigung der Leber oder an der Kontrolle der Leberregeneration beteiligt sein könnte.

Mit dieser Arbeit konnte gezeigt werden, dass Prox1 ein sehr effizientes Ziel für SUMOylierung in Hepatozyten ist. Prox1 ist mit einer einzelnen SUMO-Einheit auf Lysin 556 innerhalb einer SUMO-Konsensussequenz konjugiert. Dieser Prox1-SUMO-Schalter wird durch metabolische und zirkadiane Signale in der Mausleber reguliert. Inwiefern dieser metabolische Schalter die Aufrechterhaltung der Energiehomöostase reguliert bedarf weiterer Untersuchung.

ACKNOWLEDGEMENTS

Para y por mamá, papá y Memo:

"Porque la vida quiere que vivas tu Leyenda Personal"
- Paulo Cohelo, The Alchemist

CONTENTS

LIST OF FIGURES

LIST OF TABLES

ABBREVIATIONS

4EBP	eIF4E Binding Protein
AAV	Adeno-associated virus
ACATs	Acyl coenzyme A:cholesterol acyltransferases
ACC	Acetyl-CoA carboxylase
AICAR	5-aminoimidazole-4-carboxamide ribonicleosid
Akt	Akt or Protein kinase B (PKB)
ALT	Alanine aminotransferase
AML12	like alpha mouse liver 12 cell line
AMPK	AMP-activated protein kinase
AST	Aspartate aminotransferase
BAT	brown adipose tissue
BMAL1	Brain and muscle ARNT-like 1
cAMP	cyclic adenosine monophosphate
CLOCK	Circadian locomotor output cycles kaput
CREB	Cyclic AMP-responsive element binding protein
Cry	Cryptochrome; Cry1 and Cry2
CYP7a1	Cholesterol 7a-hydroxylase
Dex	dexamethasone
E1	SUMO-activating enzyme
E2	SUMO-conjugating enzyme
E3	SUMO E3 ligases
ERRα	Estrogen-related receptor α
FoxO	Forkhead box protein O
FSK	forskolin
FXR	Farnesoid X receptor

G6Pc   Glucose-6-phosphatase

GR   Glucocorticoid receptor

GS   Glycogen synthase

GSK3   Glycogen synthase 3-kinase

HDAC   Histone deacetylase

HDL   high-density lipoprotein

HMGCR   HMG-CoA reductase

HNF4α Hepatocyte nuclear factor 4α

HOMA-IR   Homeostatic Model Assessment for Insulin Resistance

INSIG   Insulin-induced gene

ISI   Insulin Sensitivity Index

LDH   Lactate dehydrogenase

LDL   low-density lipoprotein

LRH1   Liver receptor homolog 1 or NR5A2

LXR   Regulator of liver X receptor

MEFs   mouse embryonic fibroblasts

mTORC1   mammalian Target of rapamycin kinase complex 1

NASH   Non alcoholic steatohepatitis

NCoR   Nuclear receptor corepressor 1

Pepck   Phosphoenolpyruvate carboxykinase

Per   Period; Per1, Per2 and Per3

PGC-1α Peroxisome proliferator-activated receptorγ co-activator-1α

PI3K   Phospatidylinositol 3-kinase

PIAS   Protein Inhibitor of Activated STAT

PKA   Protein kinase A

Pros   Homeobox protein prospero

Prox1   Prospero homeobox protein 1

RanBP2	Ran binding protein 2
RORs	Retinoic acid–related orphan receptors; RORα, RORβ, and RORγ
RXR	Retinoid X receptor
S6K1	p70S6 Kinase 1
SCAP	SREBP cleavage-activating protein
SCN	suprachiasmatic nucleus
SDS-PAGE	sodium dodecyl sulfate polyacrylamide electrophoresis
SENPs	SUMO-specific isopeptidases
SIM	SUMO interacting motif
SIRT1	NAD+-dependent deacetylase sirtuin 1
SREBP	Sterol regulatory element-binding protein
STZ	streptozotocin
SUMO	Small Ubiquitin-related Modifier
SXR	Steroid and Xenobiotic Receptor
TRF	Time Restricted Feeding
TSC	Tuberous sclerosis complex
VLDL	very low-density lipoprotein
WAT	white adipose tissue
ZT	Zeitgeber

Introduction

1.1   The liver and its central role in energy homeostasis

Liver physiology and function

The liver is the biggest internal organ in the body and plays a unique and crucial role in detox-ification, digestion, protein synthesis and metabolism (Juza and Pauli, 2014). The liver has two major sources of blood supply. Oxygen-rich blood from the heart is delivered to the liver though the hepatic artery. The second blood source comes from the portal vein supplying nutrients and carrying potential damaging substances into the liver where they are absorbed and me-tabolized (Abdel-Misih and Bloomston, 2010). Hepatocytes are the dominant cell type in the liver, they constitute approximately 70 % of the cell population (Si-Tayeb, Lemaigre, and Duncan, 2010). Hepatocytes carry out most of the metabolic functions of the liver. They are equipped with detoxifying enzymes (known as cytochrome P450 enzymes) that convert toxic compounds into their inactive metabolites and/or into water-soluble molecules for proper excretion (Grant, 1991). Hepatocytes are also entirely in charge of the production and secretion of bile acids. Bile acids are molecules synthesized from cholesterol that are essential for the absorption of lipids and fat-soluble vitamins from the diet. Thus, the liver is a key player in the digestion process (Staels and Fonseca, 2009). Simultaneously, the liver is responsible for the the breakdown, storage and redistribution of nutrients. Hepatocytes regulate glucose and lipid metabolism in response to either feeding or fasting conditions to cope with the energy demand of the body. They do so through a network of nutrient sensing and signal transduction pathways. Upon food intake, glu-cose derived from carbohydrates is transported to the liver and absorbed by the hepatocytes. There, glucose is metabolized or stored as glycogen (Woerle et al., 2003). Lipids are solubilized by bile acids, processed and absorbed in the small intestine where they are packed in particles called chylomicrons for transport to the adipose tissue for storage (Bechmann et al., 2012). Chy-lomicron remnants are then absorbed by the hepatocytes (Heath et al., 2003). Dietary carbohy-drates and lipids are metabolized and packed into particles called very low-density lipoproteins (VLDLs) in the liver. VLDLs are then secreted into the circulation to deliver energy to periph-eral tissues (H. Wang and Eckel, 2009). VLDLs are processed in the bloodstream into circulating low-density lipoproteins (LDLs), which then interact with LDL receptors on the peripheral cells to deliver the cargo. Excess lipids from the peripheral tissues are packed into particles called high-density lipoproteins (HDLs) and transported back to the liver for recycling or elimination (Ouimet, Barrett, and Fisher, 2019).

During fasting, the glycogen molecules stored in the hepatocytes are broken-down to generate glucose and maintain energy homeostasis. When the glycogen depots are depleted, glucose

is synthesized *de novo* primarily in hepatocytes (Nuttall, Ngo, and Gannon, 2008). If the fasting period surpasses the capacity of hepatocytes to produce glucose, lipids are released by the adipose tissue and used as a secondary energy source in most organs (Bechmann et al., 2012). During prolonged periods of fasting and starvation the liver redirects lipid metabolism to synthesize ketone bodies as an alternative energy source for the brain (Newman and Verdin, 2014). Due to all the physiological functions of the hepatocytes described above, the liver is recognized as a central regulator of energy homeostasis.

Regulation of liver metabolism during fasting and feeding

To maintain energy homeostasis the metabolic pathways in the liver are tightly regulated during changes in nutrient availability. The activity of critical enzymes is modulated by means of allosteric regulation and post-translational modifications to allow for a fast adaptive response. In addition, physiological cues are translated into specific transcriptional metabolic programs to grant a long-term regulation and adaptation of cell metabolism.

In the feeding state, the glucose levels in the blood rise and stimulate the production and secretion of insulin from the β-cells of the pancreas. Insulin binds and activates the insulin receptors localized in the cell membrane of hepatocytes (Bugianesi, McCullough, and Marchesini, 2005). The activated kinase activity of the insulin receptor initiates a cascade of phosphorylation events on intracellular substrates (Kido, 2001). As a consequence, two major signaling pathways are activated: the Akt/protein kinase B (PKB) pathway via phospatidylinositol 3-kinase (PI3K) and the Ras-mitogen-activated protein kinase (MAPK) pathway (Avruch, 1998). The PI3K/Akt-axis mediates most of the metabolic actions of insulin signaling. For example: Akt activation promotes the conversion of glucose into glycogen, a process called glycogenesis. Akt inhibits the activity of Glycogen synthase kinase 3 (GSK3) by phosphorylation. Inhibiting GSK3 activity releases its negative control on glycogen synthase (GS), a key enzyme required in the glycogenesis pathway (Bouskila et al., 2010). In addition, Akt activity inhibits *de novo* glucose production from lactate, glycerol, and specific amino acids, a process called gluconeogenesis. Akt phosphorylates the transcription factor Forkhead box protein O (FoxO) to promote its export from the nucleus thus inhibiting the transcription of target gluconeogenic genes (Tran et al., 2003). Akt activation also promotes the synthesis of fatty acids from acetyl-CoA, a process called lipogenesis, and further processing into triglycerides for storage. Akt induces the expression and translocation into the nucleus of the sterol regulatory element-binding protein 1 (SREBP-1). SREBP-1 is a key transcription factor driving fatty acid absorption and lipogenesis (Krycer et al., 2010). In addition, the PI3K/Akt-axis promotes the activation of the mammalian target of rapamycin kinase complex 1 (mTORC1) by blocking the activity of its negative regulator, the TSC complex (for tuberous sclerosis complex) (Dibble and Cantley, 2015). mTORC1 is a master intracellular sensor that modu-

lates protein synthesis and autophagy in response to growth factors, insulin and amino acids. Activated mTORC1 phosphorylates two main effectors: p70S6 Kinase 1 (S6K1) and eIF4E Binding Protein (4EBP). Phosphorylation of S6K1 and 4EBP promotes mRNA translation by influencing the recruitment of translation initiation factors (Saxton and Sabatini, 2017). The mTORC1 pathway also promotes lipogenesis by up-regulating SREBP-1 expression through a mechanism that requires S6K1 activation (Wan et al., 2011).

Cholesterol synthesis, absorption and efflux are also tightly regulated upon changes in dietary cholesterol. SREBP cleavage-activating protein (SCAP) is a cholesterol-sensing factor that retains the transcription factor SREBP-2 in the ER membrane in response to an increase in oxysterols levels; oxysterols are oxygenated derivatives of cholesterol (Accad and Farese, 1998). The sequestration of SREBP-2 in the ER membrane is mediated by the interaction of SCAP with the insulin-induced gene proteins (INSIG-1 and INSIG-2), this interaction stabilizes the SCAP-SREBP complex at the ER blocking the processing and activation of SREBP-2 at the Golgi. Thus, SREBP-2 cannot induce the expression of enzymes required for cholesterol synthesis such as HMG-CoA reductase (HMGCR), the rate limiting enzyme in the cholesterol synthesis pathway (Luo, H. Yang, and B.-L. Song, 2020). HMGCR activity is also regulated by INSIG-1; high levels of oxysterols induce the binding of INSIG-1 to HMGCR promoting its ubiquitination and subsequent proteasomal degradation (Luo, H. Yang, and B.-L. Song, 2020). Oxysterols also activate the regulator of liver X receptor (LXR), a nuclear receptor that controls cholesterol efflux. Upon ligand binding LXR forms an heterodimer with the retinoid X receptor (RXR) and promotes the expression of cholesterol 7α-hydroxylase (CYP7a1), the rate-limiting enzyme involved in the conversion of cholesterol into bile acids (Edwards, Kennedy, and Mak, 2002) and (R. Zhu et al., 2012). The conversion of cholesterol into bile acids is the main pathway for cholesterol clearance. Because elevated concentrations of bile acids are cytotoxic, this process is controlled through a negative feedback mechanism mediated by farnesoid X receptor (FXR). FXR is a nuclear receptor that gets activated in response to an increase in bile acids (specially by chenodeoxycholic acid); its activation then results in the down-regulation of enzymes driving bile acid synthesis such as Cyp7a1 (Makishima et al., 1999) and (Parks et al., 1999). Cholesterol efflux is also driven by the liver receptor homolog 1 (LRH1 or NR5A2), which promotes the expression of transporters and enzymes required for HDL-cholesterol uptake and bile acid-synthesis (Schoonjans et al., 2002) and (Francis et al., 2003). Excess cholesterol is then converted to neutral cholesteryl esters for storage in lipid droplets or for secretion as components of lipoprotein particles; this reaction is catalyzed by acyl coenzyme A:cholesterol acyltransferases (ACATs) (Rogers et al., 2015).

In the fasting state, glucagon and glucocorticoids are secreted by the pancreas and the adrenal cortex, respectively (Woods, Hazlehurst, and Tomlinson, 2015) (Cain and Cidlowski, 2017). Binding of glucagon to its cell surface receptor results in the activation of the adenylate cyclase complex, which synthesizes the second messenger molecule cyclic adenosine monophosphate (cAMP) (Brubaker and Drucker, 2002). Increased levels of cAMP lead to the activation of protein kinase A (PKA) which is then able to enter the nucleus and phosphorylate the cyclic AMP-responsive element binding protein (CREB). CREB is a transcription factor that promotes the expression of phosphoenolpyruvate carboxykinase (Pepck) and glucose-6-phosphatase (G6Pc), enzymes that catalyze the rate-limiting and final step in gluconeogenesis, respectively (Altarejos and Montminy, 2011). Glucocorticoids interact and activate the glucocorticoid receptor (GR) by releasing it from a chaperone complex and promoting its translocation to the nucleus. The expression of Pepck is further induced by glucocorticoids after prolonged periods of fasting via the co-regulator PGC-1α (peroxisome proliferator-activated receptorγ co-activator-1α), which recruits the necessary chromatin-modifier complexes to induce transcription (Herzig et al., 2001). AMP-activated protein kinase (AMPK) is also activated in response to low cellular energy states to inhibit ATP-consuming pathways and promote ATP-generating processes. AMPK kinase activity is induced upon alterations in the cellular AMP:ATP ratio; AMP binding causes its allosteric activation and subsequent phosphorylation by the liver kinase B1 (LKB1), which is required for full AMPK activation (Cantó and Auwerx, 2009). Activation of AMPK initiates a cascade of phosphorylation events to promote fatty acid oxidation while blocking lipogenesis. For example: AMPK phosphorylates and inhibits acetyl-CoA carboxylase (ACC), the rate-limiting enzyme for fatty acid synthesis (Munday et al., 1988). Inhibition of ACC results in lower acetyl-CoA to malonyl-CoA conversion, a subsequent decrease in fatty acid synthesis and an increase in mitochondrial fatty acid oxidation. AMPK also phosphorylates and inhibits SREBP-1c thus reducing the expression of lipogenic genes (Y. Li et al., 2011). AMPK activity regulates protein synthesis through mTORC1 inactivation either directly or via the TSC complex (Steinberg and Carling, 2019). AMPK also inhibits HMGCR by phosphorylation to reduce cholesterol synthesis, as this is an energy consuming metabolic process (Clarke and Hardie, 1990).

Circadian regulation of liver metabolism

Almost every organism on Earth possesses a biological clock, an oscillating system pushed by evolution to keep organisms in tune with the light and dark cycles experienced on this planet. Thanks to the biological clock, organisms are capable to anticipate and prepare for rhythmic changes in the environment. As a result, internal metabolic processes coordinate with external cues to separate chemical reactions in a temporal manner allowing for an efficient metabolism. In response to the Earth's rotation on its axis, the rhythm of the biological clock

is close to a 24 hrs cycle. Biological circadian systems show three essential characteristics: 1) They are constant endogenous oscillators with a period of approximately 24 hrs. 2) They are a temperature-compensating system; the oscillations are minimally affected by temperature variations. 3) They can be influenced and remodeled (entrained) by external cues (Egli, 2017).

In mammals, the main input signals to the biological clock are light, temperature, activity and nutrients; these external cues are denominated Zeitgebers (for time-givers in German) (Harmer, Panda, and Kay, 2001). Light is sensed by the retina and translated into information that is processed by a brain structure called the suprachiasmatic nucleus (SCN). The SCN then transmits rhythmic information to influence physiology and behavior (Dibner, Schibler, and Albrecht, 2010). The rhythm set by the SCN promotes cell autonomous oscillations in most peripheral organs. These endogenous oscillators can be entrained by nutrients and bi-products of metabolism (Mendoza-Viveros et al., 2017). Thus, it appears that the biological clock is comprised of many rhythm-generating systems that influence themselves and each other via regulatory feedback loops (Roenneberg and Merrow, 1998). These systems are built by the molecular clock machinery; a set of oscillating factors that coordinate multiple regulatory feedback loops to organize most cellular functions. In mammals, CLOCK (for circadian locomotor output cycles kaput) and BMAL1 (for brain and muscle ARNT-like 1) have been identified as core components of the molecular clock. CLOCK and BMAL1 form a complex that activates the expression of clock-target genes, including the feedback factors Period (Per1, Per2, and Per3) and Cryptochrome (Cry1 and Cry2). Per and Cry proteins form a complex and accumulate in the nucleus to repress CLOCK-BMAL1 induced transcription including their own. Once the Per-Cry complex is degraded the activity of the CLOCK-BMAL1 complex is restored, thus generating a circadian feedback system (Mendoza-Viveros et al., 2017). In addition, the CLOCK-BMAL1 complex is regulated by another set of its own transcriptional targets, the RORs (for Retinoic acid–related orphan receptors; $ROR\alpha$, $ROR\beta$, and $ROR\gamma$) and REV-ERB (REV-ERBα and REV-ERBβ). BMAL1 expression is induced by RORs and inhibited by REV-ERB; the amount of BMAL1 protein available for CLOCK binding is modulated through this oscillating process (Mendoza-Viveros et al., 2017).

The molecular clock also converges with metabolic rhythmic signals in the peripheral organs through the interaction with intracellular energy sensors. Most genes showing circadian oscillations in the liver encode for enzymes or regulatory factors involved in glucose, fatty acid, cholesterol, bile acid, amino acid, and xenobiotics metabolism (Satchidananda Panda et al., 2002). Multiple circadian and metabolic crosstalk mechanisms have been identified. For example: Upon food intake, insulin signaling promotes the phosphorylation of BMAL1 via Akt/S6K1 to suppress BMAL1 transcriptional activity (Dang et al., 2016). During fasting, glucagon signaling induces BMAL1 expression via CREB; PGC-1α also promotes BMAL1 expression through its interaction

with RORα (Sun et al., 2015) and (C. Liu et al., 2007). AMPK also modulates the core clock system by phosphorylating and promoting the degradation of Cry proteins. In addition, the expression and nuclear localization of AMPK is under circadian regulation (Lamia et al., 2009). The cellular NAD+ sensor SIRT1 (for NAD+-dependent deacetylase sirtuin 1) is also regulated in a circadian manner; SIRT1 is activated during fasting to promote gluconeogenesis (via PGC-1α and FoxO) and cholesterol efflux (via LXRs) (X. Li et al., 2007) and (Asher et al., 2008). In addition, SIRT1 interacts with the CLOCK-BMAL1 complex to induce its transcriptional activity while it promotes Per2 degradation (Asher et al., 2008). REV-ERBα also participates in the circadian regulation of fatty acid and cholesterol metabolism as it mediates the rhythmic expression of Insig2 to modulate the activity of SREBPs (Le Martelot et al., 2009).

It is clear that the regulation of cellular metabolic processes relies heavily on the interactions between the core clock system dictated by light via the SCN and the peripheral clock driven by metabolic stimuli. Thus, it is not surprising that disruption of circadian oscillations results in a sub-optimal adsorption, metabolism and storage of nutrients by the liver.

Aberrant liver metabolism - from liver steatosis to non-alcoholic steatohepatitis

The imbalance between nutrient uptake and expenditure that contributes to systemic metabolic complications, such as obesity and type 2 diabetes, also promotes an aberrant accumulation of triglycerides in the liver, a condition defined as hepatic steatosis (Browning and Horton, 2004). The accumulation of triglycerides within the hepatocytes has been linked to a susceptibility to inflammation and cellular damage. During this vulnerable state, other pathogenic events such as insulin resistance, adipose tissue dysfunction and an altered immune system can lead to liver injury, inflammation and fibrosis (Birkenfeld and Shulman, 2014) and (Musso, Cassader, and Gambino, 2016). This critical liver state, denominated non alcoholic steatohepatitis (NASH), is a major risk factor for the development of cirrhosis and hepatocellular carcinoma (Day and James, 1998) and (Bechmann et al., 2012). An improper lipid metabolism is a main contributor to the development and progression of hepatic steatosis and NASH. Increased fatty acid uptake and *de novo* triglyceride synthesis, as well as reduced fatty acid oxidation and low triglyceride export within VLDL particles, are key metabolic pathways targeted to prevent and treat NASH. In addition, alterations in cholesterol homeostasis have been implicated in the pathogenesis of NASH. Free cholesterol overload correlates with the severity of liver dysfunction. It has been suggested that excess of cholesterol might disrupt the integrity of the mitochondria and ER membranes (Musso, Gambino, and Cassader, 2013). In addition, activation of SREBP-2 (regulator of cholesterol homeostasis) and HMGCR expression (rate-limiting enzyme for cholesterol synthesis) are increased during NASH despite the cholesterol overload (Min et al., 2012). Increased bile acid levels are also associated with liver injury and inflammation. Consistent with these observa-

tions, the therapeutic activation of FXR has been shown to promote the mobilization of liver triglycerides and the resolution of fibrosis (Musso, Cassader, and Gambino, 2016).

The metabolic pathways contributing to the progression from hepatic steatosis to more severe complications like NASH remain to be elucidated. However, it is clear that an aberrant uptake, synthesis, utilization and disposal of glucose and lipids within the hepatocytes represents a major risk factor. Thus, intensive research is being conducted in our laboratory to explore the mechanisms modulating signal transduction and gene expression upon changes in nutrient availability.

1.2 SUMOylation

Reversible post-translational protein modifications allow for a fast and dynamic response to changes in the cellular environment. Post-translational modifications regulate the activity of a target protein through various mechanisms. For example: they can induce structural conformational changes and influence protein-protein interactions. Important modifications include the addition of small chemical entities like phosphorylation or acetylation but also the attachment of entire proteins (Kerscher, Felberbaum, and Hochstrasser, 2006). The reversible attachment of a 10 kDa polypeptide called Small Ubiquitin-related Modifier (SUMO) to a target protein was discovered about 25 years ago in the context of nuclear transport (Matunis, Coutavas, and Blobel, 1996) (Mahajan et al., 1997). Since then, hundreds of SUMO targets involved in diverse cellular processes including cell cycle, signal transduction, DNA repair and transcription have been identified. Thus, SUMOylation is now recognized as a crucial regulatory mechanism of cellular function (Geiss-Friedlander and Melchior, 2007) and (E. S. Johnson, 2004).

The small ubiquitin-related modifier (SUMO)

SUMO is a small 10 kDa protein expressed in all eukaryotes and highly conserved from yeast to human. While yeast and invertebrates posses a single SUMO gene, the genome of higher plants and vertebrates encodes for more than one SUMO isoform (Flotho and Melchior, 2013). In mammals, three isoforms encoded by different genes have been identified: SUMO1, SUMO2 and SUMO3. They seem to be expressed in all tissues and in all developmental stages (Geiss-Friedlander and Melchior, 2007). A fourth human SUMO4 isoform has been detected in the kidney and immune-related tissues. However, SUMO4 seems to be unable to modify target proteins and will not be addressed further (Guo et al., 2004) and (Owerbach et al., 2005). SUMO2 and SUMO3 share 97 % identity in their amino acid sequence and are referred to as SUMO2/3. On the other hand the level of similarity between SUMO1 and SUMO2/3 is only about 50 % (Flotho and Melchior, 2013). Consistent with the differences observed between the amino acid sequences, SUMO1 and SUMO2/3 have distinct mechanistic functions. SUMO2/3 contains a SUMO attach-

ment site at the N-terminal unfolded region which grants it the unique ability to form SUMO chains (Tatham et al., 2001). There is also a greater cellular pool of un-conjugated SUMO2/3 than SUMO1. While the conjugation of SUMO2/3 can be induced in response to a number of stresses including heat shock and oxidizing agents, the levels of conjugated SUMO1 are not affected upon these stimuli (Saitoh, 2000). In addition, SUMO1 and SUMO2/3 modify different substrates *in vivo*. Despite these differences, SUMO1 and SUMO2/3 are conjugated to target proteins through the same enzymatic process.

The SUMO conjugation pathway

The reversible conjugation of SUMO to a target is achieved through an ATP-dependent enzymatic process (Gareau and Lima, 2010) and (Geiss-Friedlander and Melchior, 2007). For a schematic representation see Fig.1.1. All SUMO isoforms are synthesized with a number of extra amino acid residues at the C-terminal that need to be cleaved to expose the glycine-glycine (GG) motif required for conjugation. This process is mediated by cysteine proteases also called SUMO-specific isopeptidases (SENPs). The mature SUMO is then activated by the SUMO-activating enzyme E1, an heterodimer of Aos1 and Uba2, via an ATP-dependent reaction. A high energy SUMO-adenylate intermediate is used to form a thioester bond with the catalytic cysteine residue of the E1 enzyme. Afterwards, SUMO is transferred from the E1 to the active cysteine of Ubc9, the E2 SUMO-conjugating enzyme , to also form a thioester bond. Finally, SUMO is attached to a lysine residue on the target protein via an isopeptide bond through a reaction catalized by Ubc9. The bond is created between the carboxyl group of the glycine residue at the SUMO's C-terminal and the ε-amino group of an acceptor lysine residue on the target protein. Ubc9 is able to recognize substrates carrying a specific amino acid sequence called SUMO consensus motif (ΨKX(D/E)), a sequence consisting of a large hydrophobic residue (Ψ) followed by the lysine to be modified (K) and an acidic amino acid (D/E). This four-amino acid sequence is sufficient to mediate the interaction between the E2 and the substrate. Nevertheless, SUMOylation of most proteins *in vivo* requires the aid of SUMO E3 ligases such as the PIAS family (for Protein Inhibitor of Activated STATs) and RanBP2 (for Ran binding protein 2). SUMO-E3 ligases promote SUMOylation by mediating a more stable interaction between Ubc9 and the target.

SUMO conjugation is reversed by the highly active SENPs which also catalyze the cleavage of the isopeptide bond between the SUMO moiety and the substrate. This feature makes SUMOylation a reversible and very dynamic process.
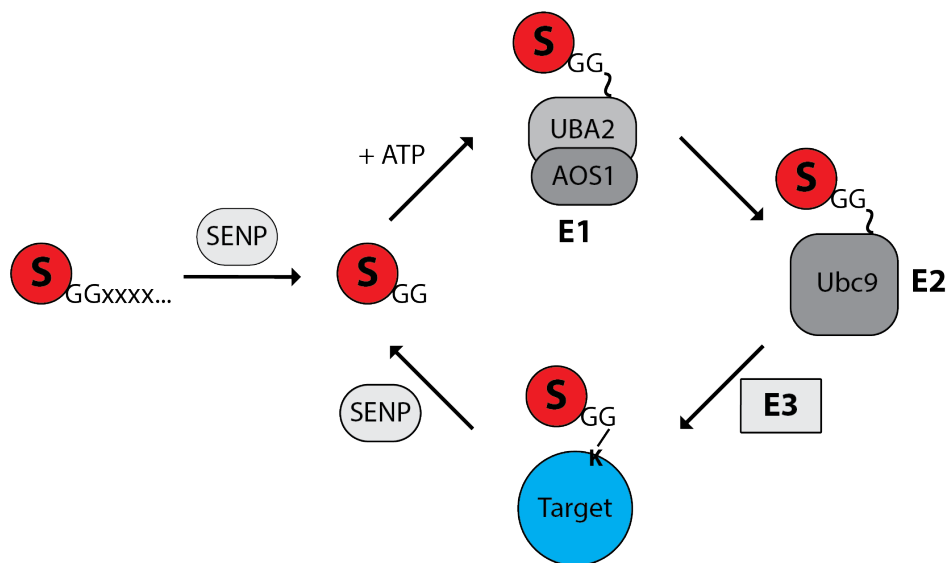
Figure 1.1: **Schematic representation of the SUMO conjugation pathway**
The nascent SUMO protein is matured by SUMO-specific isopeptidases (SENPs) that cleave the extra residues at the C-terminal to reveal the glycine-glycine (GG) motif required for conjugation. The mature SUMO is then activated by the E1 SUMO activating enzyme in an ATP-consuming reaction. SUMO is then transfered to the E2 SUMO conjugating enzyme which catalyzes the formation of an isopeptide bond between the SUMO moiety and the substrate. The attachment of SUMO to a target protein often requires the assistance of SUMO E3 ligases. SUMO can be cleaved from the substrate by highly active SENPs making SUMOylation a reversible and dynamic process.

Target recognition and regulation

Various mechanisms regulating the conjugation of SUMO to a target protein have been discovered. In addition to the SUMO consensus motif described above, a phosphorylation-dependent motif has been identified (ΨKX(D/E)xxSP), where a regulatory serine-phosphorylation site (S) followed by a proline (P) are adjacent to the SUMO consensus motif (X.-J. Yang and Grégoire, 2006). The influence of phosphorylation on SUMO conjugation seems to be target specific. Phosphorylation has been shown to promote SUMOylation by inducing a stronger interaction between the target and the Ubc9 (Mohideen et al., 2009). On the other hand, phosphorylation has been shown to block SUMOylation by masking the SUMO motif or by changing the target's subcellular localization (Desterro, Rodriguez, and Hay, 1998) and (J.-Y. Lin, Ohshima, and Shimotohno, 2004). Phosphorylation cascades represent a major signal transduction mechanism in the cell. Thus, the phosphorylation-mediated regulation of SUMO conjugation represents a mechanism to translate phosphorylation signals to SUMOylation based responses.

SUMOylation can also be promoted by non-covalent interactions between the target and the SUMO moiety loaded on Ubc9 (Ubc9-SUMO thioester). This interaction is mediated by a SUMO

interacting motif (SIM) on the substrate. The canonical SIM consists of a β-strand structure that is inserted between the α-helix and the β-strand of SUMO (Kerscher, 2007). It has been reported that SIMs can promote SUMOylation outside of a SUMO consensus motif (Meulmeester et al., 2008) and (Chang et al., 2011).

E3 ligases represent an additional mechanism for target recognition and regulation because specific E3 ligases interact preferentially with specific SUMO targets. Thus, the regulation of a particular E3 ligase (for example: through changes in its expression or cellular localization) can influence SUMOylation of a particular target protein (Yunus and Lima, 2009) and (Makhnevych et al., 2007).

As described above, SUMO1 and SUMO2/3 are similar but not identical proteins. They seem to have non-redundant functions in the cell as a number of target proteins are selectively modified either with SUMO1 or SUMO2/3 (Rosas-Acosta et al., 2005), (Vertegaal et al., 2006) and (Becker et al., 2013). Furthermore, poly-SUMO chains, which are mainly formed with SUMO2/3, provide the substrate with a new and unique interface for binding partners (Fu et al., 2005). In addition, it has been reported that some SENPs show a clear preference for one SUMO isoform or the other (Alegre and Reverter, 2011) and (Di Bacco et al., 2006). Conjugation of a target protein with a specific SUMO isoform can determine the fate and function of the SUMOylated species. Isoform specificity can be granted by the target protein itself or by external factors like interaction partners, including the SUMO enzymes. For example: RanGAP1 can be equally modified with SUMO1 and SUMO2/3 *in vivo* and *in vitro*. However, only RanGAP1 modified with SUMO1 is able to form a stable interaction with the RanBP2 complex and so get protected from SENPs; SUMOylation of RanGAP1 by SUMO2/3 is rapidly reversed *in vivo* (S. Zhu et al., 2009). SUMO isoform specificity can also be granted by the substrate itself via SIMs that mediate non-covalent interactions with higher affinity to a specific isoform. The SUMO specific SIM for SUMO1 has been described as the canonical amino acid sequence plus a serine residue that introduces a negative charge when phosphorylated. A phosphorylated SIM has a higher binding affinity to SUMO1 than to SUMO2/3 (Hecker et al., 2006). A SUMO2/3 specific SIM has also been identified in USP25. The SIM on USP25 contains a seven-amino acids hydrophobic core that recruits SUMO2/3 more efficiently than SUMO1 (Meulmeester et al., 2008). The mechanism regulating isoform preference is currently a hot research topic in the SUMOylation field.

SUMOylation in transcription

There are multiple and target specific consequences of SUMOylation (Geiss-Friedlander and Melchior, 2007) and (Flotho and Melchior, 2013). At the molecular level, attachment of a SUMO moiety can either generate new binding interfaces or physically block a binding site. Not just

protein-protein interactions, but also interactions with macro molecules like DNA and RNA are regulated by SUMO conjugation. SUMOylation has been shown to regulate the activity of transcription factors by promoting changes in nuclear localization, inhibiting proteasomal degradation and influencing DNA binding affinity (Geiss-Friedlander and Melchior, 2007). Furthermore, SUMOylation has been identified as a key modulator of nuclear receptors. SUMO conjugation has been shown to influence dimerization and modulate the dissociation or recruitment of co-activators and co-repressor complexes (Treuter and N. Venteclef, 2011). Because nuclear receptors represent a central sensing mechanism, SUMOylation is considered part of the system regulating energy homeostasis.

SUMOylation in liver metabolism

The liver metabolism is tightly regulated upon changes in nutrient availability. The regulatory network driven by post-translational modifications in response to metabolic cues has mainly been studied in the context of phosphorylation. Nevertheless, isolated studies have demonstrated that SUMOylation also participates in the regulation of liver metabolism:

The transcriptional activity of LRH1, a nuclear receptor controlling reverse cholesterol transport, is regulated by SUMOylation. Mutation of the main SUMO site on LRH1 increases its transcriptional activity; whole body loss of LRH1 SUMOylation is sufficient to protect mice against atherosclerosis by enhancing the transcription of genes involved in reverse cholesterol transport (Stein et al., 2014). Another protein regulated by SUMOylation in the context of liver metabolism is SREBP-1c, a transcription factor that promotes the expression of lipogenic genes. In response to a fasting signal, PKA phosphorylates SREBP-1c, which promotes its conjugation with SUMO. SUMOylation on SREBP-1c targets it for proteasomal degradation and the subsequent repression of the lipogenic program (Lee et al., 2014). SUMOylation has also been implicated in the control of anti-inflammatory pathways in the liver. LRH1 together with the regulator of liver receptor proteins (LXRs) are responsible for the repression of pro-inflammatory genes during the hepatic acute phase response. SUMOylation of LRH1 and LXRs promotes the recruitment and stabilization of the Nuclear receptor corepressor-1 (NCoR) complex on the promoters of inflammatory genes (Venteclef et al., 2010) and (Kim et al., 2015).

An indirect link between SUMOylation and liver steatosis has also been reported. The expression of SENP3 is higher in steatotic livers from human and rat. In addition, SENP3 expression is increased by fatty acids in the hepatocyte cell line L02 while SENP3 knock-down reduced the accumulation of lipids within the cells (Y. Liu et al., 2016).

1.3   Project background

Because different physiological cues would trigger SUMOylation of specific substrates, Prof. Dr. Stephan Herzig and Prof. Dr. Frauke Melchior teamed up to identify SUMO targets that are differentially modified in response to changes in nutrient availability. To do so, Dr. Janina Becker, a previous member of the Melchior laboratory, established a protocol to enrich endogenous SUMO targets from liver tissue using monoclonal anti-SUMO1 and anti-SUMO2/3 antibodies (Becker et al., 2013). This tool was used to enrich SUMO modified proteins by immunoprecipitation using liver tissue of mice that were either fasted (16 hrs) or re fed (2 hrs). The isolated proteins were then analyzed by mass spectrometry (Becker, 2012). Over two hundred SUMO candidates were identified; some of them were differentially modified between the fasted and re fed conditions. The target showing the most remarkable differences was the Prospero homeobox protein 1 (Prox1). According to the mass spectrometry data, Prox1 is weakly SUMOylated during fasting but highly modified in the re fed state. In addition, the data showed that Prox1 has a preference for the SUMO2 isoform over SUMO1. These observations have been confirmed (Becker, 2012), (Dittner, 2016) and (Alfaro N., 2016).

1.4   The prospero homeobox protein 1 (Prox1)

The structure of Prox1

Prox1 is a 82.3 kDa protein that belongs to the family of homeobox transcription factors highly conserved in vertebrates (Zinovieva et al., 1996); for a schematic representation of the Prox1 structure see Fig.1.2. Prox1 contains a unique motif consisting of a homeo domain and an associated prospero domain at the C-terimnal region. Together they form a single structural unit required for sequence specific binding to DNA (Ryter, Doe, and Matthews, 2002). A nuclear export signal is located within the homeo domain and masked by the prospero domain. Structural studies performed with the *Drosophila* homolog Pros (for homeobox protein prospero) showed that the homeo-prospero unit serves not only to align Pros on the DNA but also to mask the nuclear export signal (Ryter, Doe, and Matthews, 2002). The regulation of the DNA binding capacity and the exposure of the nuclear export signal are not directly coupled and are probably mediated by different structures (Yousef and Matthews, 2005). A DNA recognition sequence for the homeo-prospero domain 5' AGCATGCCTG 3' has been reported (Yousef and Matthews, 2005). Prox1 contains a nuclear localization signal and two nuclear receptor binding motifs (LxxLL) and (IxxLL) at the N-terminal region (K.-H. Song, T. Li, and Chiang, 2006) (Steffensen et al., 2004).

Prox1 in development and cancer

Prox1 has been thoroughly characterized in the context of organ development and cancer. Prox1 knock-out mice are not viable, they die before birth due to multiple developmental defects
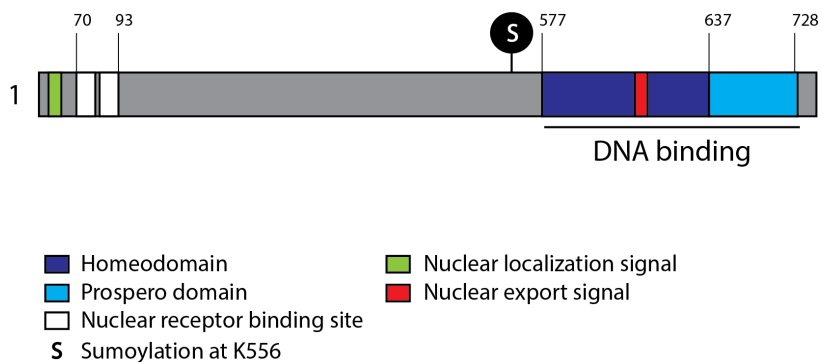
Figure 1.2: **Schematic representation of Prox1**
Functional domains are highlighted. The main SUMOylation site at lysine (K) residue 556 within a SUMO consensus motif (ΨKXE) is marked with an "S". Figure adapted from (Elsir, Eriksson, et al., 2010).

(Wigle, Chowdhury, et al., 1999). Prox1 has been shown to play an important role in the embryonic development of the central nervous system and neurogenesis in the adult brain (Elkouris et al., 2011), (Kaltezioti et al., 2010) and (Karalay et al., 2011). Prox1 is an essential regulator of lymphatic vasculature development as it is the first marker for lymphatic endothelial cell determination; Prox1 knock-out leads to complete loss of lymphatic vasculature (Wigle and Oliver, 1999). Prox1 is also required for lymphatic cell commitment; Prox1-deficient endothelial cells fail to express lymphatic markers, and instead conserve a blood vascular endothelial phenotype (N. C. Johnson et al., 2008). Prox1 heterozygous mice have a defect in the lymphatic vascular system that promotes adipose tissue accumulation and obesity (Harvey et al., 2005). In addition, Prox1 is essential for liver development as it regulates proliferation and migration of hepatocytes from the liver bud. Prox1 knock-out mouse embryos show a 70 % reduction in liver size due to developmental problems (Sosa-Pineda, Wigle, and Oliver, 2000) and (Burke and Guillermo Oliver, 2002).

Prox1 has also been studied in the context of tumor formation. Prox1 exerts both tumor suppressive and oncogenic properties in a cell type dependent manner. Increased levels of Prox1 correlate with high-grade brain tumors; it is suggested that Prox1 is acting as a progenitor cell marker (Elsir, Eriksson, et al., 2010). In that line, increased expression of Prox1 in colon cancer is associated with low prognosis as it promotes progression from a benign to a malignant phenotype (Petrova et al., 2008). It has been suggested that Prox1 is influencing cancer cell migration and invasion by enhancing transcription of genes involved in cell adhesion and migration (Elsir, Smits, et al., 2012). On the other hand, Prox1 seems to act as a tumor suppressor in hepatocellular carcinoma; it has been shown that overexpression of Prox1 decreases tumor cell growth while transient depletion results in an accelerated tumor cell proliferation *in vitro* (Shimoda et al., 2006).

Prox1 as a co-regulator of nuclear receptors

Multiple studies have demonstrated that, besides its role as a canonical DNA-binding factor, Prox1 acts a transcriptional co-regulator of nuclear receptors in the liver.

Prox1 has been shown to interact and repress hepatic LRH1 (regulator of reverse cholesterol transport and bile acid synthesis) (Qin et al., 2004) and (Stein et al., 2014). Prox1 interacts with LRH1 through its nuclear receptor binding motif (LxxLL) to reduce the binding affinity of LRH1 to DNA, thus inhibiting CYP7a1 expression (Qin et al., 2004). Prox1 also represses the activity of Steroid and Xenobiotic Receptor (SXR) *in vitro* (Azuma et al., 2011). SXR is a sensor of toxic substances that regulates the expression of enzymes required for detoxification. Prox1 also interacts with the ERRα/PGC-1α complex; the estrogen-related receptor α (ERRα) together with its co-activator PGC-1α control several aspects of energy metabolism (Giguère, 2008). PGC-1α and Prox1 seem to have opposite effects, PGC-1α acts as a co-activator while Prox1 has a repressive effect on the ERRα transcriptional activity (Charest-Marcotte et al., 2010). Chip-on-chip analyses showed that genes enriched by the Prox1/ERRα/PGC-1α complex contained ERRα binding sites but no homeobox-like motifs. Moreover, Prox1 seems to interact with the ERRα/PGC-1α complex through its DNA binding unit. Thus, it was proposed that Prox1 exerts its activity as a co-regulator by interacting with other transcription factors and not necessarily through its DNA binding capacity (Charest-Marcotte et al., 2010). Prox1 also acts as a co-repressor of hepatocyte nuclear factor 4α (HNF4α), a key regulator of lipid metabolism. Prox1 competes with PGC-1α via its nuclear receptor binding motifs and recruits the repressive chromatin-modifier LSD1/NuRD complex to inhibit HNF4α activity *in vitro* (Ouyang et al., 2013) and (K.-H. Song, T. Li, and Chiang, 2006). Furthermore, it has been demonstrated that hepatic Prox1 interacts with the chromatin-modifier Histone deacetylase 3 (HDAC3) within the NCoR complex via its N-terminal. HDAC3 and Prox1 are co-recruited to HNF4α to act as direct repressors of a number of genes critical to maintain a proper lipid homeostasis in the mouse liver (Armour et al., 2017).

A link between Prox1 and the molecular clock in the liver has also been identified. The expression of Prox1 could be under circadian control as chip-on-chip experiments have shown that the CLOCK/BMAL1 complex is enriched at the promoter region of Prox1 (Dufour et al., 2011) and (Takeda and Jetten, 2013). In addition, Prox1 itself seems to be recruited to the promoters of BMAL1 and CLOCK. Furthermore, BMAL1 and Prox1 seem to have common target genes which show an enrichment for fatty acid and carbohydrate metabolism (Dufour et al., 2011). Prox1 has been shown to interact and repress the transcriptional activity of the RORs, which regulate the circadian expression of BMAL1 and CLOCK (Takeda and Jetten, 2013). In addition, co-localization experiments suggest that RORγ promotes the nuclear localization of Prox1 *in vitro* (Takeda and Jetten, 2013).

Prox1 in the liver metabolism

In addition to its molecular function as a co-regulator further research done by us and others have addressed the relevance of hepatic Prox1 *in vivo*:

A constitutive and liver specific Prox1 knock-out mouse model has been characterized using an Albumin_Cre driver (Goto et al., 2017). Constitutive ablation of Prox1 resulted in glucose intolerance, insulin resistance and lower glycogen storage when analyzed in six weeks-old male mice. Furthermore, the constitutive knock-out of Prox1 resulted in the up-regulation of gluconeogenic genes and down-regulation of genes involved in glycolysis; it was also reported that knock-down of Prox1 reduced the glycolytic rate *in vitro*. Higher circulating levels of the markers for liver injury and impaired function were detected in the constitutive Prox1 knock-out animals (Goto et al., 2017).

In our hands, knock-down of Prox1 in eight weeks-old male mice (after liver development) via an AAV_Prox1-miRNA showed a different phenotype (Dittner, 2016). The liver weight of the Prox1 knock-down animals was 20 % higher than the controls but no differences were detected in the glycogen content. No signs of glucose intolerance, insulin resistance or liver damage were observed. Triglycerides and cholesterol accumulation in the liver were slightly reduced in the Prox1 knock-down mice during feeding, while it was not affected in the fasted state. There was also a slight reduction in the serum cholesterol levels in the Prox1 knock-down mice, while the serum triglycerides levels were mildly increased, in both fasted and fed conditions. Further investigation by mass spectrometry revealed that the livers of the Prox1 knock-down mice had a lower content of cholesteryl esters in both fasted and fed conditions, while free cholesterol remained unchanged. A trend towards lower cholesteryl esters was also observed in the serum. An FPLC lipoprotein profile revealed a slight reduction in the HDL-associated cholesterol in the Prox1 knock-down mice in the fed state but not during fasting. Higher amounts of VLDL-associated triglycerides were also detected in the Prox1 knock-down mice specially in the fed state. Transcriptome and proteome analyses revealed that pathways involved in triglyceride metabolism were up-regulated in the Prox1 knock-down mice, while pathways in drug and steroid metabolism were down-regulated. Down-regulation at the mRNA level of HMGCR, the rate-limiting enzyme for cholesterol synthesis, as well as CYP7a1, the rate-limiting enzyme for bile acid synthesis, was corroborated by qPCR analysis. Furthermore, knock-down of Prox1 in mice challenged with a high fat diet resulted in a higher degree of steatosis as compared to the control animals (Dittner, 2016).

In line, it has been shown that knock-down of Prox1 via an AAV_shRNA in the liver of male mice led to the accumulation of lipids within this organ; knock-down of Prox1 in the liver of female mice showed a weaker phenotype (Armour et al., 2017).

These studies demonstrate that hepatic Prox1 plays an important function in the regulation of energy homeostasis. The rs340874 single-nucleotide polymorphism in the 5' untranslated region of the Prox1 gene has been associated with altered lipid metabolism, high fasting glucose levels and type 2 diabetes (Kretowski et al., 2015). Yet, little is known regarding the mechanisms regulating the activity of Prox1.

Prox1 SUMOylation

It has been reported that Prox1 is a SUMO target *in vitro* and that its transcriptional activity can be modulated by SUMOylation (Shan et al., 2008) (Pan et al., 2009). Overexpression experiments performed in Huh7 and HEK293T cells showed that Prox1 can be modified by the SUMO1 isoform and that Prox1 is modified on lysine residues 353 and 556, both localized within putative SUMO consensus motifs (Shan et al., 2008). A different study, where Prox1 was co-transfected with SUMO1 or SUMO2/3 on a synthetic expression-modification system in *Escherichia coli*, proposed that Prox1 is target for SUMO1 but not for SUMO2/3 modification (Pan et al., 2009). However, previous experiments performed by Claudia Dittner at the Melchior laboratory have confirmed that hepatic Prox1 is predominantly conjugated with the SUMO2 isoform *in vivo* and that the main SUMO acceptor site is lysine residue 556 *in vitro* (Dittner, 2016). In addition, it has been demonstrated that full length Prox1 has a preference for the SUMO2 isoform at the level of SUMO conjugation *in vitro* (Alfaro N., 2016).

The impact of SUMOylation on the activity of Prox1 seems to be context specific. It has been proposed that SUMOylation inhibits the co-repressor activity of Prox1 by reducing its interaction with HDAC3 in HEK293T cells (Shan et al., 2008). In EA.hy926 cells, a cell line with characteristics of vein endothelial cells, SUMOylation was shown to stabilize Prox1 at the VEGFR3 promoter resulting in an up-regulation of lymphatic endothelial cell markers (Pan et al., 2009).

Taking into consideration that Prox1 has cell-specific functions as a canonical transcription factor and as a co-regulator, we have previously analyzed whether SUMOylation affects the interaction of endogenous Prox1 with chromatin in a hepatocyte-like cell line using a salt-gradient extraction protocol. In our experimental set-up both the unmodified and the SUMOylated species of Prox1 showed a similar binding affinity to chromatin (Alfaro N., 2016). In addition, we have show by immunofluorescence experiments done in HeLa cells that SUMOylation does not affect the nuclear localization of Prox1 (Alfaro N., 2016).

It is clear that the regulation and functional consequences of Prox1 SUMOylation are cell specific. Furthermore, is appears that this modification is drastically affected by the experimental conditions. Thus, the function of hepatic Prox1 SUMOylation will be investigated with an integral combination of *in vivo* and *in vitro* experiments.

1.5 Aim of the study

Prox1 is a highly efficient SUMO target in the mouse liver. It is differentially modified by SUMOylation during fasting and feeding conditions and it shows a clear preference for the SUMO2 isoform. The underlying mechanisms regulating the nutrition-dependent Prox1 SUMO-switch are currently unknown. Moreover, the impact of SUMO conjugation on the transcriptional activity of Prox1 remains to be elucidated.

To address how the Prox1 SUMO-switch is regulated *in vivo* I analyzed the status of Prox1 SUMOylation in the liver of fasted and fed mice at different time points through their active phase. I also investigated whether Prox1 is expressed and/or modified in other metabolic tissues. I also analyzed the levels of SUMOylated Prox1 in the liver of young and old mice to assess whether the conjugation of Prox1 with SUMO is affected upon aging.

To identify upstream signals modulating the conjugation of Prox1 with SUMO, I screened a set of chemicals and hormones mimicking the main fasting and feeding signals in a hepatocyte-like cell line and in primary hepatocytes.

To investigate the role of Prox1 SUMOylation in the context of adult liver metabolism, I characterized a SUMO-deficient K556R Prox1 knock-in mouse model. By inducing Cre recombination using an adeno-associated virus (AAV) vector under a hepatocyte-specific promoter, the conjugation of Prox1 with SUMO was blocked specifically in hepatocytes and after liver development. A liver transcriptome analysis of the SUMO-deficient K556R Prox1 knock-in mouse model was performed in both fasted and fed conditions. In addition, wild-type Prox1 and the SUMO-deficient K556R variants were purified from liver tissue samples in order to identify SUMO-dependent interaction partners of Prox1.

To further investigate the implications of the Prox1 SUMO-switch in the control of liver metabolism I investigated how the K556R Prox1 knock-in mice cope with the metabolic burden of a high cholesterol diet. In addition, I assessed how the conjugation of Prox1 with SUMO behaves in mouse models of liver steatosis and fibrosis.

The overall aim of this project is to clarify the function of the Prox1 SUMO-switch in the mouse liver and to identify its regulatory signals.

2.1 Regulation of Prox1 SUMOylation in vivo

Prox1 SUMOylation is regulated by food intake

We have previously shown that Prox1 is strongly SUMOylated in cell culture and in the mouse liver. Moreover, we identified that hepatic Prox1 is highly modified by SUMOylation in the fed state while the levels of SUMOylated Prox1 decrease during fasting conditions. To investigate further how Prox1 SUMOylation behaves in response to nutrient availability, the levels of SUMOylated Prox1 were analyzed after different fasting or feeding time points in the liver of wild type C57BL/6N male mice. As nocturnal animals, mice consume most of their food during their active phase which comprises the dark period from zeitgeber (ZT) 12 to 24. Thus, the study was performed through the dark phase. Both the un-modified species around 97 kDa and the SUMOylated version of Prox1, which runs at 120 kDa, were easily detected by immunoblotting (Fig.2.1.A). Right at the beginning of the dark phase (time point = 0) about 15 % of the total Prox1 pool was modified by SUMOylation in random fed mice (*ad libitum*). Prox1 was de-SUMOylated after 3 hrs of fasting and remained un-modified though the dark phase when the mice had no access to food. On the other hand, the levels of Prox1 SUMOylation were maintained and showed a tendency to increase when food was available (Fig.2.1.A). The expression of Prox1 at the protein level was constant between the fasted and fed conditions and through the dark phase (Fig.2.1.A). The nutritional state of the mice upon fasting and feeding was corroborated by detecting the levels of phosphorylated S6K1 as an indirect read-out for Akt/mTORC1 activation upon nutrient intake (Fig.2.1.A). Changes in body weight, blood glucose and insulin levels were also monitored (Fig.2.1.B). The expression of the Prox1 putative target genes CYP7a1 and HMGCR was investigated; the expression of BMAL1 was used to track the circadian state through the dark phase (Fig.2.1.C). The differences observed on Prox1 SUMOylation between fasting and feeding show the maximum amplitude 3-6 hrs into the dark phase; the same is true for the regulation of CYP7a1 and HMGCR expression. Taken these results into consideration, the optimal sampling time for future studies was set between ZT 15 and 18.

The response of the SUMO-loading machinery to changes in nutrient availability was also investigated. The expression of the E1 sub-unit Sae1 at the mRNA level was reduced during fasting and increased during feeding (Fig.2.1.D). The mRNA levels of the E2 enzyme gene Ube2i were mildly reduced during fasting (Fig.2.1.D). Whether these transcriptional changes actually influence global SUMOylation or SUMOylation of Prox1 remains to be investigated.
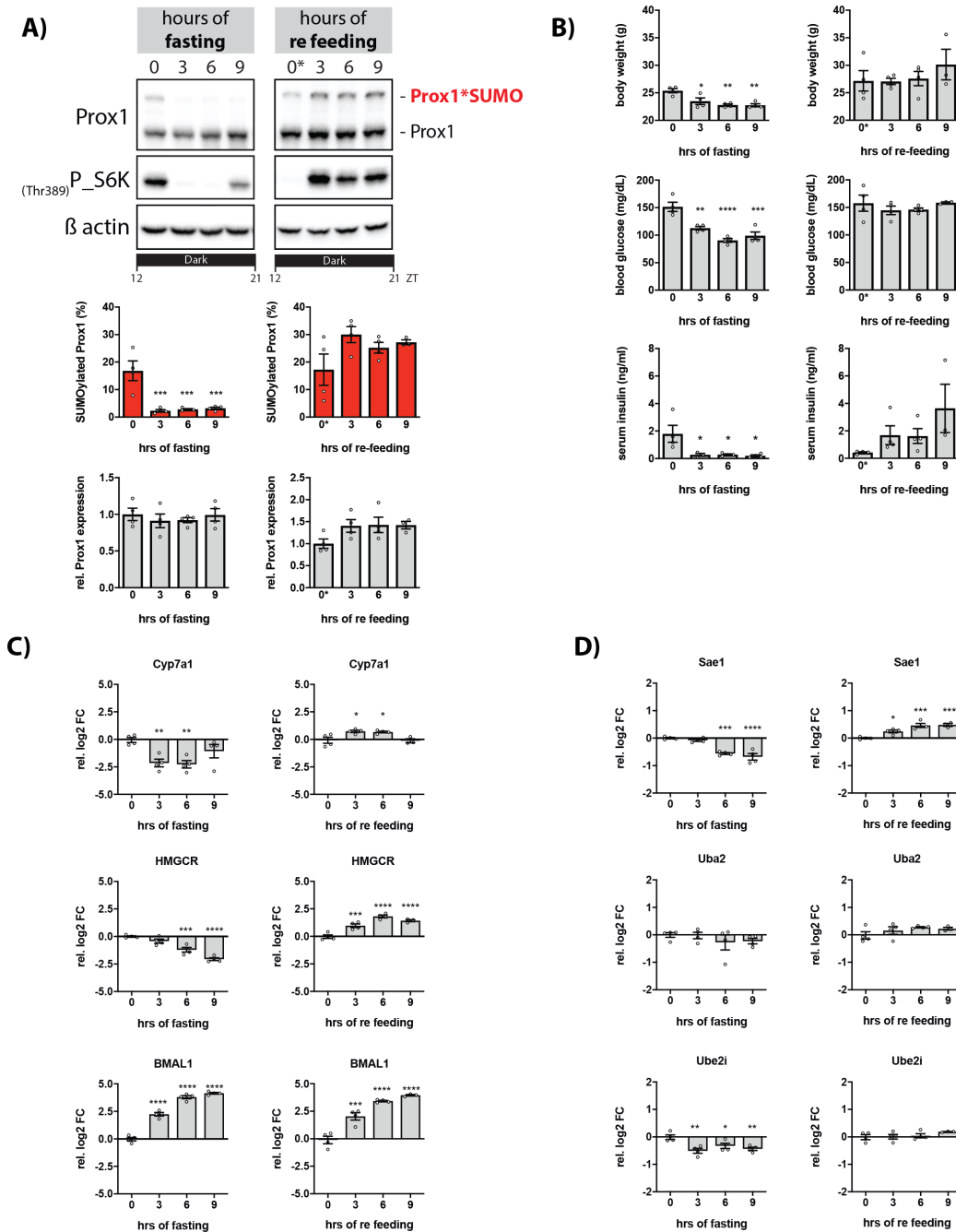
Figure 2.1: **Prox1 SUMOylation is regulated by food intake**
8 weeks-old C57BL/6N male mice were fasted: food was removed at ZT 12 or re fed: all groups were fasted for 8 hrs during the light phase (ZT 4-12) for synchronization, the food was re-introduced at ZT 12. Tissues were collected at ZT 12, 15, 18 and 21 (n=4). A) Liver lysates analyzed by immunoblotting using anti-Prox1 and anti-P_S6K(Thr389) antibodies; β actin was detected for input control. The quantification of SUMOylated Prox1 (%) and relative Prox1 expression are shown. B) Body weight, glucose and insulin levels. C) and D) Expression analysis at the mRNA level by qPCR, data presented as relative log2 fold change (FC) normalized to the housekeeping gene TBP. (A-D) Every dot represents one individual mouse. Data: mean $\pm$ SEM. Significance was determined by one-way ANOVA with Dunnett´s multiple comparison test relative to samples collected at ZT 12. * $P \leq 0.05$, ** $P \leq 0.01$, *** $P \leq 0.001$, **** $P \leq 0.0001$.

The regulation of Prox1 SUMOylation has a diurnal component

A temporal organization of nutrient intake and utilization is essential to maintain energy home-ostasis. In mammals, light is a main external signal that synchronizes the biological clock with the environment via the SCN located in the brain (Mendoza-Viveros et al., 2017). However, food is a dominant zeitgeber for the peripheral clock in the liver (Damiola et al., 2000) and (Stokkan, 2001). During the beginning stages of this work I was unable to detect the nutrition-dependent SUMO-switch on Prox1 when following the fasting and re feeding protocol commonly used in the laboratory. Despite the nocturnal behavior of mice, this protocol relies on an overnight fast of approximately 16 hrs (from ZT 12 to 4) followed by a defined re feeding time during the light (rest) phase.

This protocol was applied on wild type C57BL/6N young male mice to assess the kinetics of Prox1 SUMOylation upon 1, 2 and 4 hrs of re feeding; all tissue samples were collected between ZT 4 and 6. In this study, the levels of Prox1 SUMOylation were not influenced by food intake and were mildly affected by an overnight fast when compared to the *ad libitum* controls (Fig.2.2.A); note the changes on S6K1 phosphorylation and blood glucose levels upon food availability. This protocol was applied in three independent studies in which Prox1 SUMOylation was just mildly affected by the nutritional state of the animals during the light phase (data not shown). Thus, I suspected that the time of feeding and/or tissue collection influences whether a responsive Prox1 SUMO-switch is detected.

To test this idea the status of Prox1 SUMOylation was investigated after a 16 hrs overnight fast in samples collected either at ZT 4 or at ZT 5. Both fasted groups showed lower blood glucose and insulin levels as compare to the *ad libitum* controls (Fig.2.2.B). However, the loss of Prox1 SUMOylation upon fasting was only observed in samples collected at ZT 4; these samples also present high S6K1 phosphorylation levels (Fig.2.2.B).
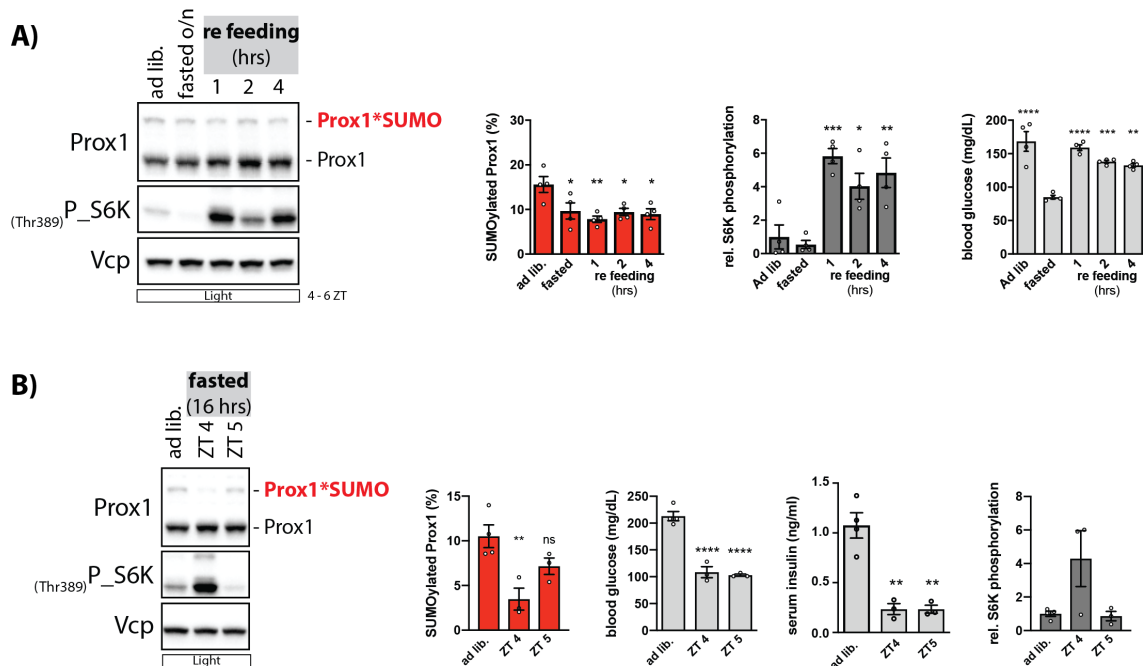
Figure 2.2: **The Prox1 SUMO-switch is not active during the light phase**
A) 8 weeks-old C57BL/6N male mice were fasted for 14 to 16 hrs (ZT 10-4) and re fed for 1, 2 or 4 hrs. A control group was fed *ad libitum* (ad lib.). Tissues were collected from ZT 4 to 6 (n=4). Liver lysates were analyzed by immunoblotting using anti-Prox1 and anti-P_S6K(Thr389) antibodies; Vcp was detected for input control. The quantification of SUMOylated Prox1 (%) and the blood glucose levels are shown. B) 8 weeks-old C57BL/6N male mice were fasted for 16 hrs; one group was fasted from ZT 12 to 4 and the other was fasted from ZT 13 to 5 (n=3-4). Liver lysates were analyzed as described above. The quantification of SUMOylated Prox1 (%), blood glucose and insulin levels are shown.(A-B) Every dot represents one individual mouse. Data: mean ± SEM. Significance was determined by one-way ANOVA with Dunnett´s multiple comparison test relative to samples collected *ad libitum*. * $P \leq 0.05$, ** $P \leq 0.01$, *** $P \leq 0.001$, **** $P \leq 0.0001$.

Taking these results into consideration, I hypothesized that the Prox1 SUMO-switch becomes unresponsive as the light phase progresses. If true, it is reasonable to think that the regulation of the Prox1 SUMO-switch has a diurnal component. Previous studies done in mice have shown that a temporal feeding restriction to the rest phase can uncouple the circadian rhythmicity in the mouse liver from the central pacemaker at the SCN (Damiola et al., 2000) and (Stokkan, 2001). Thus, a time restricted feeding protocol (TRF) confined to the light phase was implemented to elucidate whether Prox1 SUMOylation is influenced by light via the central pacemaker or by food via the peripheral clock in the liver.

Mice had access to food only during the light phase for seven days; a control group was fed *ad libitum*. The day of the study termination the food was removed from both groups right before the dark phase. The food was re-introduced to only half of each group the next day at the beginning

of the light phase. Tissue samples were collected 3 hrs later at ZT 3. For a schematic representation of the experimental set-up see Fig.2.3.A, red arrows indicate time of tissue collection.
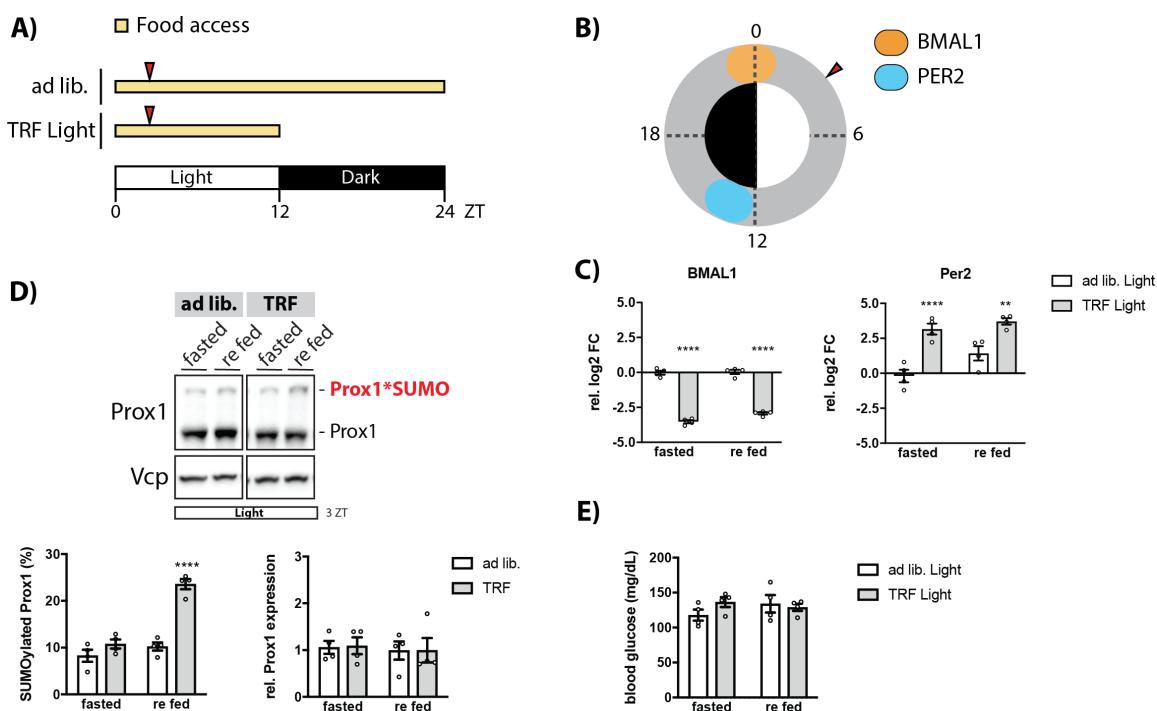
Figure 2.3: **The Prox1 SUMO-switch is influenced by the peripheral clock in the liver**
8 weeks-old C57BL/6N male mice were kept on a time restricted feeding protocol during the light phase (TRF Light) for 7 days. A) Schematic representation of the experimental set-up. Mice in the TRF group had assess to food only between ZT 0 and 12. A control group was kept *ad libitum* (ad lib.). To finalize the study the food was removed from both groups at ZT 12. The food was re-introduced to half of each group at ZT 0 and the tissues were collected at ZT 3 (red arrows) in the fasted and re fed sate (n=4). B) Schematic representation of BMAL1 and Per2 expression in the mouse liver, figure adapted from (Mure et al., 2018). C) Expression analysis at the mRNA level by qPCR of BMAL1 and Per2, data presented as relative log2 fold change (FC) normalized to the housekeeping gene TBP. D) Liver lysates analyzed by immunoblotting using anti-Prox1 and anti-P_S6K(Thr389) antibodies; β actin was detected for input control. The quantification of SUMOylated Prox1 (%) and relative Prox1 expression are shown. E) Blood glucose levels. (C-E) Every dot represents one individual mouse. Data: mean $\pm$ SEM. Significance was determined by two-way ANOVA with Sidak´s multiple comparison test between different conditions. * $P \leq 0.05$, ** $P \leq 0.01$, *** $P \leq 0.001$, **** $P \leq 0.0001$.

To corroborate that the TRF protocol shifted the peripheral clock in the liver the expression of core clock components was analyzed. It has been reported that the expression of BMAL1 peaks right at the beginning of the light phase around ZT 0, while Per2 expression peaks at the beginning of the dark phase at ZT 13 (Mure et al., 2018); see Fig.2.3.B. The expression of BMAL1 was

drastically reduced while the expression of Per2 was highly increased at ZT 3 in mice on a TRF protocol as compared to the controls (Fig.2.3.C). These results suggest that the oscillations of the peripheral clock in the liver were altered in mice entrained by the TRF protocol confined to the light phase. As observed before, the status of Prox1 SUMOylation was not affected by food availability during the light phase in mice kept *ad libitum* (Fig.2.3.D). In entrained mice, the levels of Prox1 SUMOylation where significantly increased when food was available, while SUMO conjugation was not influenced by food deprivation (Fig.2.3.D). Both groups showed comparable blood glucose levels in both fasting and feeding conditions (Fig.2.3.E). These results suggest that there is a factor regulating the responsiveness of the Prox1 SUMO-switch to food availability. This signal has a diurnal component that is not mediated by light, but rather by the peripheral clock in the liver. I hypothesize that the Prox1 SUMO-switch in the liver requires synchronization between nutritional and diurnal cues for it to be responsive.

It has been shown that a temporal feeding restriction to the dark phase can synchronize the circadian clock and metabolic regulators in the mouse liver to optimize metabolism (Hatori et al., 2012). The status of hepatic Prox1 SUMOylation was analyzed in mice on a TRF protocol during the dark phase to further investigate its diurnal regulation. Mice had access to food only during the dark phase for seven days, a control group was fed *ad libitum*. The day of the study termination the food was removed from both groups right before the light phase. The food was re-introduced to only the half of each group at the beginning of the dark phase. Tissue samples were collected 3 hrs later at ZT 15. For a schematic representation of the experimental set-up see Fig.2.4.A, blue arrows indicate time of tissue collection. The conjugation of Prox1 with SUMO was promoted by food availability in both groups (Fig.2.4.B). As observed before, Prox1 SUMOylation was lost upon food deprivation during the dark phase in mice kept *ad libitum* (Fig.2.4.B). However, the levels of Prox1 SUMOylation were not influenced upon fasting in entrained mice (Fig.2.4.B). In addition, the expression of Prox1 at the protein level was increased in the TRF group during fasting (Fig.2.4.B). Interestingly, the fasting blood glucose levels were significantly higher in entrained animals (Fig.2.4.C).

These observations further support that the Prox1 SUMO-switch is responding not only to variations in nutrient availability. If the de-SUMOylation of Prox1 was completely dependent on fasting cues, a similar response between the TRF fed mice and the *ad libitum* controls would be expected; all animals were fasted for the same time and at the same time. I conclude that the Prox1 SUMO-switch is influenced by a set of metabolic and diurnal signals that are naturally in line on healthy mice living in a 12/12 hrs light/dark cycle and with unlimited access to food. Therefore, to assess the function of Prox1 SUMOylation *in vivo*, the upcoming studies presented in this work were performed within the active (dark) phase of the mice between ZT 15 and 17.

Figure 2.4: **The Prox1 SUMO-switch is regulated by metabolic and diurnal cues**
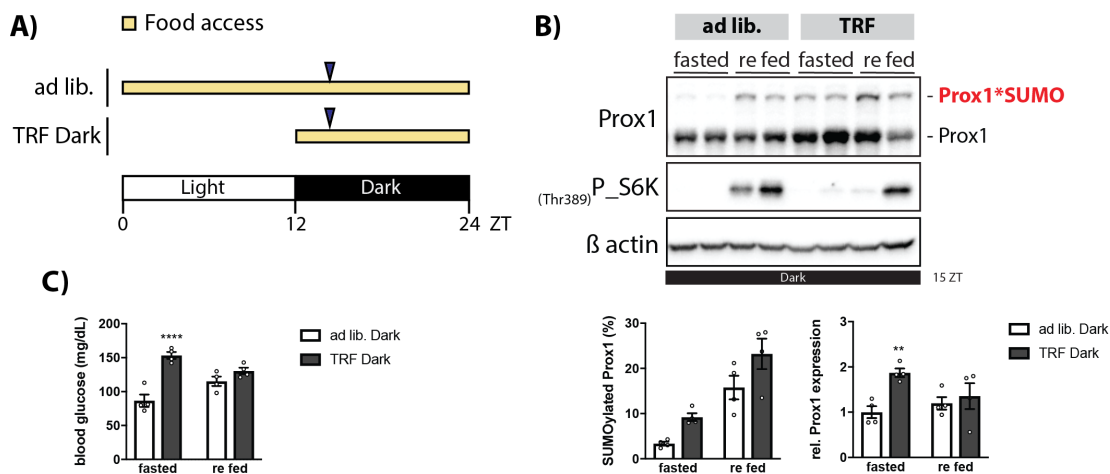8 weeks-old C57BL/6N male mice were kept on a time restricted feeding protocol during the dark phase (TRF Dark) for 7 days. A) Schematic representation of the experimental set-up. Mice in the TRF group had access to food only between ZT 12 and 24. A control group was kept *ad libitum* (ad lib.). To finalize the study the food was removed from both groups at ZT 0. The food was re-introduced to half of each group at ZT 12 and the tissues were collected at ZT 15 (blue arrows) in the fasted and re fed sate (n=4). B) Liver lysates analyzed by immunoblotting using anti-Prox1 and anti-P_S6K(Thr389) antibodies; β actin was detected for input control. The quantification of SUMOylated Prox1 (%), relative Prox1 expression are shown. C) Blood glucose levels. (B-C) Every dot represents one individual mouse. Data: mean $\pm$ SEM. Significance was determined by two-way ANOVA with Sidak´s multiple comparison test between different conditions. * P $\leq$ 0.05, ** P $\leq$ 0.01, *** P $\leq$ 0.001, **** P $\leq$ 0.0001.

Prox1 in other metabolic tissues and old mice

The expression and modification status of Prox1 was investigated in the liver, inguinal and gonadal white adipose tissue depots (iWAT and gWAT, respectively), the brown adipose tissue (BAT), the gallbladder (GB), the kidney, the pancreas (panc.) and the gastrocnemius muscle (GC.). As observed before, Prox1 was highly expressed and modified in the liver (Fig.2.5) In addition to the liver, Prox1 was detected in the gallbladder (Fig.2.5). However, due to the low abundance of Prox1 in the gallbladder its modification status remains to be elucidated. A lower molecular weight species of around 60 kDa was barely detected in the liver and in both WAT depots, while it was very abundant in the BAT. A Prox1 knock-down experiment is required to confirm whether this 60 kDa band represents an unspecific target of the antibody used or a lower molecular species of Prox1. Nevertheless, these results suggest that the full version of Prox1 is mainly expressed and modified in the liver.

ad libitum

| liver | iWAT | gWAT | BAT | GB | liver | kidney | panc. | GC. |

Prox1

- **Prox1*SUMO**
- Prox1

GAPDH

ß actin

Ponceau S
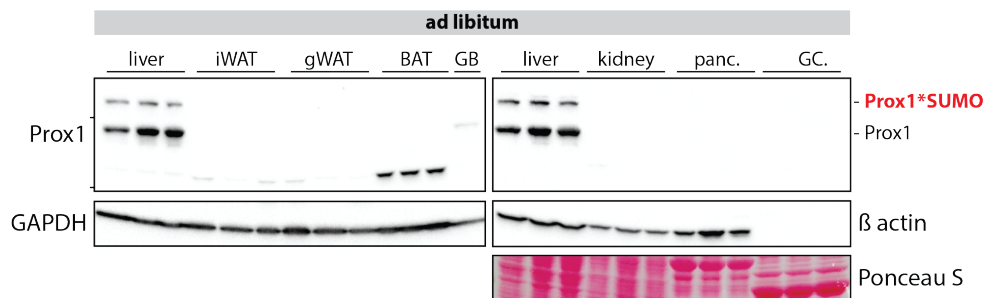
Figure 2.5: **Prox1 is expressed and modified mainly in the liver**
Analysis of Prox1 expression and SUMOylation in the metabolic organs of 8 weeks-old C57BL/6N male mice fed *ad libitum* (n=3). Gallbladders were pooled due to the small size and low protein abundance in this tissue. Lysates were analyzed by immunoblotting using an anti-Prox1 antibody; β actin and GAPDH were detected for input control. Given the low expression of β actin in the muscle, a Ponceau S staining was used for input control. White adipose tissue - inguinal and gonadal (iWAT and gWAT respectively), brown adipose tissue (BAT), gallbladder (GB), pancreas (panc.), gastrocnemius muscle (GC.).

To investigate how hepatic Prox1 behaves in older animals its expression and modification status were analyzed in nine and thirty-six weeks-old mice fed *ad libitum*. The expression of Prox1 as well as its SUMOylation status were comparable between young and older animals (Fig.2.6).

ad libitum

| 9 weeks | 36 weeks |

Prox1

- **Prox1*SUMO**
- Prox1

ß actin
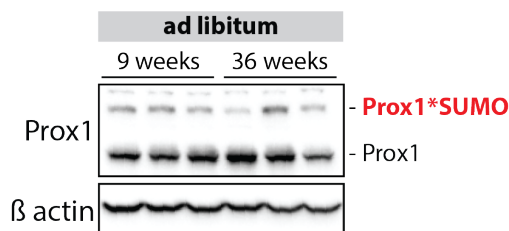
Figure 2.6: **Prox1 SUMOylation in the liver of young vs old mice**
The status of Prox1 SUMOylation was analyzed in liver samples of 9 and 36 weeks-old C57BL/6N mice fed *ad libitum* (n=3). Lysates were analyzed by immunoblotting using an anti-Prox1 antibody; β actin was detected for input control.

2.2 Upstream regulation of Prox1 SUMOylation

Prox1 is highly SUMOylated in the mouse liver. The levels of Prox1 SUMOylation are drastically decreased when mice have no access to food. Thus, it is possible that upon fasting cues 1) Prox1 is actively de-SUMOylated or 2) its conjugation with SUMO is somehow blocked. To investigate further the nutritional regulation of Prox1 SUMOylation potential signals were explored *in vitro*.

Prox1 SUMOylation in vitro - technical challenge

The status of Prox1 SUMOylation was first assessed in the non-tumor hepatocyte cell line AML12 (for like alpha mouse liver 12). To mimic a strong fasting signal, the cells were treated with a combination of glucagon, forskolin (FSK), which is an activator of the adenylate cyclase complex, and dexamethasone (Dex), a synthetic agonist of the glucocorticoid receptor. In a parallel experiment, AML12 cells were treated with either insulin or glucose to mimic two of the main feeding signals. Surprisingly, the expected modified species of Prox1 running at 120 kDa was not detected. Instead, a higher-molecular weight species of around 180 kDa was observed (see Fig.2.7 A and B, red mark at 120 kDa). The nature of this hyper-modified version of Prox1 requires further investigation and does not resemble the dynamic SUMOylated species observed *in vivo*.
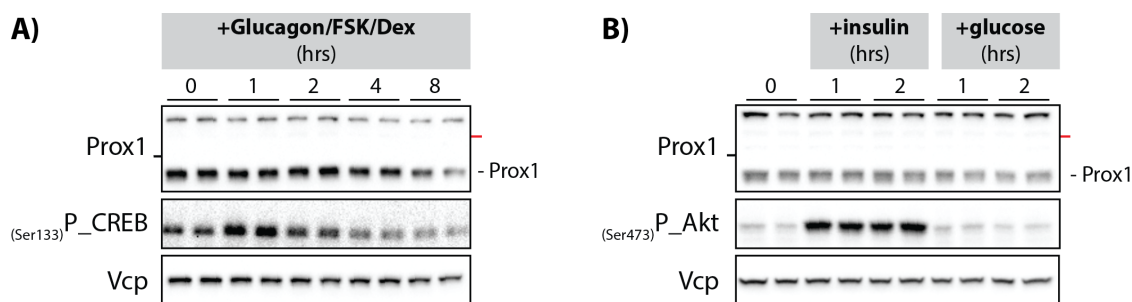
Figure 2.7: **Prox1 modification pattern in AML12 cells**
A) AML12 cells were incubated in low-serum low-glucose media for 2 hrs before stimulation. Cells were treated with a combination of 100 nM glucagon, 100 µM forskolin (FSK) and 100 nM dexamethasone (Dex) for 1, 2, 4 and 8 hrs. B) AML12 cells were incubated in low-serum low-glucose media for 20 hrs before stimulation. Cells were treated with either of 100 nM insulin or 11 mM glucose for 1 and 2 hrs. Lysates were analyzed by immunoblotting using anti-Prox1, anti-P_CREB(Ser133) and anti-P_Akt(Ser473) antibodies; Vcp was detected for input control. Red mark at 120 kDa.

Given these results, the analysis switched to primary hepatocytes as this *in vitro* system conserves many signaling pathways observed *in vivo*. Primary hepatocytes were isolated from the liver of eight weeks-old male mice and seeded on collagen pre-coated plates. The monolayer of primary cells was then treated with a Dex/FSK combination together with insulin or the PKA inhibitor, the H89 compound (Fig.2.8.A). In a second experiment, primary hepatocytes were treated

with insulin or AICAR (for 5-aminoimidazole-4-carboxamide ribonicleoside), which is an AMPK activator (Fig.2.8.B). Surprisingly, the modified species of Prox1 running at 120 kDa was barely detected (see Fig.2.8.A-B, red mark at 120 kDa). On the other hand, the 180 kDa variant was quite abundant as seen in the AML12 lysates. The response of targeted signaling pathways was conserved in the monolayer of primary hepatocytes. The activation of the adenylate cyclase complex by FSK resulted in a quick phosphorylation of CREB, this downstream effect was impaired when the activity of PKA was blunted by the H89 compound (Fig.2.8.A). Activation of the insulin/Akt pathway was confirmed by detecting Akt phosphorylation. AMPK activation by AICAR resulted in a rapid phosphorylation of its direct target ACC (Fig.2.8.B). These results suggest that the canonical signaling pathways are maintained in monolayer cultures of primary hepatocytes. However, it appears that there is a complex signaling network regulating the conjugation of Prox1 with SUMO *in vivo*.
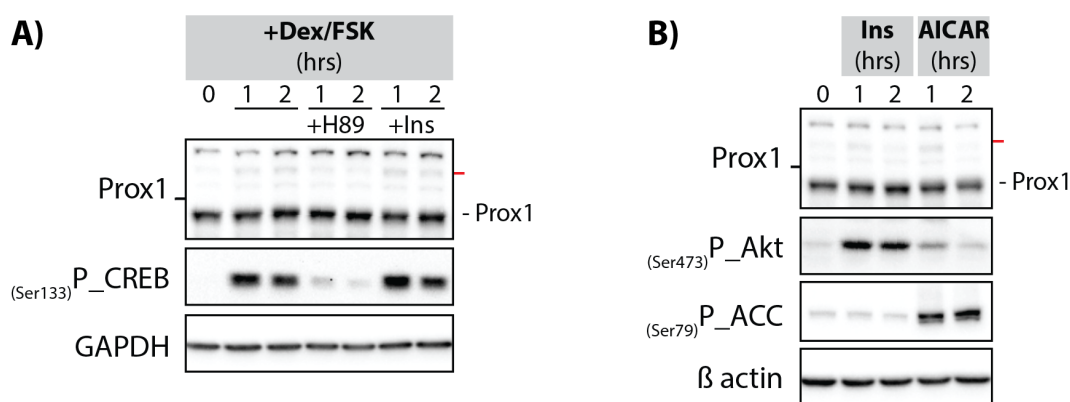
Figure 2.8: **Prox1 modification pattern in primary hepatocytes cultured as monolayer**
Primary hepatocytes were isolated from the liver of 8 weeks-old C57BL/6N male mice and seeded on a collagen pre-coated plate. The primary cells were incubated overnight in low-serum low-glucose media. A) Cells were treated with a combination of 100 nM dexamethasone (Dex) and 100 μM forskolin (FSK) for 1 and 2 hrs. Additionally, the cells were treated with either 10 μM H89 (PKA inhibitor) or 100 nM insulin. B) Cells were treated with either 100 nM insulin or 1 mM AICAR (AMPK activator) for 1 and 2 hrs. Lysates were analyzed by immunoblotting using anti-Prox1, anti-P_CREB(Ser133), anti-P_Akt(Ser473) and anti-P_ACC(Ser79) antibodies; GAPDH and β actin were detected for input control. Red mark at 120 kDa.

With the guidance of Dr. Anja Zeigerer, our laboratory has established a protocol to culture primary hepatocytes in a collagen sandwich. The collagen sandwich structure acts as an extracellular matrix that helps the primary hepatocytes to re-polarize and re-acquire key structural and functional attributes observed *in vivo* (Zeigerer et al., 2017). Therefore, the Prox1 modification pattern was analyzed in primary cells cultured in the collagen sandwich. For this, primary hepatocytes were isolated from the liver of eight weeks-old male mice and seeded onto collagen

self-coated plates. After letting the cells attach, the second collagen layer was added on top. The hepatocyte morphology was assessed for the following four days, the day of cell seeding is determined as day one. The hepatocytes showed many lateral membrane contacts already after one day in culture and multiple bile canalicular structures were observed a day later (Fig.2.9.A; see magnification). The development of bile canaliculi is related to the reorganization and stabilization of hepatocyte morphology, metabolism and gene expression (Reif et al., 2015). Therefore, the modification pattern of Prox1 in polarized hepatocytes on days three and four was analyzed. The modification pattern of Prox1 was comparable to the one observed in liver lysates showing a modified species running at 120 kDa (Fig.2.9.B).
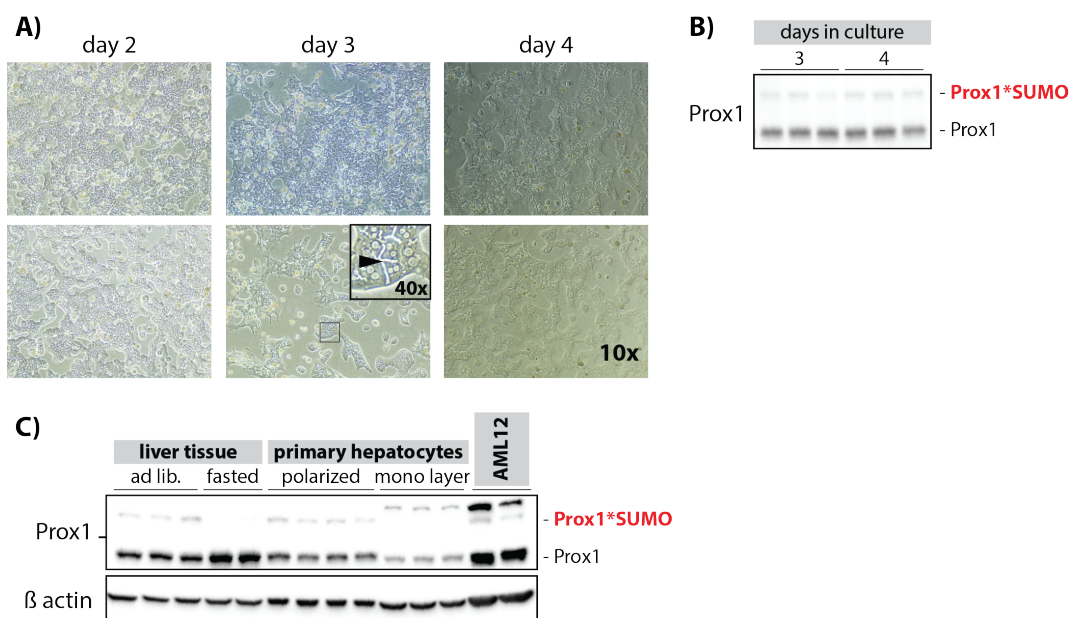
Figure 2.9: **Prox1 SUMOylation is maintained in polarized primary hepatocytes**
Primary hepatocytes were isolated from the liver of 8 weeks-old C57BL/6N male mice and seeded on a collagen self-coated plate (day 1), a second collagen layer was added on top after 6 hrs. The cells were cultured for up to 5 days in the collagen sandwich. A) The cell morphology was assessed daily via light microscopy. B) Lysates from primary polarized hepatocytes were analyzed by immunoblotting using an anti-Prox1 antibody. C) Lysates (40 µg total protein) from liver tissue of *ad libitum* fed or fasted mice, primary polarized hepatocytes, primary hepatocytes cultured as monolayer and AML12 cells were analyzed by immunoblotting using an anti-Prox1 antibody; β actin was detected for input control.

For a final comparison the same amount of total protein isolated either from the liver of *ad libitum* fed or fasted mice, from primary polarized hepatocytes, from primary hepatocytes cultured as a monolayer and from AML12 cells was analyzed by immunoblotting (Fig.2.9.C). With these results I conclude that the regulation of Prox1 SUMOylation is mediated by an intrinsic system

in hepatocytes that requires a complex regulatory network. This system seems to be lost in many *in vitro* models. Note that the dynamic modified species of Prox1 observed *in vivo* is not predominant in primary cells kept as monolayer or in AML12 cells.

Mimicking fasting and feeding signals in polarized primary hepatocytes

In order to identify the regulatory signals of the Prox1 SUMO-switch, the main fasting cues were mimicked on polarized primary hepatocytes. For this, a protein isolation protocol was optimized to detect both the unmodified and the SUMOylated species of Prox1 in lysates from the collagen sandwich culture.

Polarized primary hepatocytes were stimulated with a combination of forskolin (FSK) and dexamethasone (Dex) for 1 hr. A co-treatment was performed with the PKA inhibitor, the H89 compound. Treatment with FSK/Dex resulted in lower levels of Prox1 SUMOylation independently of PKA activity (Fig.2.10.A).

To investigate whether the regulation is mediated via the activation of the adenylate cyclase complex and/or the glucocorticoid receptor, single FSK or Dex treatments were performed in polarized primary hepatocytes. The levels of Prox1 SUMOylation were affected by the FSK, but not by the Dex treatment (Fig.2.10.B). It appears that the effects on Prox1 SUMOylation are mediated by the downstream signals of cAMP accumulation.

Given the signaling mechanism of the glucocorticoid receptor, a longer Dex treatment was performed to allow for the transcription and translation of a potential mediator. A dexamethasone treatment of up to 16 hrs did not affect the levels of Prox1 SUMOylation in polarized primary hepatocytes (Fig.2.10.C).

Figure 2.10: Upstream regulation of Prox1 SUMOylation - FSK vs Dex treatment
Primary hepatocytes were isolated and cultured in a collagen sandwich as described above. Prior to the treatment the cells were incubated in low-serum low-glucose media overnight. A) Cells were treated with a combination of 100 µM forskolin (FSK) and 100 nM dexamethasone (Dex) for 1 hr. Additionally, the cells were treated with 10 µM H89 (PKA inhibitor). B) Cells were treated with either 100 µM forskolin (FSK), 100 nM dexamethasone (Dex) or both for 1 hr. C) Cells were treated with 100 nM dexamethasone (Dex) for 4, 8 and 16 hrs. Lysates were analyzed by immunoblotting using anti-Prox1, anti-P_CREB(Ser133) and anti-P_Akt(Ser473) antibodies; GAPDH, Vcp and β actin were detected for input control. For A) and B) the quantification of SUMOylated Prox1 (%) and relative expression are shown.

Insulin is one of the main feeding signals to the liver. Thus, the status of Prox1 SUMOylation upon insulin stimulation was analyzed in polarized primary hepatocytes. A combinatory treatment of insulin and FSK was tested to mimic the cAMP-dependent regulation of the insulin pathway upon fasting. Surprisingly, treating the cells with insulin for 1 hr resulted in lower levels of Prox1 SUMOylation (Fig.2.11.A). Note that the inhibition of Prox1 SUMOylation was stronger with the insulin treatment alone than in combination with FSK. These results suggest that insulin also

activates a signal on polarized primary hepatocytes that hampers the conjugation of Prox1 with SUMO.

It is possible that the observed de-SUMOylation on Prox1 upon insulin stimulation is due to the activation of a negative feedback loop. Therefore, an acute insulin treatment was tested. An insulin stimulation for 15 and 30 min inhibited the conjugation of Prox1 with SUMO in polarized primary hepatocytes (Fig.2.11.B).

Figure 2.11: **Upstream regulation of Prox1 SUMOylation - insulin treatment**
Primary hepatocytes were isolated and cultured in a collagen sandwich as described above. Prior to the treatment the cells were incubated in low-serum low-glucose media overnight. A) Cells were treated with either 100 nM insulin for 1 hr or with a combination of 100 nM insulin and 100 μM forskolin (FSK) for 1 and 4 hrs. B) Cells were treated with 100 nM insulin for 15 and 30 min. Lysates were analyzed by immunoblotting using anti-Prox1, anti-P_Akt(Ser473) and anti-P_CREB(Ser133) antibodies; Vcp and β actin were detected for input control. The quantification of SUMOylated Prox1 (%) is shown.

The response of the Prox1 SUMO-switch to insulin was further analyzed in an alternative *in vitro* system. Liver slices obtained from an eight weeks-old male mouse were treated with insulin for 15 and 30 min. A parallel experiment was performed under the presence of the calcium chelator EGTA, with the aim to loose the calcium-dependent cell-cell junctions for a better diffusion of insulin. An acute insulin stimulation did not inhibit the conjugation of Prox1 with SUMO in liver slices (Fig.2.12).

Taking these results into consideration, I conclude that the conjugation of Prox1 with SUMO is regulated by signals that are not completely conserved when the hepatocytes are removed from the body.
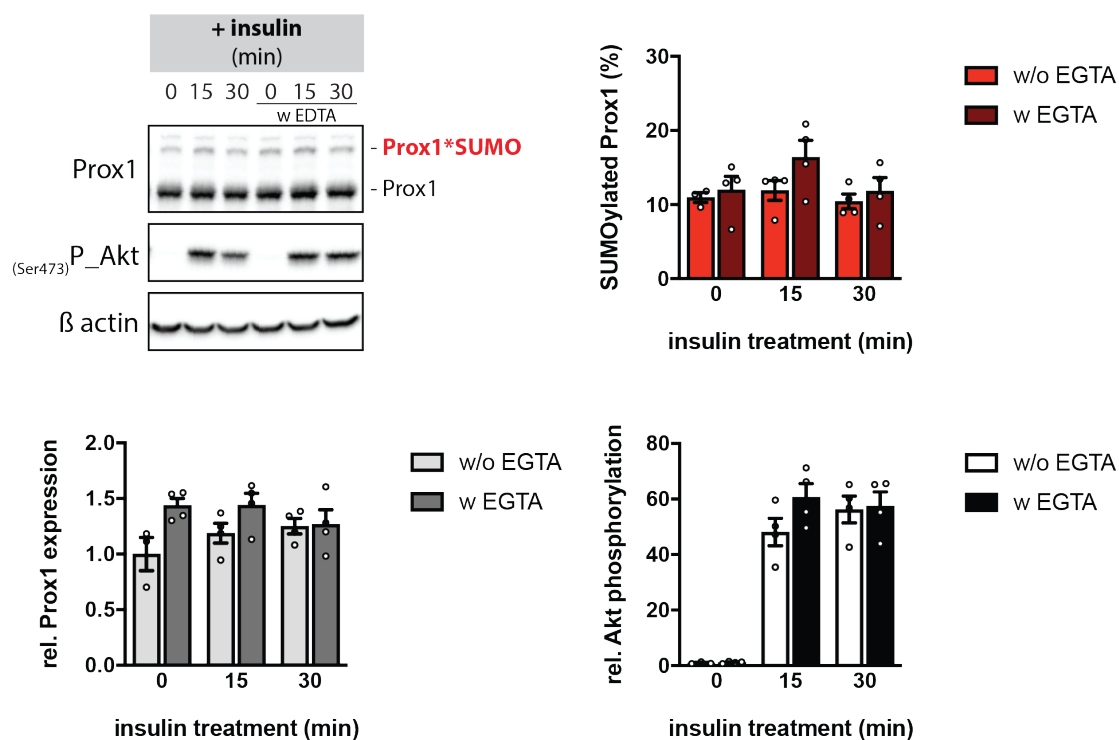
Figure 2.12: **Insulin treatment in liver slices**
Precision-cut liver slices were obtained from an 8 weeks-old C57BL/6N male mouse. Each slice was cultured individually and allow for recovery, prior to the treatment the liver slices were incubated in low-serum low-glucose media overnight. The liver slices were treated with 100 nM insulin for 15 and 30 min. Additionally, half of the samples were incubated together with 20 nM EGTA. Lysates were analyzed by immunoblotting using anti-Prox1 and anti-P_Akt(Ser473) antibodies; β actin was detected for input control. The quantification of SUMOylated Prox1 (%), relative Akt phosphorylation and relative Prox1 expression are shown.

To investigate whether the Prox1 SUMO-switch is regulated by the intracellular low-energy sensor AMPK, polarized primary hepatocytes were stimulated with AICAR, for 1, 2 and 4 hrs. Activation of AMPK resulted in a time dependent loss of Prox1 SUMOylation that was proportional to increasing levels of ACC phosphorylation (Fig.2.13.A). ACC phosphorylation was used as an indirect read-out of AMPK activation.
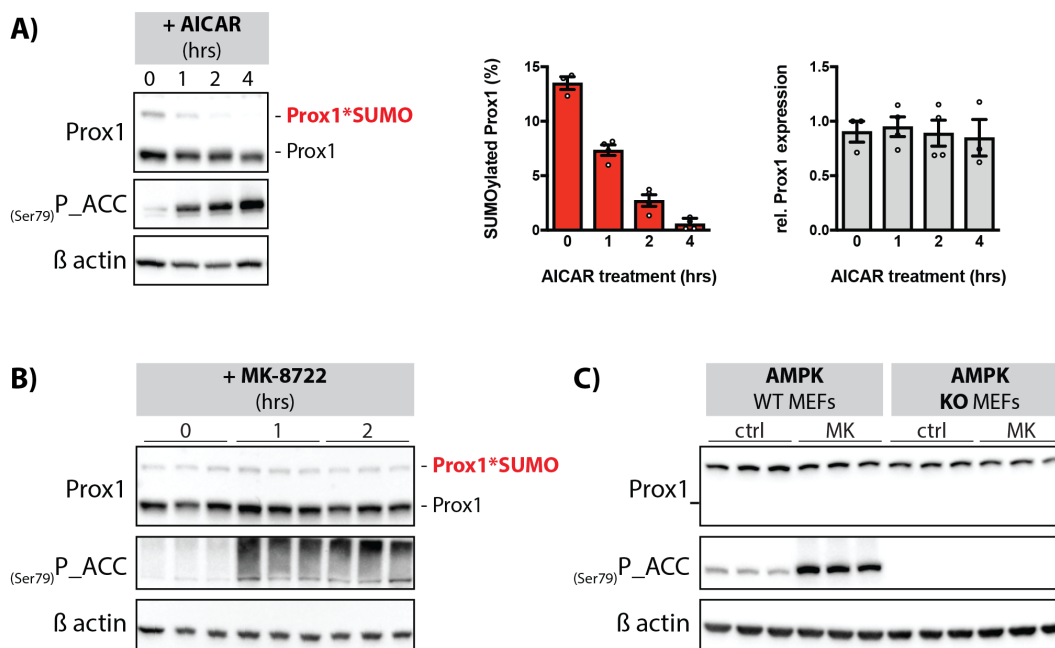
Figure 2.13: **Upstream regulation of Prox1 SUMOylation by AMPK**
A) Primary hepatocytes were isolated and cultured in a collagen sandwich as described above. Prior to the treatment the cells were incubated in low-serum low-glucose media overnight. Cells were treated with 0.9 mM AICAR (AMPK activator) for 1, 2 and 4 hrs. B) Polarized primary hepatocytes were incubated in low-serum low-glucose media overnight then treated with 5 µM MK-8722 ((Makhnevych et al., 2007)) for 1 and 2 hrs. C) Wild type (WT) and AMPK knock-out (KO) MEFs were treated with 0.9 mM AICAR for 1 hr. Lysates were analyzed by immunoblotting using anti-Prox1 and anti-P_ACC(Ser79) antibodies; β actin was detected for input control. For A) the quantification of SUMOylated Prox1 (%) and relative Prox1 expression are shown.

The role of AMPK in the regulation of the Prox1 SUMO-switch was further investigated by treating polarized primary hepatocytes with the MK-8722 compound, a selective and very potent activator of AMPK (Makhnevych et al., 2007). The levels of Prox1 SUMOylation were not affected by the MK-8722 treatment (Fig.2.13.B). Activation of the AMPK pathway was confirmed by detecting ACC phosphorylation. Note that phosphorylated ACC is detected at a higher molecular level than previously observed upon AICAR treatment.

Taking into consideration the opposing results obtained between the AICAR and MK-8722 treatments, it was necessary to address the participation of AMPK in the regulation of the Prox1

SUMO-switch with an alternative approach. Therefore, the status of Prox1 SUMOylation was assessed in AMPK knock-out mouse embryonic fibroblasts (MEFs), which are known to have the required enzymatic machinery for SUMOylation (Cossec et al., 2018). However, the modification pattern of Prox1 in cultured MEFs does not resemble that observed *in vivo* (Fig.2.13.C).

The results obtained so far are inconclusive. Thus, the implications of AMPK in the regulation of the Prox1 SUMO-switch will be further investigated.

To assess whether the Prox1 SUMO-switch is regulated by the intracellular nutrient sensor mTORC1, its activity was inhibited in polarized primary hepatocytes with rapamycin. The expression and SUMOylation levels of Prox1 were not affected by a rapamycin treatment of 2 and 4 hrs (Fig.2.14.A). A prolonged incubation with rapamycin for 24 hrs strongly blocked the conjugation of Prox1 with SUMO and increased the expression of Prox1 at the protein level (Fig.2.14.B).

The levels of Prox1 SUMOylation were not affected by different concentrations of glucose and serum in polarized primary hepatocytes (data not shown).
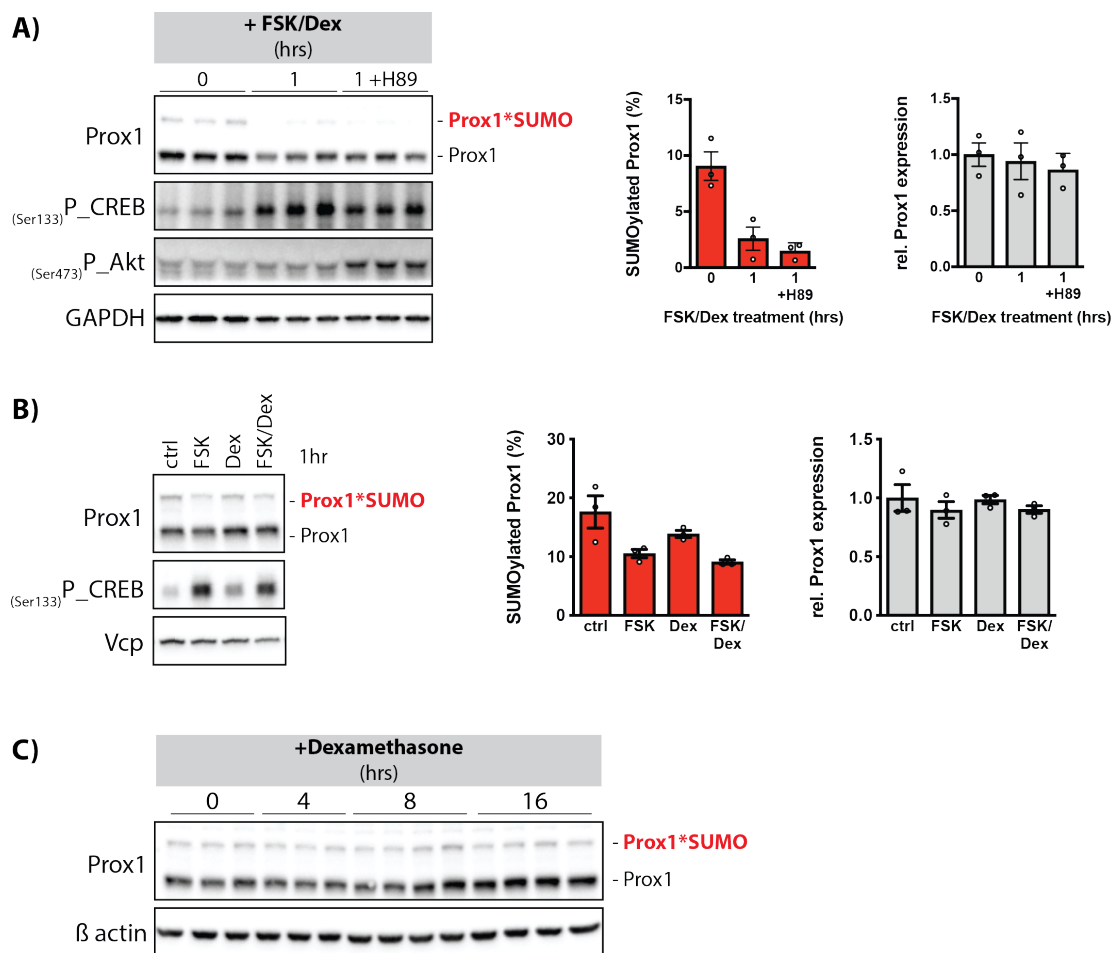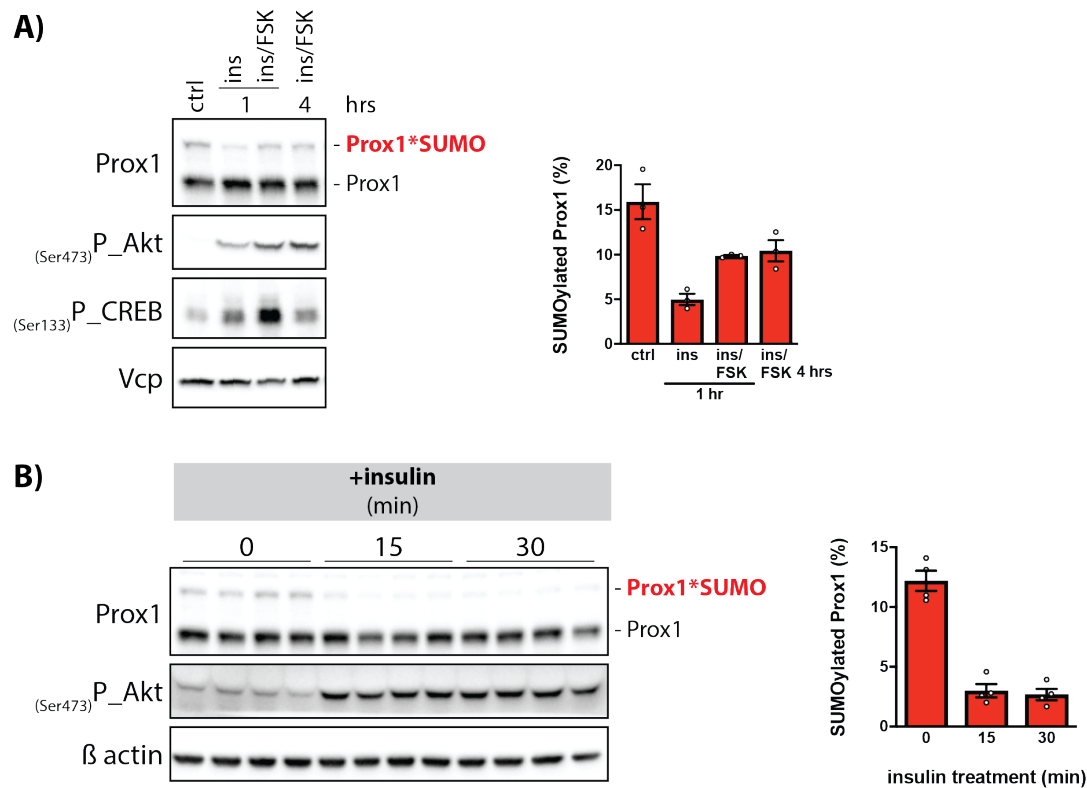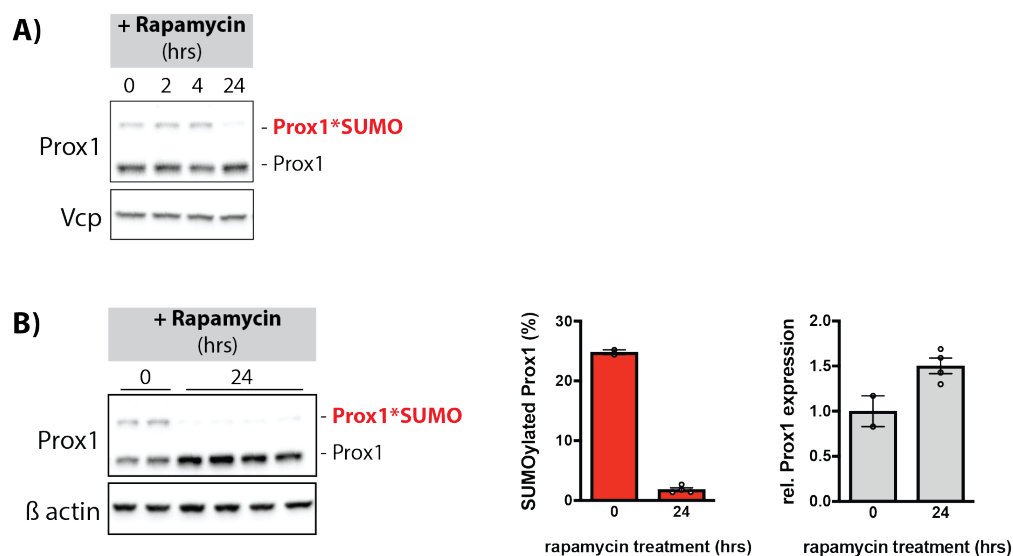

Figure 2.14: **Upstream regulation of Prox1 SUMOylation - rapamycin treatment**
A) Primary hepatocytes were isolated and cultured in a collagen sandwich as described above. Prior to the treatment the cells were incubated in low-serum low-glucose media overnight. Cells were treated with 20 nM rapamycin for 2, 4 and 24 hrs. B) Polarized primary hepatocytes were stimulated with rapamycin for 24 hrs as described above. Lysates were analyzed by immunoblotting using an anti-Prox1 antibody; Vcp and β actin were detected for input control. The quantification of SUMOylated Prox1 (%) and relative Prox1 expression are shown.

The regulation of the Prox1 SUMO-switch by bile acids was also investigated. For this, polarized primary hepatocytes were stimulated with chenodeoxycholic acid (CDCA), a primary bile acid, for 2, 4 and 24 hrs. A short incubation with CDCA resulted in a rapid de-SUMOylation of Prox1 without affecting the protein levels (Fig.2.15). On the other hand, longer incubation with CDCA not only blocked the conjugation of Prox1 with SUMO but it also decreased the total protein amount (Fig.2.15).
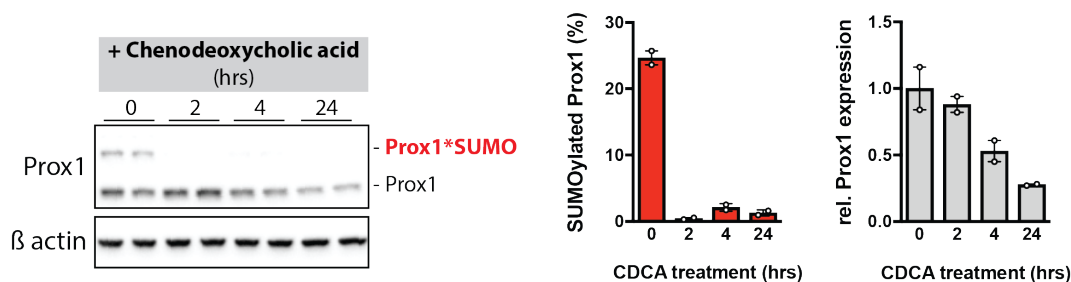
Figure 2.15: **Regulation of Prox1 expression and SUMOylation by bile acids**
Primary hepatocytes were isolated and cultured in a collagen sandwich as described above. Prior to the treatment the cells were incubated in low-serum low-glucose media overnight. Cells were treated with 25 μM chenodeoxycholic acid (CDCA) for 2, 4 and 24 hrs. Lysates were analyzed by immunoblotting using an anti-Prox1 antibody; β actin was detected for input control. The quantification of SUMOylated Prox1 (%) and relative Prox1 expression are shown.

There is still a lot of research to be done in order to clarify the regulatory signals modulating the conjugation of Prox1 with SUMO in hepatocytes. Thanks to the collagen sandwich protocol, some potential pathways regulating the Prox1 SUMO-switch were identified. The activation of AMPK, the inhibition of mTORC1 and increased levels of bile acids are all inter-connected. It has been published that chenodeoxycholic acid can activate AMPK (Noh et al., 2011) and it is well known that AMPK inhibits mTORC1 activity (Zoncu, Efeyan, and Sabatini, 2010). Thus, it will be interesting to investigate this signaling crosstalk in detail.

2.3 SUMO-deficient K556R Prox1 knock-in mouse model

The dynamic conjugation of SUMO to a substrate can result in multiple functional outcomes through the generation or disruption of binding sites for interacting partners. In order to elucidate the function of hepatic Prox1 SUMOylation it was necessary to alter the modification without affecting the expression of Prox1 itself. Thus, a conditional SUMO-deficient Prox1 knock-in mouse model was generated together with Taconic Biosciences. These animals are genetically engineered to express wild-type Prox1 until Cre-recombination is induced. The genomic region coding for the wild-type variant is removed upon Cre recombination allowing the expression of a Prox1 mutant carrying a lysine to arginine mutation at position 556; lysine 556 (K556) is the proposed main SUMO-acceptor site.

Prox1 is mainly SUMOylated on lysine residue 556 in vivo

In order to induce Cre-recombination only in hepatocytes and only after the liver has fully developed, an adeno-associated virus (AAV) was used as a vector to overexpress the Cre recombinase protein under the control of the hepatocyte-specific LP1 promoter (Cre_AAV). A control AAV vector coding for an untranslatable Cre recombinase under the LP1 promoter was also generated (Ctrl_AAV). For a pilot experiment eight weeks-old male mice were injected with either the Ctrl_AAV, the Cre_AAV, or phosphate-buffered saline (PBS). The status of Prox1 SUMOylation was analyzed three weeks later. The conjugation of hepatic Prox1 with SUMO was blocked in mice injected with the Cre_AAV; the total protein levels were not affected (Fig.2.16.A). With these results we can confirm that Prox1 is modified by a single SUMO moiety on K556 in the liver. The levels of Prox1 at the mRNA level had a trend to be lower in the livers of the mice injected with the Cre_AAV (Fig.2.16.A).

Therefore, the expression of Prox1 was assessed in wild-type (+/+), heterozygous (f/+) and homozygous (f/f) littermates of the K556R Prox1 mouse line. The expression of Prox1 at the protein level was comparable between all genotypes (Fig.2.16.B). However, the (f/+) animals had double the amount of Prox1 mRNA as compared to the (+/+) littermates while the quadruple the amount was detected in (f/f) mice. These results suggest that the increase in Prox1 mRNA comes from the incorporation of our engineered allele (Fig.2.16.B). Nevertheless, the elements added to our genomic design are capable of stopping the translation of the mutant variant until Cre recombination is induced (Fig2.16.B). It is important to keep this observation in mind for the interpretation of the upcoming results.
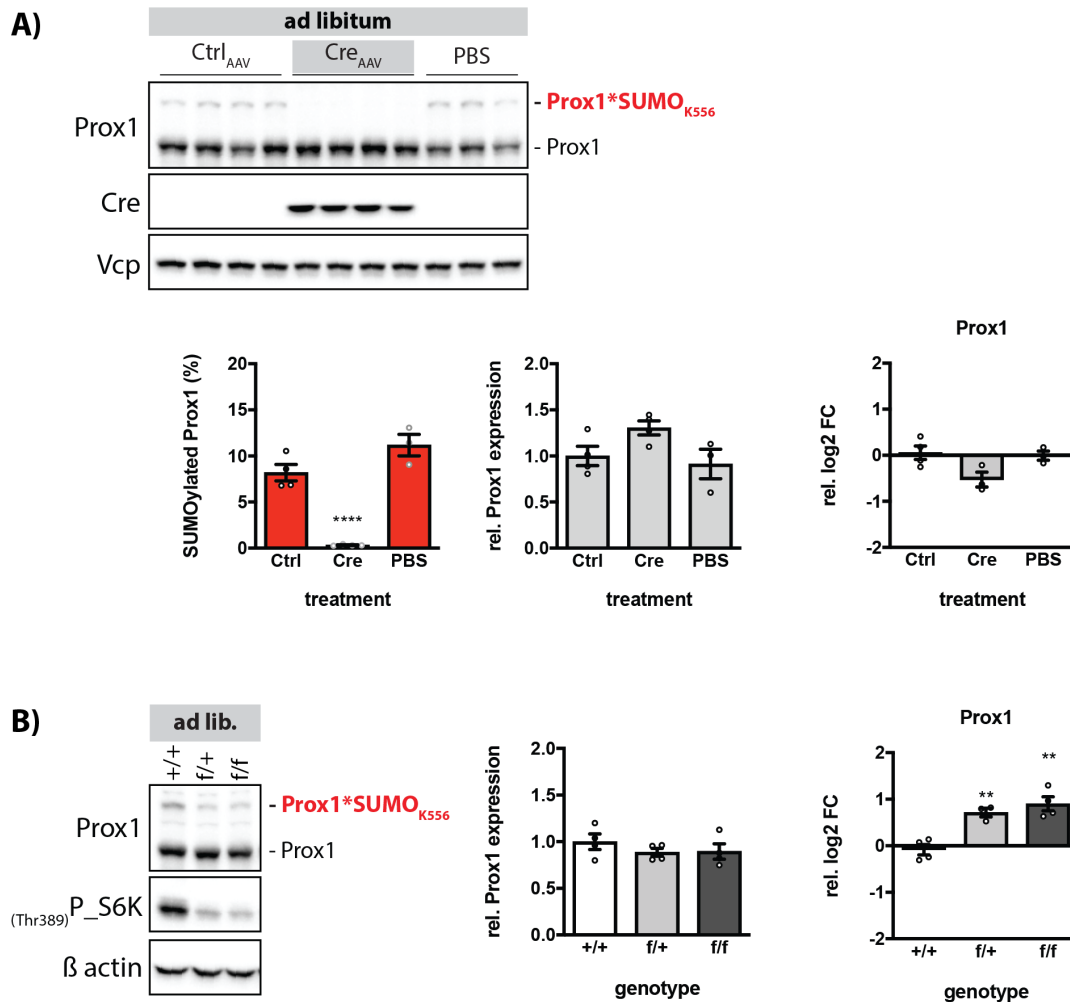
Figure 2.16: **The SUMO-deficient K556R Prox1 knock-in mouse model**
A) 8 weeks-old K556R Prox1 (f/f) male mice were injected with phosphate-buffered saline (PBS), a control AAV (Ctrl_AAV) or with an AAV to overexpress Cre recombinase (Cre_AAV) (n=3). Liver tissue samples were collected 3 weeks later, from mice fed *ad libitum*. B) The expression and SUMOylation status of Prox1 was analyzed in wild-type (+/+), heterozygous (f/+) and homozygous (f/f) litter mates of the K556R Prox1 mouse line (n=4). (A-B) Liver lysates were analyzed by immunoblotting using anti-Prox1, anti-Cre and anti-P_S6K(Thr389) antibodies; Vcp and β actin were detected for input control. The quantification of SUMOylated Prox1 (%) and relative Prox1 expression are shown. Expression analysis at the mRNA level by qPCR, data presented as relative log2 fold change (FC) normalized to the housekeeping gene TBP. Every dot represents one individual mouse. Data: mean $\pm$ SEM. Significance was determined by one-way ANOVA with Dunnett´s multiple comparison test relative to A) PBS or B) (+/+) samples. * P $\leq$ 0.05, ** P $\leq$ 0.01, *** P $\leq$ 0.001, **** P $\leq$ 0.0001.

Recombination specificity in the K556R Prox1 knock-in mouse model

The hepatocyte-specificity of the Cre recombination driven by the Cre_AAV was confirmed. For this, a liver fractionation of mice injected with either the Ctrl_AAV or the Cre_AAV was performed. The hepatocytes were isolated from the non-parenchymal liver cells such as sinusoidal endothelial cells, kupffer cells or hepatic stellate cells. The expression of Prox1 at the mRNA level and the Cre recombination event were analyzed in both the hepatocyte (hep.) and non-hepatocyte (non.h.) fractions. The liver fractionation was controlled by detecting the expression of albumin, a hepatocyte-specific marker, as well as Stab1, Emr1 and Vim, which are markers of sinusoidal endothelial cells, kupffer cells and hepatic stellate cells, respectively. Albumin expression was enriched in the hepatocyte fraction while Stab1, Emr1 and Vim expression were restricted to the non-hepatocyte fraction (Fig.2.17.A). Prox1 mRNA was detected mainly in hepatocytes (Fig.2.17.A). To control for Cre recombination, a PCR was performed using primers designed to detect either the constitutive allele or the conditional knock-in (K.I.) after Cre-mediated recombination. Amplification with these primers gives a product of 280 bp for the constitutive allele and a 235 bp for the conditional K.I. allele. The conditional K.I. allele was only detected in the hepatocyte fraction of mice injected with the Cre_AAV (Fig.2.17.B). These results confirm that the SUMO-deficient K556R Prox1 is expressed specifically in hepatocytes.
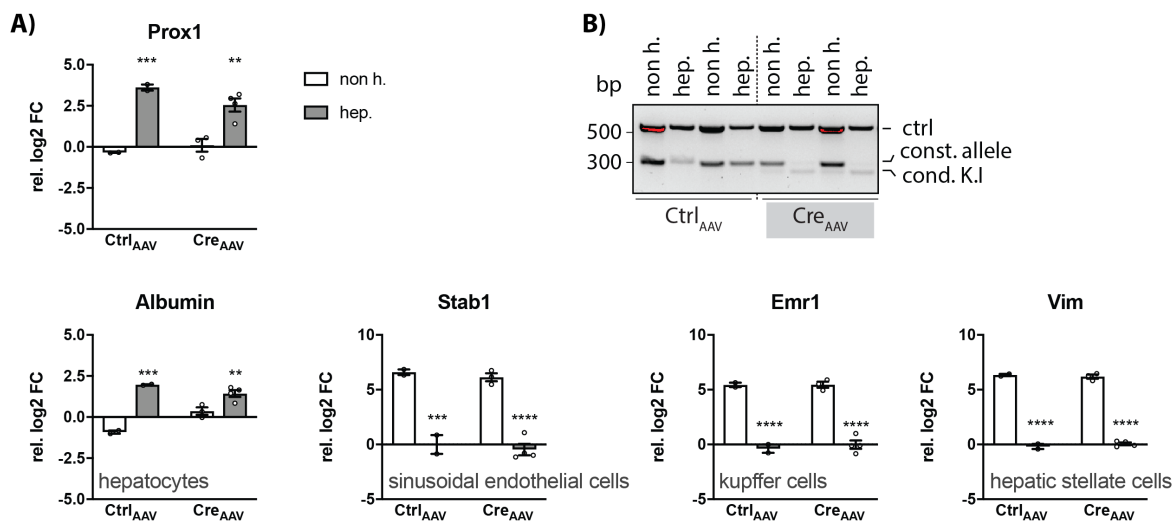
Figure 2.17: **Hepatocyte-specificity of the K556R Prox1 knock-in mouse model**
8 weeks-old K556R Prox1 (f/f) male mice were injected with a control AAV (Ctrl_AAV) or an AAV to overexpress Cre recombinase (Cre_AAV) (n=2-4). Hepatocytes (hep.) were isolated from the non-hepatocyte (non.h.) faction. A) Expression analysis at the mRNA level by qPCR, data presented as relative log2 fold change (FC) normalized to the housekeeping gene TBP. B) Amplification reaction by PCR detecting the constitutive allele (280 bp) or the conditional K.I. allele after Cre mediated recombination (235 bp); control product (585 bp). (A) Every dot represents one individual mouse. Data: mean $\pm$ SEM. Significance was determined by two-way ANOVA with Sidak´s multiple comparison test between different conditions. * P $\leq$ 0.05, ** P $\leq$ 0.01, *** P $\leq$ 0.001, **** P $\leq$ 0.0001.

2.4 Blocking Prox1 SUMOylation in the liver of male mice fed a standard chow diet

The function of hepatic Prox1 SUMOylation was first investigated in young male mice fed a standard chow diet in a 12/12 hrs light/dark cycle. For this, eight weeks-old male mice were injected with phosphate-buffered saline (PBS), the Ctrl_AAV or the Cre_AAV. Three weeks after injection the mice underwent a set of *in vivo* characterization analyses. The study was completed eleven weeks after the AAV injection. The relevant tissues were collected and weighted in the fasted and re fed state at ZT 15-17. In addition, blood serum samples were prepared for further analysis. The status of Prox1 SUMOylation was analyzed by immunoblotting. The conjugation of Prox1 with SUMO was blocked in the liver of the mice injected with the Cre_AAV without affecting the total protein levels (Fig.2.18). From now on these animals will be denominated "SUMO-deficient Prox1(liver)" mice. About 10 % of the Prox1 pool was SUMOylated in the re fed control groups (Fig.2.18). Higher levels of Prox1 SUMOylation have been previously detected in wild type C57BL/6N male mice upon re feeding. Given the longer exploratory analysis done to the livers before freezing, it is possible that a portion of Prox1 was de-SUMOylated *post-mortem* in this study.
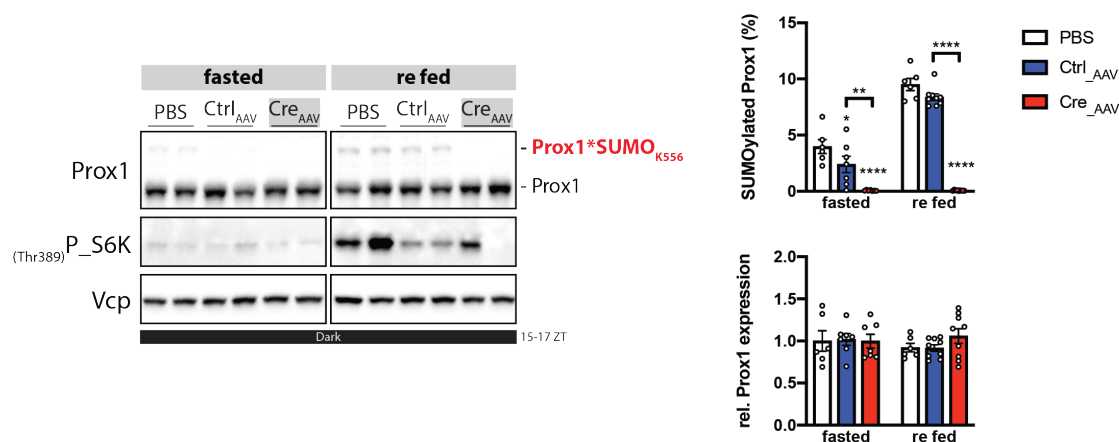
Figure 2.18: **Blocking hepatic Prox1 SUMOylation in male mice fed a standard diet**
8 weeks-old K556R Prox1 (f/f) male mice were injected with phosphate-buffered saline (PBS), a control AAV (Ctrl_AAV) or with an AAV to overexpress Cre recombinase (Cre_AAV). 11 weeks after the AAV injection the study was terminated. Fasted: The food was removed at ZT 7, tissues were collected 8 hrs later between ZT 15 and 16. Re fed: Mice were fasted for 8 hrs (ZT 4-12) for synchronization. The food was re-introduced at ZT 12 right before the start of the dark phase, tissues were collected between ZT 16 and 17 (n=6-9). Liver lysates were analyzed by immunoblotting using anti-Prox1 and anti-P_S6K(Thr389) antibodies; Vcp was detected for input control. The quantification of SUMOylated Prox1 (%) and relative Prox1 expression are shown. Every dot represents one individual mouse. Data: mean $\pm$ SEM. Significance was determined by two-way ANOVA with Tukey´s multiple comparison test between different conditions. * $P \leq 0.05$, ** $P \leq 0.01$, *** $P \leq 0.001$, **** $P \leq 0.0001$.

In vivo characterization

To investigate whether the Prox1 SUMO-switch in hepatocytes has an impact on systemic glucose handling the SUMO-deficient Prox1(liver) mice were subjected to a glucose tolerance test (GTT). To perform the GTT mice were fasted for 5 to 6 hrs then challenged with a high dose of glucose via an intraperitoneal injection. The clearance of glucose from the circulation was tracked over a period of 2 hrs; the acute insulin levels were also measured. The first GTT was performed four weeks after the AAV injection. The SUMO-deficient Prox1(liver) mice clear the glucose overload in a comparable degree to the control groups (Fig.2.19.A). The fasting blood glucose levels, the insulin response and the calculated Insulin Sensitivity Index (ISI), as well as the Homeostatic Model Assessment for Insulin Resistance (HOMA-IR) were comparable between all groups (Fig.2.19.A). In a second GTT performed eight weeks after the AAV injection the SUMO-deficient Prox1(liver) mice coped with the glucose challenge similarly than the control animals (Fig.2.19.B).

To investigate whether the Prox1 SUMO-switch in hepatocytes has an impact on insulin signaling, the SUMO-deficient Prox1(liver) mice were subjected to an insulin tolerant test (ITT). To per-

form the ITT, mice were fasted for 5 hrs then challenged with insulin via an intraperitoneal injection. The clearance of glucose from the circulation was tracked over a period of 2 hrs. The SUMO-deficient Prox1(liver) mice coped with the insulin dose similarly than the control animals (Fig.2.20).

Taken these results into consideration, I conclude that blocking Prox1 SUMOylation in hepatocytes does not affect systemic glucose handling nor insulin sensitivity in young male mice.

To investigate whether the Prox1 SUMO-switch in hepatocytes has an impact on systemic lipid metabolism, the circulating levels of triglycerides and cholesterol were monitored seven weeks after the AAV injection. For this, blood samples were collected at ZT 14 in the fasted and *ad libitum* state. The plasma triglycerides and cholesterol levels in the SUMO-deficient Prox1(liver) mice were comparable to the controls in both conditions (Fig.2.21).

The body weight and the body composition were monitored through the course of this study. The control and the SUMO-deficient Prox1(liver) mice gained a comparable amount of body weight (Fig.2.22.A). The body composition of the SUMO-deficient Prox1(liver) mice was influenced by age to a degree comparable to the control animals (Fig.2.22.B).

These *in vivo* results suggest that blocking Prox1 SUMOylation in hepatocytes has little impact on the systemic metabolism of young male mice fed a standard healthy diet.
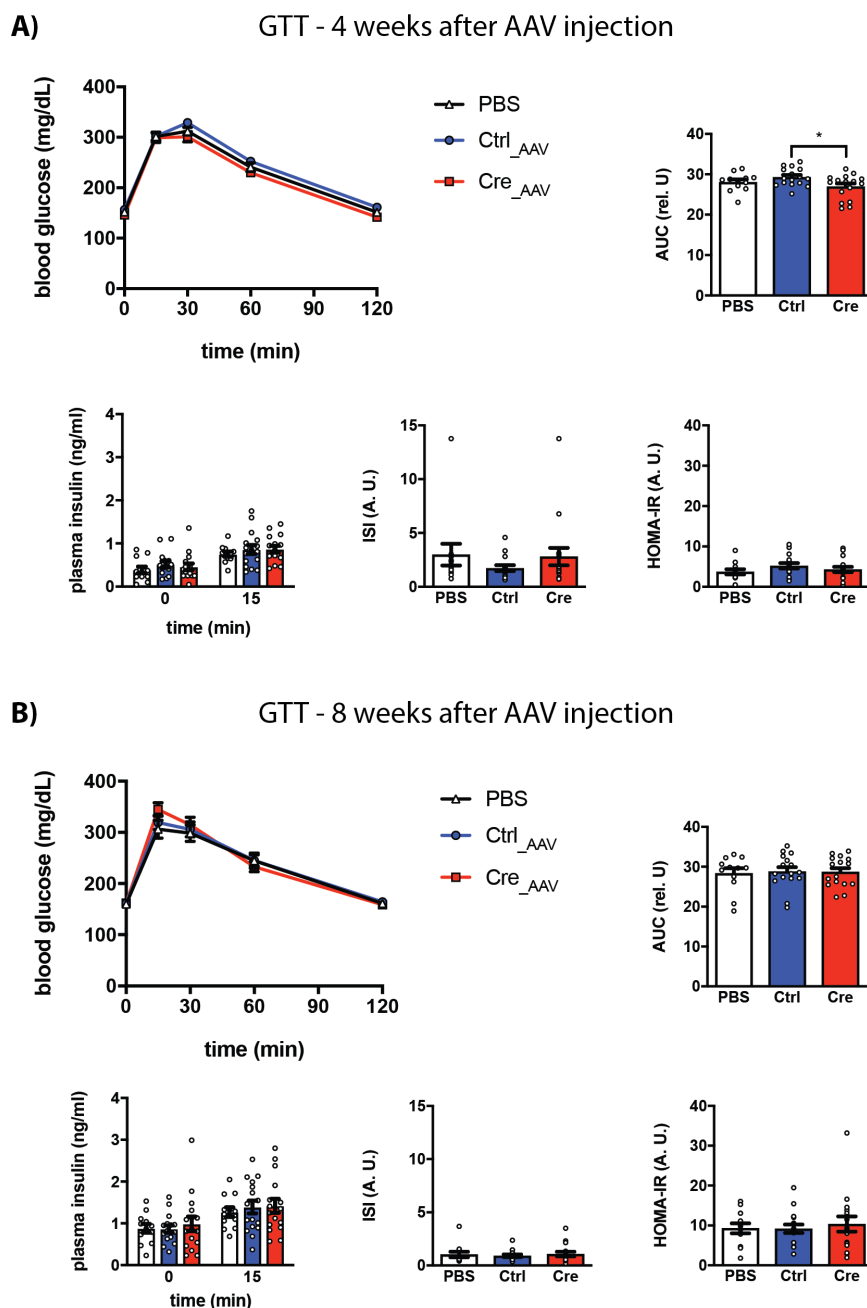
Figure 2.19: **Glucose Tolerance Test (GTT) in the SUMO-deficient Prox1(liver) mice**
8 weeks-old (f/f) male mice were injected with phosphate-buffered saline (PBS), a control AAV (Ctrl_AAV) or with an AAV to overexpress Cre recombinase (Cre_AAV). A) GTT done 4 weeks after the AAV injection. B) GTT done 8 weeks after the AAV injection. For the GTT mice were fasted for 5 to 6 hrs then challenged with 1.5 g/kg glucose via an intraperitoneal injection. Blood samples were collected at time points: 0, 15, 30, 60 and 120 min after the glucose injection (n=12-18). (A-B) AUC: area under the curve. The calculated Insulin Sensitivity Index (ISI), Homeostatic Model Assessment for Insulin Resistance (HOMA-IR) and plasma insulin levels at time points: 0 and 15 min are shown. Every dot represents one individual mouse. Data: mean $\pm$ SEM. Significance was determined by one-way ANOVA with Tukey´s multiple comparison test between different conditions for AUC, ISI and HOMA-IR. For plasma insulin levels significance was determined by two-way ANOVA with Sidak´s multiple comparison test between different conditions. * P $\leq$ 0.05.
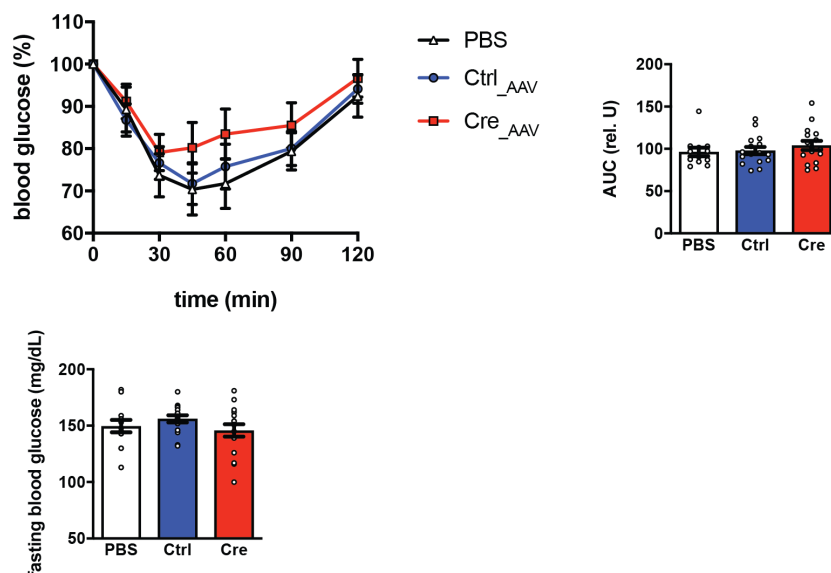
Figure 2.20: Insulin Tolerance Test (ITT) in the SUMO-deficient Prox1(liver) mice
8 weeks-old (f/f) male mice were injected with phosphate-buffered saline (PBS), a control AAV (Ctrl_AAV) or with an AAV to overexpress Cre recombinase (Cre_AAV). An ITT was performed 9 weeks after the AAV injection. For this, mice were fasted for 5 hrs then challenged with 1.2 U/kg insulin via an intraperitoneal injection. Blood samples were collected at time points: 0, 15, 30, 45, 60, 90 and 120 min after the insulin injection (n=12-18). The blood glucose levels (% of fasting blood glucose) and AUC: area under the curve are shown. Every dot represents one individual mouse. Data: mean ± SEM. Significance was determined by one-way ANOVA with Tukey´s multiple comparison test between different conditions.

Plasma triglycerides and cholesterol - 7 weeks after AAV injection
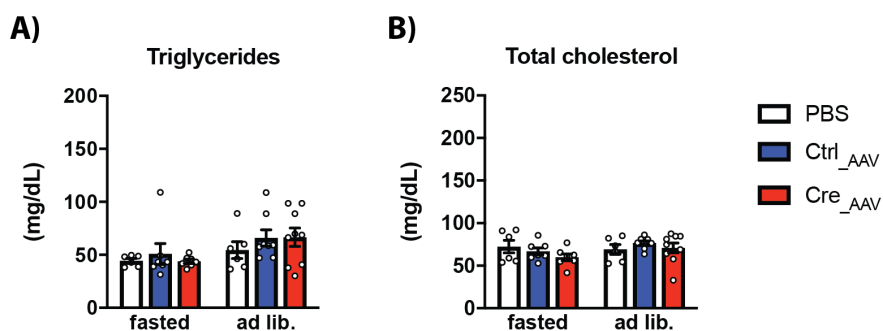
Figure 2.21: **Plasma triglycerides and cholesterol in the SUMO-deficient Prox1(liver) mice**
Blood samples were collected 7 weeks after the AAV injection from the tail vein of mice injected with phosphate-buffered saline (PBS), a control AAV (Ctrl_AAV) or with an AAV to overexpress Cre recombinase (Cre_AAV). Mice were either fasted for 4 hrs or kept *ad libitum*, sampling was done at ZT 14 (n=6-9). A) Colorimetric measurement of triglycerides. B) Colorimetric measurement of total cholesterol. Every dot represents one individual mouse. Data: mean $\pm$ SEM. Significance was determined by two-way ANOVA with Sidak´s multiple comparison test between different conditions.

A)

B)
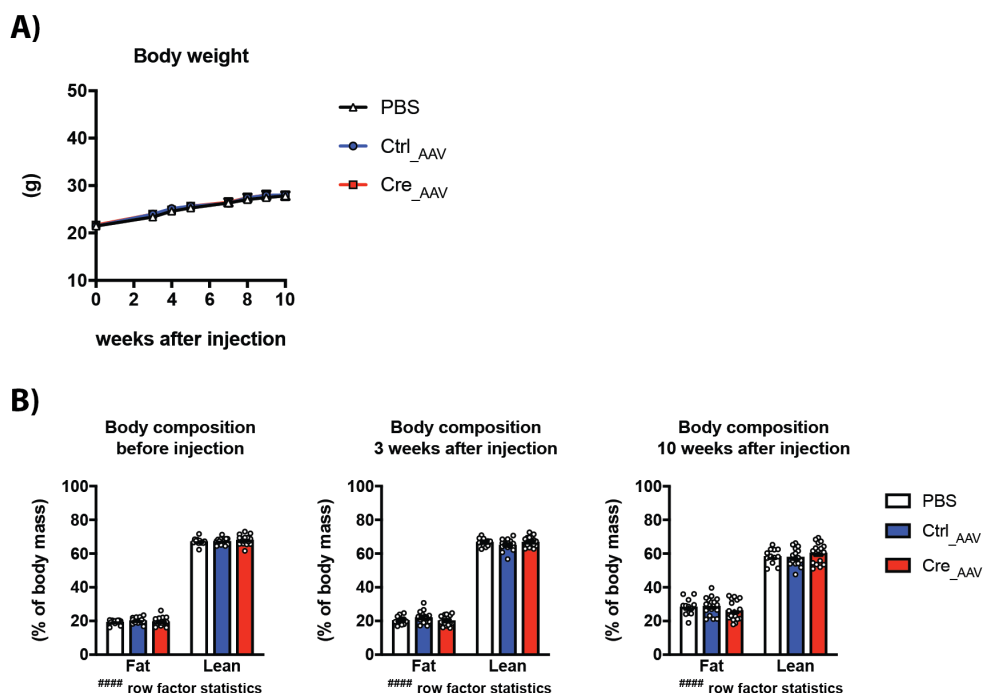
Figure 2.22: **Body composition in the SUMO-deficient Prox1(liver) mice**
8 weeks-old (f/f) male mice were injected with phosphate-buffered saline (PBS), a control AAV (Ctrl_AAV) or with an AAV to overexpress Cre recombinase (Cre_AAV) (n=12-18). A) Body weight records. B) Echo-MRI measurements done before, 3 and 10 weeks after the AAV injections. (B) Every dot represents one individual mouse. Data: mean $\pm$ SEM. Significance was determined by two-way ANOVA with Tukey´s multiple comparison test between different conditions. Row factor statistics: #### $P \leq 0.0001$.

Analysis of tissue and serum samples

To further analyze the consequences of blocking Prox1 SUMOylation in hepatocytes, the study was terminated eleven weeks after the AAV injection. The relevant tissues and blood samples were collected in the fasted (8 hrs) and re fed (4-5 hrs) state at ZT 15-17 as described above. The body weight and blood glucose levels were recorded right before the tissue collection. Changes on body weight and blood glucose levels upon fasting or re feeding were comparable between the control and the SUMO-deficient Prox1(liver) mice (Fig.2.23.A). The weight of the liver, the inguinal and gonadal white adipose tissue (WAT) depots and the gastrocnemius muscle (GC) were comparable between all groups (Fig.2.23.B). These results suggest that blocking Prox1 SUMOylation in the hepatocytes has little effect on whole body metabolism.

Study termination -11 weeks after AAV injection
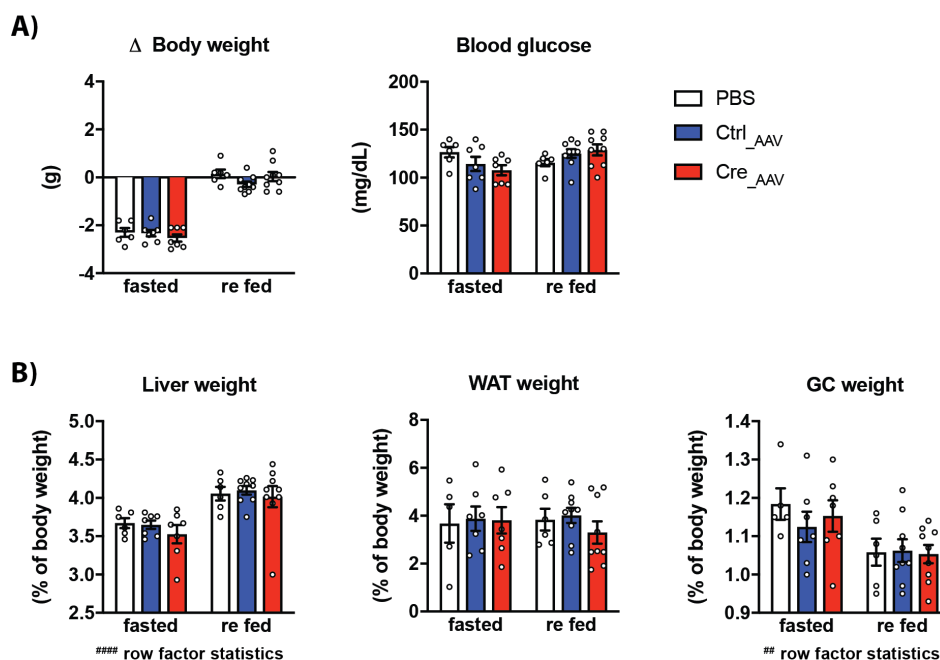
Figure 2.23: **Body/tissue weight and blood glucose levels in SUMO-deficient Prox1(liver) mice**
8 weeks-old (f/f) male mice were injected with phosphate-buffered saline (PBS), a control AAV (Ctrl_AAV) or with an AAV to overexpress Cre recombinase (Cre_AAV). 11 weeks after the AAV injection the study was terminated. Fasted: 8 hrs (ZT 7 to 15). Re fed: fasted for 8 hrs (ZT 4 to 12) and re fed for 4-5 hrs (ZT 12 to 16-17), (n=6-9). A) Body weight changes and blood glucose levels. B) Tissue weights (% relative to the total body weight); liver, inguinal and gonadal white adipose tissue (WAT) and gastrocnemius muscle (GC) are shown. (A-B) Every dot represents one individual mouse. Data: mean $\pm$ SEM. Significance was determined by two-way ANOVA with Tukey´s multiple comparison test between different conditions. Row factor statistics: ## $P \leq 0.01$, #### $P \leq 0.0001$.

To further investigate the metabolism of the SUMO-deficient Prox1(liver) mice, the blood serum was analyzed using a colorimetric-based serum analyzer. The circulating levels of triglycerides, cholesterol, low density lipoprotein (LDL) and high density lipoprotein (HDL) as well as the markers for liver injury and impaired function alanine aminotransferase (ALT), aspartate aminotransferase (AST) and lactate dehydrogenase (LDH) were measured. The SUMO-deficient Prox1(liver) mice showed no significant differences in the circulating metabolites tested as compared to the controls (Fig.2.24). These results show that mice injected with the Ctrl_AAV or Cre_AAV have no signs of liver damage or impaired function.
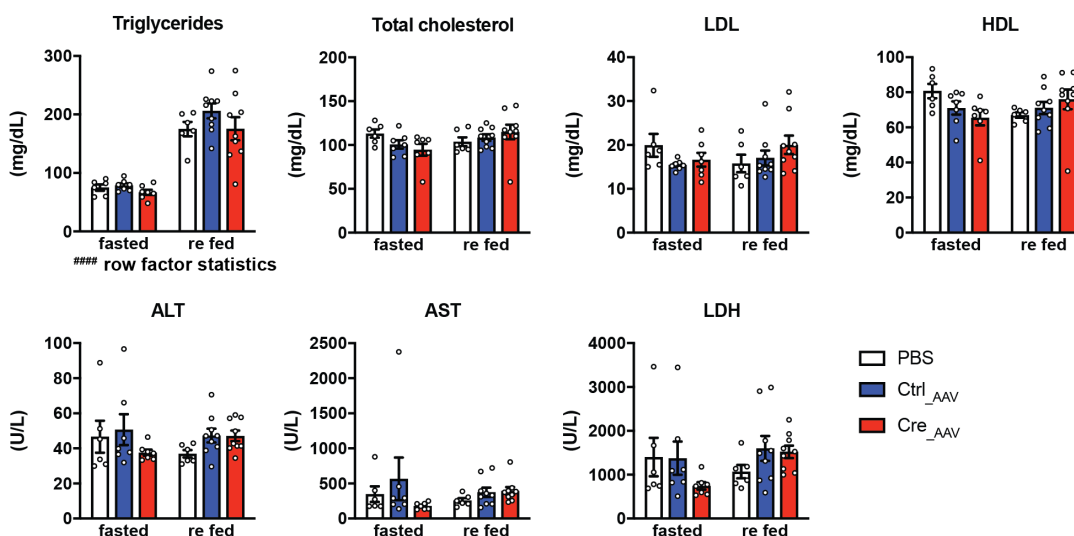
Figure 2.24: **Serum analysis in the SUMO-deficient Prox1(liver) mice**
8 weeks-old (f/f) male mice were injected with phosphate-buffered saline (PBS), a control AAV (Ctrl_AAV) or with an AAV to overexpress Cre recombinase (Cre_AAV). 11 weeks after the AAV injection the study was terminated. Fasted: 8 hrs (ZT 7 to 15). Re fed: fasted for 8 hrs (ZT 4 to 12) and re fed for 4-5 hrs (ZT 12 to 16-17). Blood was collected by decapitation and processed for serum analysis using a colorimetric-based serum analyzer (n=6-9). Levels of triglycerides, total cholesterol, low density lipoprotein (LDL), high density lipoprotein (HDL), alanine aminotransferase (ALT), aspartate aminotransferase (AST) and lactate dehydrogenase (LDH) are shown. Every dot represents one individual mouse. Data: mean $\pm$ SEM. Significance was determined by two-way ANOVA with Tukey´s multiple comparison test between different conditions. Row factor statistics: #### P $\leq$ 0.0001.

The liver morphology of the SUMO-deficient Prox1(liver) mice was analyzed by the pathology core facility of our research center. The analysis and interpretation were lead by Dr. Annette Feuchtinger and done by Dr. Andreas Parzefall. No differences in liver morphology were detected between the control and the SUMO-deficient Prox1(liver) mice (Fig.2.25.B).

Changes in glycogen and lipid deposition in the liver were also investigated. The glycogen accumulation upon feeding was observed to a comparable degree in the control and in the SUMO-deficient Prox1(liver) mice (Fig.2.25.A.B). The triglycerides and cholesterol content in the liver during fasting and feeding was not altered in the SUMO-deficient Prox1(liver) mice (Fig.2.25.B).

Blocking the conjugation of Prox1 with SUMO in hepatocytes showed no metabolic consequences in young male mice fed a standard healthy diet. Therefore, more research is required to clarify the function of the hepatic Prox1 SUMO-switch.

Liver morphology and metabolites - 11 weeks after AAV injection
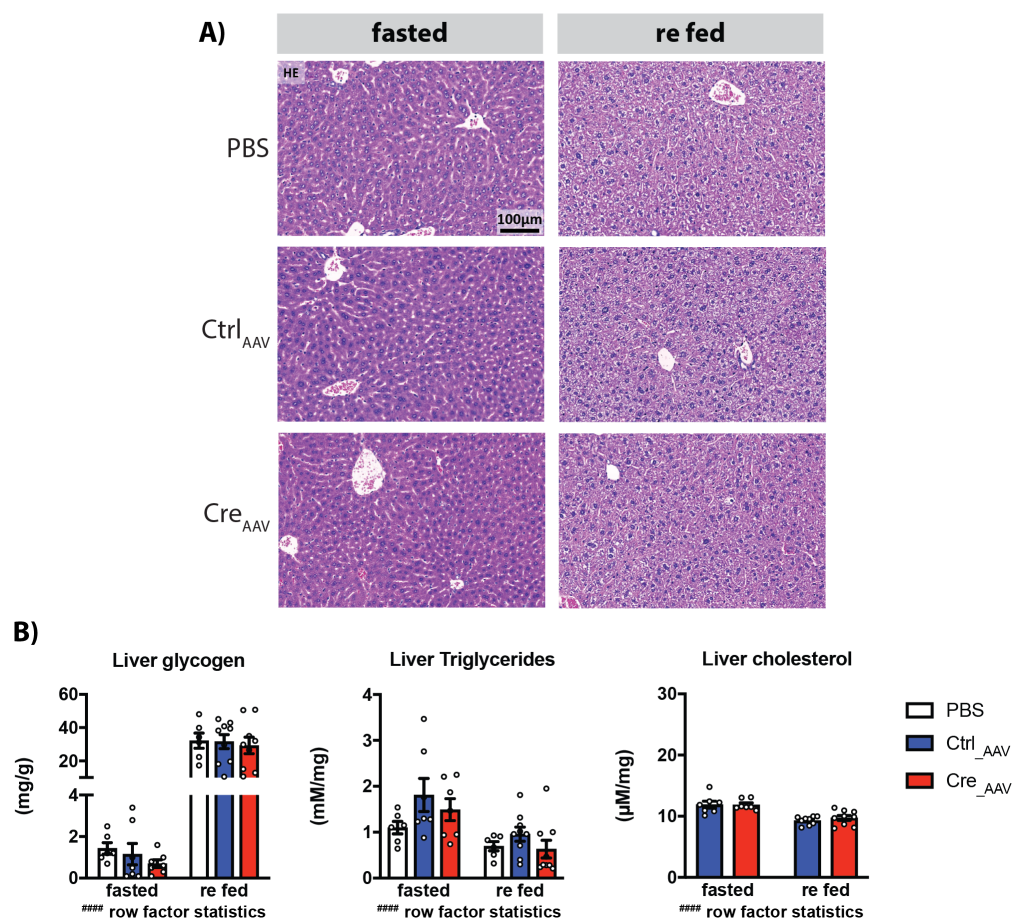
Figure 2.25: **Liver morphology and metabolites in the SUMO-deficient Prox1(liver) mice**
8 weeks-old (f/f) male mice were injected with phosphate-buffered saline (PBS), a control AAV (Ctrl_AAV) or with an AAV to overexpress Cre recombinase (Cre_AAV). 11 weeks after the AAV injection the study was terminated. Fasted: 8 hrs (ZT 7 to 15). Re fed: fasted for 8 hrs (ZT 4 to 12) and re fed for 4-5 hrs (ZT 12 to 16-17), (n=6-9). A) Liver morphology analyzed via hematoxylin and eosin staining, representative images. B) Colorimetric measurement of glycogen, triglycerides and total cholesterol content within the liver. (B) Every dot represents one individual mouse. Data: mean $\pm$ SEM. Significance was determined by two-way ANOVA with Sidak´s multiple comparison test between different conditions. Row factor statistics: ### P $\leq$ 0.001, #### P $\leq$ 0.0001.

RNA sequencing analysis and data processing

To address the impacts of SUMO conjugation on the transcriptional activity of Prox1, the liver transcriptome of the SUMO-deficient Prox1(liver) mice was analyzed. RNA was extracted from the livers of mice injected with either the Ctrl_AAV or with the Cre_AAV in both the fasted and re fed conditions (Fig.2.26.A). Five representative samples of each group were sequenced by the Genome Sequencing facility at our research center lead by Elisabeth Graf. With the mapped raw counts a differential expression analysis was performed using the DESeq2 R-package from Bio-conductor (Love, Huber, and Anders, 2014). A statistical threshold was set to an adjusted pvalue (padj) < 0.05; DESeq2 uses the Benjamini-Hochberg to adjust for multiple testing. A threshold for the effect size was set to a log2 fold change (FC) of < - 0.5 or > 0.5. A log2 FC shrinkage was performed to generate more accurate estimates.

A principal component analysis (PCA) was performed to visualize global changes in the transcriptome. The liver transcriptome showed major changes in response to the nutritional state of the mice but was not affected by the SUMOylation status of Prox1 (Fig.2.26.A). Data from the differential expression analysis showed that fourteen genes were differentially regulated in the SUMO-deficient Prox1(liver) mice during fasting, while only one gene was differentially expressed in the re fed state (Fig.2.26.B). This observation is quite remarkable as it is during feeding when the SUMOylation status differs the most between the control and the SUMO-deficient Prox1(liver) mice. It is important to address the down-regulation of Prox1 detected in fasted mice. As explained above, the mRNA levels of Prox1 are halved upon Cre recombination (Fig.2.16.B). Lower levels of Prox1 mRNA were detected in the re feeding condition, although no statistical significance was reached (data not shown).

To investigated whether Prox1 is a potential direct regulator of the differentially expressed genes, the Cistrome Data Browser (Mei et al., 2017) and (Zheng et al., 2019) was utilized to explore a published liver Prox1 chip-seq analysis (Armour et al., 2017). According to this data, Prox1 is enriched at the promoters of the following genes affected during fasting: Nt5e, Dpy19l3, Ces4a, Tbc1d30, Insig2, Hsb3b2 and Tubb2a. Prox1 is also localized at the promoter of Atxn1, the only differentially expressed gene detected in the re fed condition. The expression of the putative Prox1 target genes as well as the expression of the known Prox1 target Cyp7a1 according to the RNA-seq data is presented Fig.2.27. The occupancy score (S) of the target genes was identified using BETA (S. Wang et al., 2013). The score (S) of Prox1 on the Cyp7a1 promoter was used as a reference.
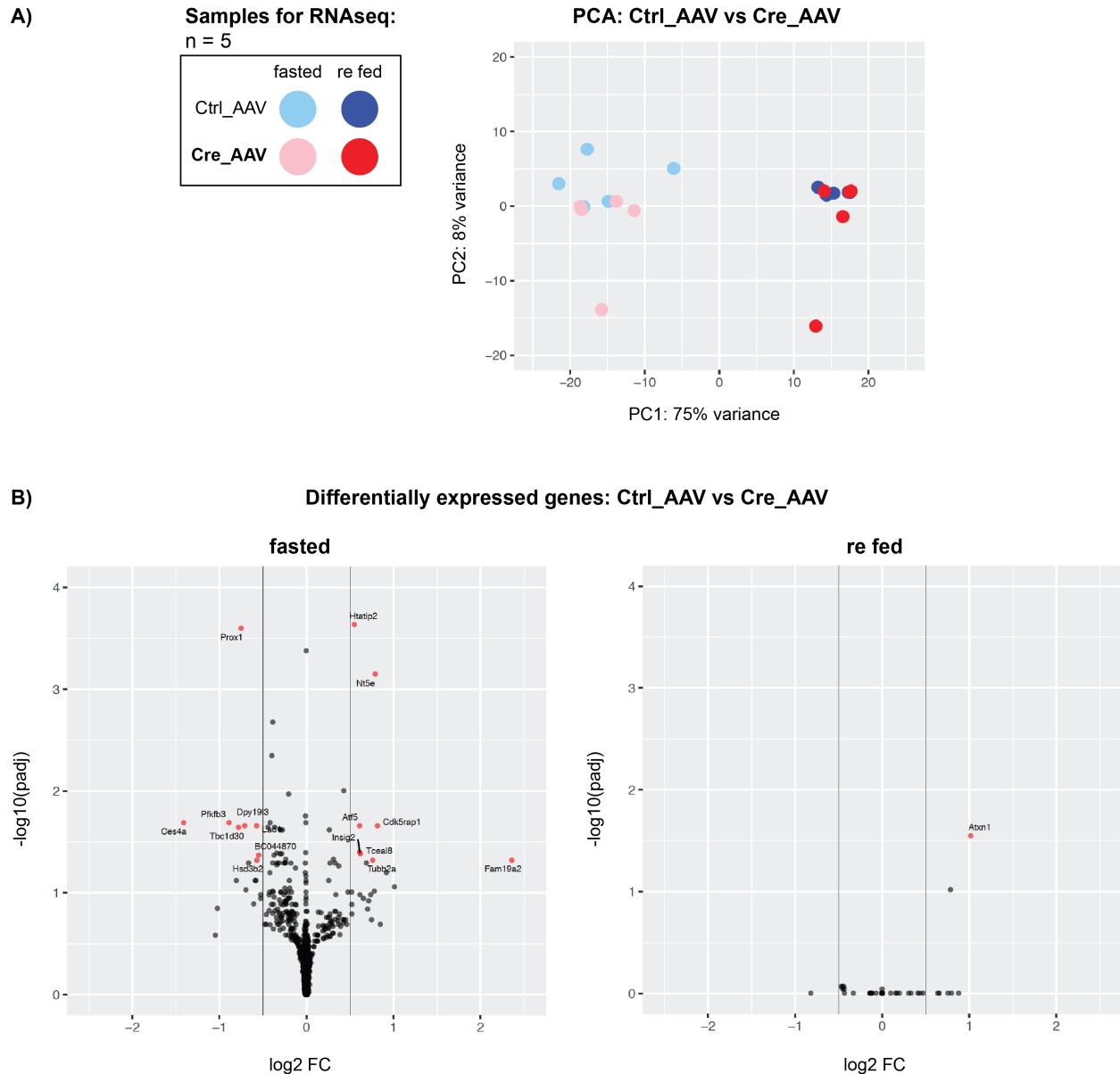
Figure 2.26: **Transcriptome analysis of the SUMO-deficient Prox1(liver) mice**
8 weeks-old (f/f) male mice were injected with a control AAV (Ctrl_AAV) or with an AAV to over-express Cre recombinase (Cre_AAV). 11 weeks after the AAV injection the livers were collected. Fasted: 8 hrs (ZT 7 to 15). Re fed: fasted for 8 hrs (ZT 4 to 12) and re fed for 4-5 hrs (ZT 12 to 16-17). Total RNA was isolated and processed for mRNA sequencing (n=5). The transcriptome was analyzed using the DESeq2 R-package from Bioconductor (Love, Huber, and Anders, 2014). A statistical threshold to extract the differentially expressed genes was set to an adjusted pvalue (padj) < 0.05 and a log2 fold change (FC) of < - 0.5 or > 0.5. A) Principal component analysis (PCA) of the complete transcriptome. B) Volcano plots showing in red the differentially expressed genes.
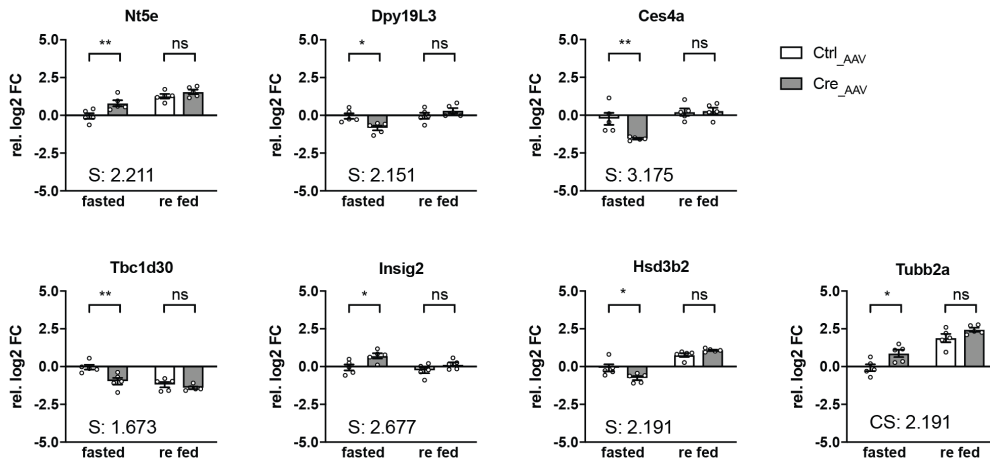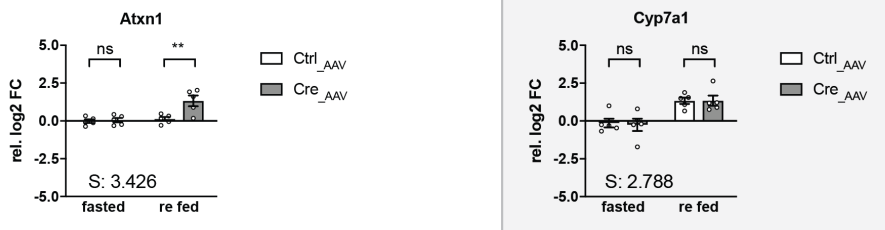
Figure 2.27: **Putative Prox1 target genes in the SUMO-deficient Prox1(liver) mice**
The transcriptome analysis of the SUMO-deficient Prox1(liver) mice was done as described above. The identified differentially expressed genes were compared to a published chip-seq analysis (Armour et al., 2017) using the Cistrome Data Browser (Mei et al., 2017) and (Zheng et al., 2019). The expression of the putative Prox1 target genes according to the RNA-seq data is shown as well as the occupancy score (S) identified using BETA (S. Wang et al., 2013). Cyp7a1 was used as a reference gene. Every dot represents one individual mouse. Data: mean $\pm$ SEM. Significance was determined by two-way ANOVA with Sidak´s multiple comparison test between different conditions. * P $\leq$ 0.05, ** P $\leq$ 0.01.

Known functions of the Prox1 putative target genes were investigated further in the literature; the results are listed in (Fig.2.28).

Gene	Coding protein	Function
Nt5e	ecto-5'-nucleotidase or CD73	catalyzes extracellular AMP to adenosine convertion
Dpy19l3	Probable C-mannosyltransferase	mediates C-mannosylation of tryptophan residues
Ces4a	Carboxylesterase 4A	probable carboxylesterase
Tbc1d30	TBC1 domain family member 30	GTPase-activating protein
Insig2	Insulin induced gene 2	blocks processing of sterol regulatory element binding proteins (SREBPs)
Hsd3b2	3 beta-hydroxysteroid dehydrogenase/Delta 5-4-isomerase type 2	oxidative conversion of Delta$_5$-ene-3-beta-hydroxy steroid and ketosteroids
tubb2a	Tubulin Beta 2A Class IIa	major constituent of microtubules
Ataxin1	Ataxin 1	chromatin-binding factor, transcriptional repressor of the Notch signaling pathway

Figure 2.28: **Analysis of the putative Prox1 target genes**
Main function of the putative Prox1 target genes according to the literature. References: Nt5e - (Peng et al., 2008); Dpy19L3 - (Niwa et al., 2016); Ces4a - (Lian, Nelson, and Lehner, 2018); Tbc1d30 - (Ishibashi et al., 2009); Insig2 - (Yabe, Brown, and Goldstein, 2002); Hsd3b2 - (Simard et al., 2005); tubb2a - (H. Lin et al., 2017); Atxn1 - (Tong et al., 2011).

Nt5e, also known as cluster of differentiation 73 (CD73), has been implicated in the regulation of liver fibrosis. CD37 knock-out mice are protected from liver fibrosis and show significantly less collagen content in the liver (Peng et al., 2008). There is less information regarding Dpy19L3, which has been characterized as a C-mannosyltransferase involved in Wnt signaling in human cell lines (Niwa et al., 2016). Ces4a has been annotated as a probable carboxylesterase (Lian, Nelson, and Lehner, 2018). Carboxylesterases hydrolyze a wide range of xenobiotic and endogenous compounds including lipid esters. Furthermore, liver-specific knock-down of the related gene, Ces3, results in lower plasma levels of triglycerides, total cholesterol and VLDL and a higher content of lipids in the liver (Lian, Wei, et al., 2012). These observations were associated with lipid droplet mobilization and increased fatty acid oxidation (Lian, Wei, et al., 2012). Tbc1d30 is a GTPase-activating protein probably participating in intracellular membrane traffic (Ishibashi et al., 2009). Moreover, its activity on Rab8A links it to lipid droplet fusion (Wu et al., 2014). Insig2 for Insulin induced gene 2 mediates the feedback control of cholesterol synthesis by blocking the processing of SREBPs (Yabe, Brown, and Goldstein, 2002). As the name suggests, the Insig2 promoter is activated by insulin (Fernández-Alvarez et al., 2010). Hsd3b2 is in charge of the oxidative conversion of Delta5-ene-3-beta-hydroxy steroid and ketosteroids. Hsd3b2 expression is regulated via the LXRα, LRH1 and GATA4/6 (Simard et al., 2005). Tubb2a, the major constituent of microtubules, has been shown to be down-regulated in human patients with liver failure (Peng et al., 2008). The only differentially expressed gene in the re fed state, Atxn1, is a chromatin-binding factor known to act as a transcriptional repressor. In drosophila, Atxn1 was described as

a member of the co-repressor complex SMRT (silencing mediator of retinoid and thyroid receptors) controlling some aspects of the Notch signaling pathway (Tong et al., 2011).

Although some of the putative Prox1 target genes are linked to the regulation of liver metabolism, the transcriptional changes induced by blocking Prox1 SUMOylation in hepatocytes are so subtle that no conclusion can be made regarding its function. It is possible that the Prox1 SUMO-switch in hepatocytes becomes mostly relevant when the liver has to cope with some sort of metabolic burden. It is also reasonable to think that this regulatory mechanism could be conserved in males but that it is actually more relevant in females. Therefore, a second study was conducted where the SUMO-deficient Prox1(liver) mice, both males and females, where challenged with a high cholesterol diet.

2.5 Blocking Prox1 SUMOylation in the liver of mice fed a high cholesterol diet

Prox1 has been identified as a regulator of lipid metabolism in the liver. Hepatocyte-specific knock-down of Prox1 affected the serum levels of total and HDL-associated cholesterol. (Dittner, 2016). In line, loss of Prox1 in hepatocytes affected the expression of a cluster of genes involved in cholesterol and bile acid metabolism in the liver (Dittner, 2016). Given these observations, the role of hepatic Prox1 SUMOylation on cholesterol homeostasis was investigated. For this, Prox1 SUMOylation was blocked in the hepatocytes of male and female mice challenged with a high cholesterol (2 %) diet. A custom-made control diet with 0 % cholesterol was used as control. Eight weeks-old male and female mice were injected with either the Ctrl_AAV or the Cre_AAV and placed on the high cholesterol or the control diet. Three weeks after the AAV injection and diet start the animals underwent a set of *in vivo* characterization analyzes similar to those described above. The animals were kept on a 12/12 hrs light/dark cycle; the study was completed fourteen weeks after the AAV injection and diet start. On the day of the study termination the relevant tissues were collected and weighted in the fasted and re fed state at ZT 15-17. In addition, blood serum samples were prepared for analysis.

The conjugation of Prox1 with SUMO was abolished in the liver of mice injected with the Cre_AAV, in both males and females (Fig.2.29.A-B). The expression of Prox1 at the protein level was comparable between all groups (Fig.2.29.A-B). These animals are again denominated "SUMO-deficient Prox1(liver)" mice.
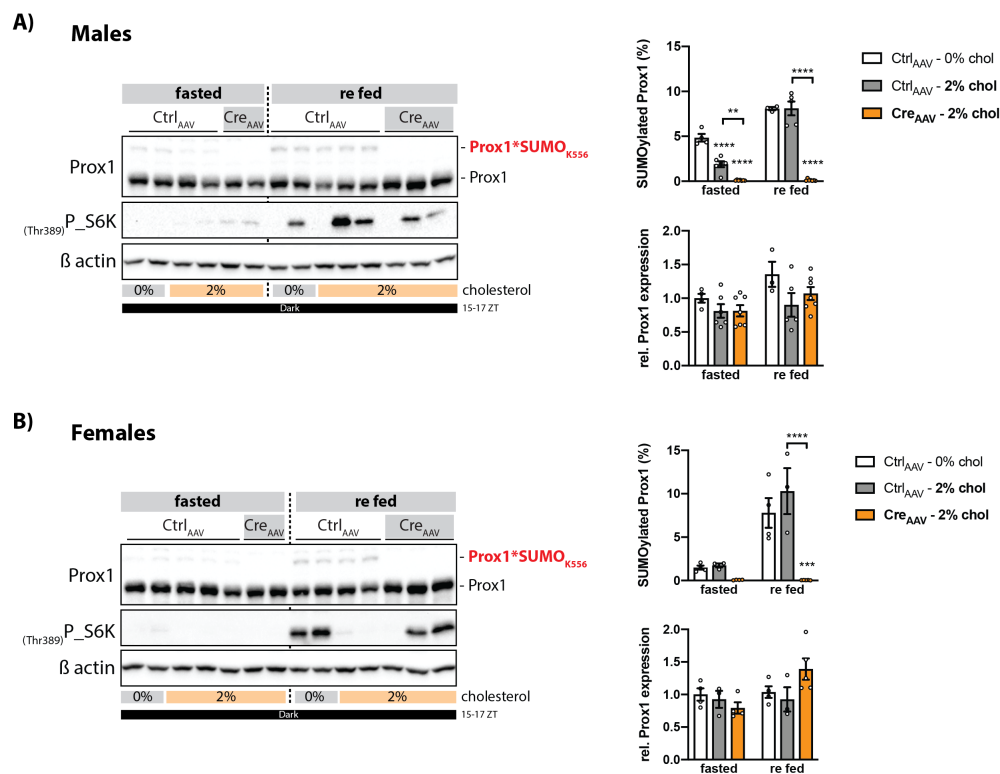
Figure 2.29: **Blocking hepatic Prox1 SUMOylation in mice fed a high cholesterol diet**
8 weeks-old K556R Prox1 (f/f) mice were injected with a control AAV (Ctrl_AAV) or with an AAV to overexpress Cre recombinase (Cre_AAV) and placed on a high cholesterol (2 %) or control (0 %) diet. 14 weeks after the AAV injection and the diet start the study was terminated. Fasted: The food was removed at ZT 7, tissues were collected 8 hrs later between ZT 15 and 16. Re fed: Mice were fasted for 8 hrs (ZT 4-12) for synchronization. The food was re-introduced at ZT 12 right before the start of the dark phase, tissues were collected between ZT 16 and 17. Liver lysates were analyzed by immunoblotting using anti-Prox1 and anti-P_S6K(Thr389) antibodies; β actin was detected for input control. A) Male mice (n=4-7). B) Female mice (n=3-5). The quantification of SUMOylated Prox1 (%) and relative Prox1 expression are shown. Every dot represents one individual mouse. Data: mean $\pm$ SEM. Significance was determined by two-way ANOVA with Tukey´s multiple comparison test between different conditions. * $P \leq 0.05$, ** $P \leq 0.01$, *** $P \leq 0.001$, **** $P \leq 0.0001$.

In vivo characterization

The role of the Prox1 SUMO-switch on systemic glucose handling was investigated in mice challenged with the high cholesterol diet. For this, a glucose tolerance test (GTT) was performed four weeks after the AAV injection and diet start, as described above. Male and female mice fed the high cholesterol diet showed no differences in systemic glucose handling as compared to animals fed the control diet; the SUMO-deficient Prox1(liver) mice handled the glucose challenge in a comparable degree to that of the control animals (Fig.2.30). These results suggest that male and female mice on a high cholesterol challenge can maintain glucose homeostasis despite the loss Prox1 SUMOylation in hepatocytes.

The metabolic status of the animals was tracked by measuring the plasma cholesterol levels. Blood samples taken four and seven weeks after the AAV injection and diet start were collected at ZT 14 from *ad libitum* fed mice. Samples taken after ten weeks were collected at ZT 11 in the fasted and *ad libitum* fed conditions. The circulating levels of cholesterol after four and seven weeks were not only comparable between the control and the SUMO-deficient Prox1(liver) mice fed the high cholesterol diet, but also to the control mice fed the control diet, in both males and females (Fig.2.31.A-B). After ten weeks, the fasted and *ad libitum* cholesterol levels were also comparable between all groups (Fig.2.31.A-B). These results suggest that the cholesterol overload from the diet had been metabolized to the same degree in both the control and the SUMO-deficient Prox1(liver) mice.

The body weight and the food intake were also recorded through the course of this study. The body weight gain and the food intake were comparable between all groups, in both males and females (Fig.2.32.A-B). Echo-MRI measurements performed right before and thirteen weeks after the AAV injection and diet start showed that the body composition of male and female mice was not affected by the high cholesterol challenge or by the loss of Prox1 SUMOylation (Fig.2.32.A-B).

The *in vivo* results obtained suggest that male and female mice were capable of metabolizing a dietary cholesterol overload despite the loss of Prox1 SUMOylation in hepatocytes.

GTT - 4 weeks after AAV injection and diet start
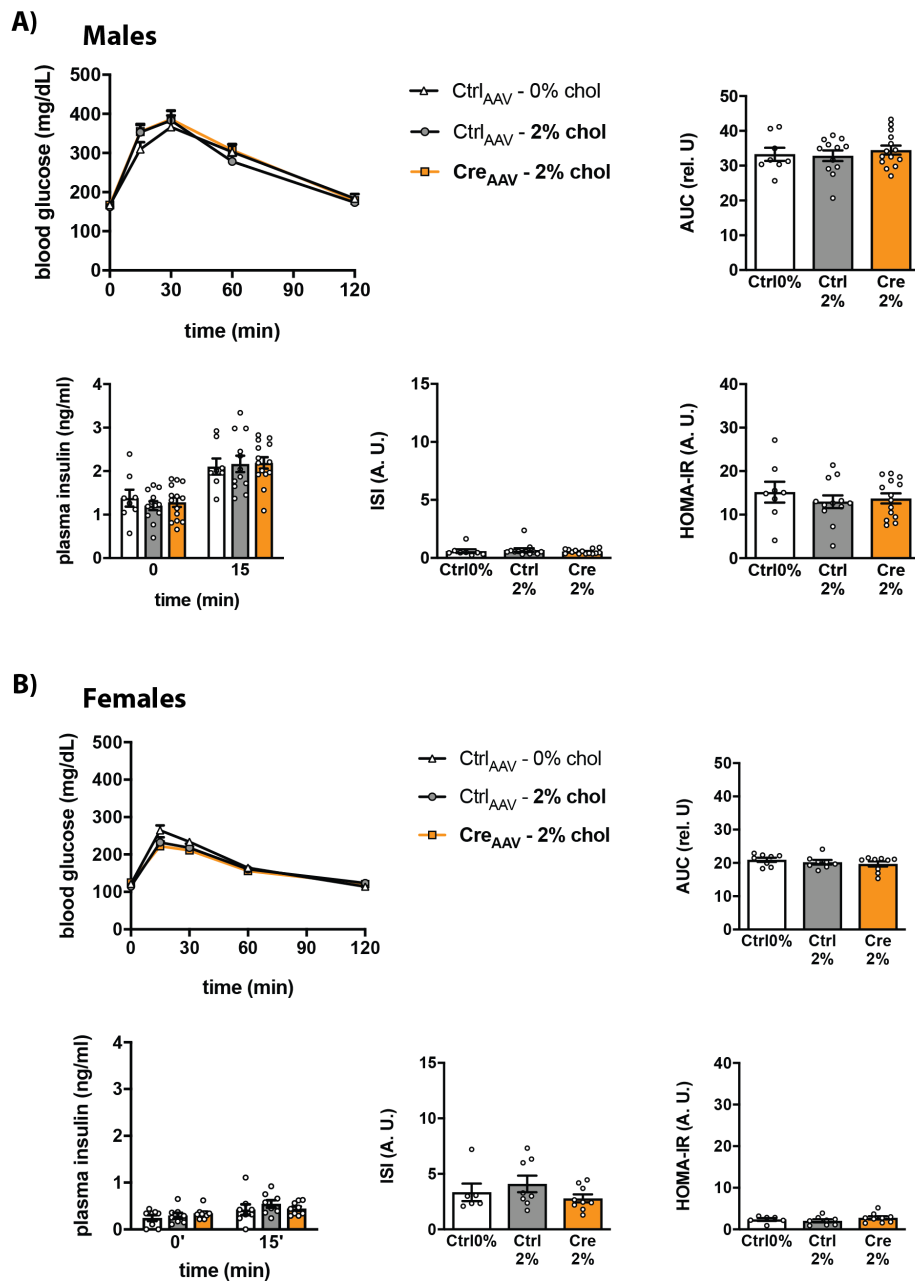
Figure 2.30: **High cholesterol challenge: GTT in the SUMO-deficient Prox1(liver) mice**
8 weeks-old (f/f) mice were injected with a control AAV (Ctrl_AAV) or with an AAV to overexpress Cre recombinase (Cre_AAV) and placed on a high cholesterol (2 %) or control (0 %) diet. A GTT was done 4 weeks after the AAV injection and diet start. For the GTT mice were fasted for 6 hrs then challenged with 2 g/kg glucose via an intraperitoneal injection. A) Male mice (n=8-14). B) Female mice (n=6-10). (A-B) The calculated Insulin Sensitivity Index (ISI), Homeostatic Model Assessment for Insulin Resistance (HOMA-IR) and plasma insulin levels at time points: 0 and 15 min are shown. Every dot represents one individual mouse. Data: mean $\pm$ SEM. Significance was determined by one-way ANOVA with Tukey´s multiple comparison test between different conditions for AUC, ISI and HOMA-IR. For plasma insulin levels significance was determined by two-way ANOVA with Sidak´s multiple comparison test between different conditions.

A) **Males**

B) **Females**
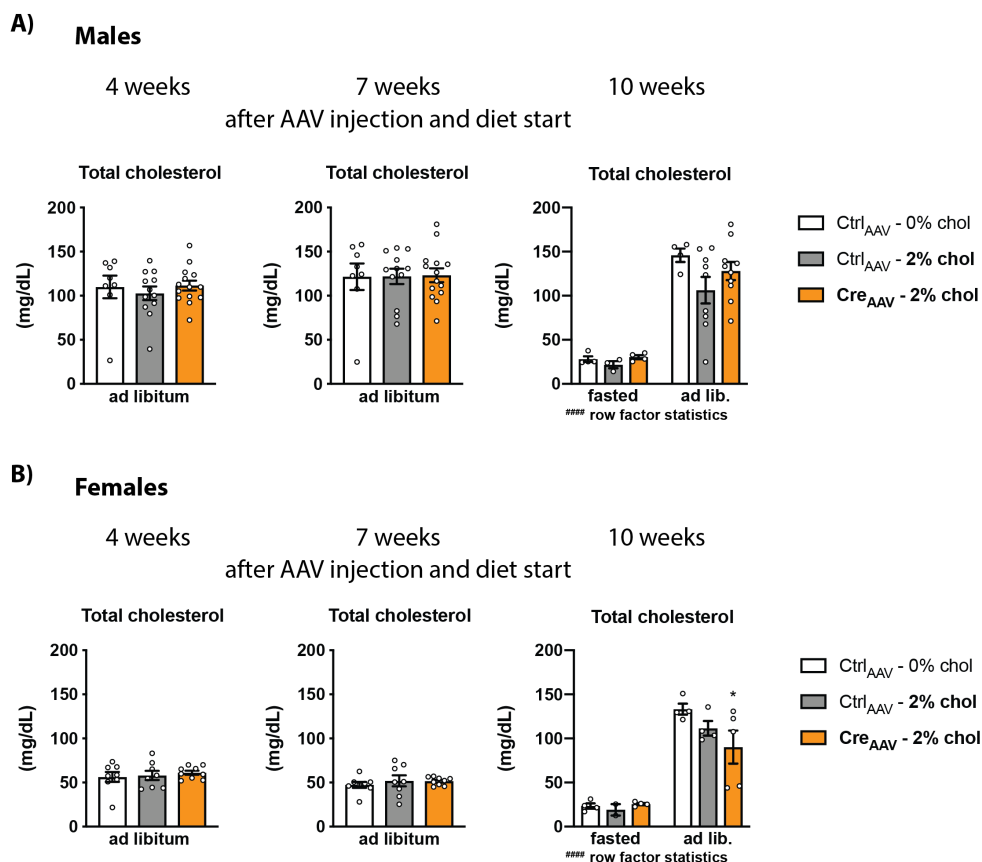
Figure 2.31: **High cholesterol challenge: Tracking plasma cholesterol levels**
8 weeks-old (f/f) mice were injected with a control AAV (Ctrl_AAV) or with an AAV to overexpress Cre recombinase (Cre_AAV) and placed in a high cholesterol (2 %) or control (0 %) diet. Tail vein blood samples collected 4 and 7 weeks after the AAV injection and diet start were obtained from *ad libitum* fed mice at ZT 14 (males n=8-14; females n=6-10). Samples collected after 10 weeks were obtained from fasted or *ad libitum* fed mice at ZT 11. The cholesterol levels from A) Male mice and B) Female mice are shown. (A-B) Every dot represents one individual mouse. Data: mean $\pm$ SEM. Significance was determined by two-way ANOVA with Sidak´s multiple comparison test between different conditions. * $P \leq 0.05$. Row factor statistics: #### $P \leq 0.0001$.

Figure 2.32: **High cholesterol challenge: Body weight, food intake and body composition**
8 weeks-old (f/f) mice were injected with a control AAV (Ctrl_AAV) or with an AAV to overexpress
Cre recombinase (Cre_AAV) and placed in a high cholesterol (2 %) or control (0 %) diet. The body
weight was recorded every 2 weeks for a period of 14 weeks. The daily food intake was recorded
every 2 weeks for a period of 10 weeks. Echo-MRI measurements were done before and 13 weeks
after the AAV injection and diet start. Data from A) Male mice (n=8-14) and B) Female mice (n=6-
10) is shown.(A-B) Every dot represents one individual mouse. Data: mean $\pm$ SEM. Significance
was determined by two-way ANOVA with Tukey´s multiple comparison test between different
conditions. Row factor statistics: #### $P \leq 0.0001$.

Analysis of tissue and serum samples

To further investigate the consequences of a high cholesterol challenge in mice lacking hepatic Prox1 SUMOylation, the study was terminated fourteen weeks after the AAV injection and diet start. The relevant tissues and blood samples were collected in the fasted (8 hrs) and re fed (4-5 hrs) state at ZT 15-17, as described above. The body weight and blood glucose levels were recorded right before the tissue collection. The changes in body weight and blood glucose levels upon fasting or re feeding were comparable between the control and the SUMO-deficient Prox1(liver) mice fed the high cholesterol diet and the control animals fed the control diet, in both males and females (Fig.2.33.A-B). The liver weight of the control and the SUMO-deficient Prox1(liver) mice fed the high cholesterol diet were comparable between each other, in both males and females (Fig.2.33.A-B). The liver weight of male mice fed the high cholesterol diet was significantly higher than the control mice fed the control diet (Fig.2.33.A). The liver weight of female mice fed the high cholesterol diet was just slightly higher than the control mice fed the control diet; this observation was only significant in the SUMO-deficient Prox1(liver) female mice upon re feeding (Fig.2.33.B).

To further investigate the metabolism of the SUMO-deficient Prox1(liver) mice on a high cholesterol challenge, the blood serum levels of triglycerides, cholesterol, LDL, HDL and bile acids as well as markers for liver injury and impaired function ALT, AST and LDH were measured. The circulating levels of triglycerides and cholesterol were comparable between mice fed the high cholesterol diet and mice fed the control diet, in both males and females; no differences were detected in the SUMO-deficient Prox1(liver) mice (Fig.2.34.A-B). The circulating levels of HDL-associated cholesterol were not affected by the high cholesterol diet and were comparable between the SUMO-deficient Prox1(liver) mice and the control animals, in both males and females (Fig.2.34.A-B). The LDL-associated cholesterol was increased by the high cholesterol diet in males and females but was not affected by the loss of Prox1 SUMOylation (Fig.2.34.A-B). The circulating levels of total bile acids in the male cohort upon fasting or re feeding were comparable between all groups. On the other hand, a couple of control female mice fed either the high cholesterol or the control diet showed remarkably elevated levels of total bile acids; none of the SUMO-deficient Prox1(liver) female mice showed increased levels of circulating bile acids (Fig.2.34.B). There were no significant differences in the markers for liver injury ALT and AST in the male cohort (Fig.2.34.A). However, increased levels of ALT and AST were detected in control female mice fed the high cholesterol diet (Fig.2.34.B).

Study termination - 14 weeks after AAV injection and diet start

A) **Males**
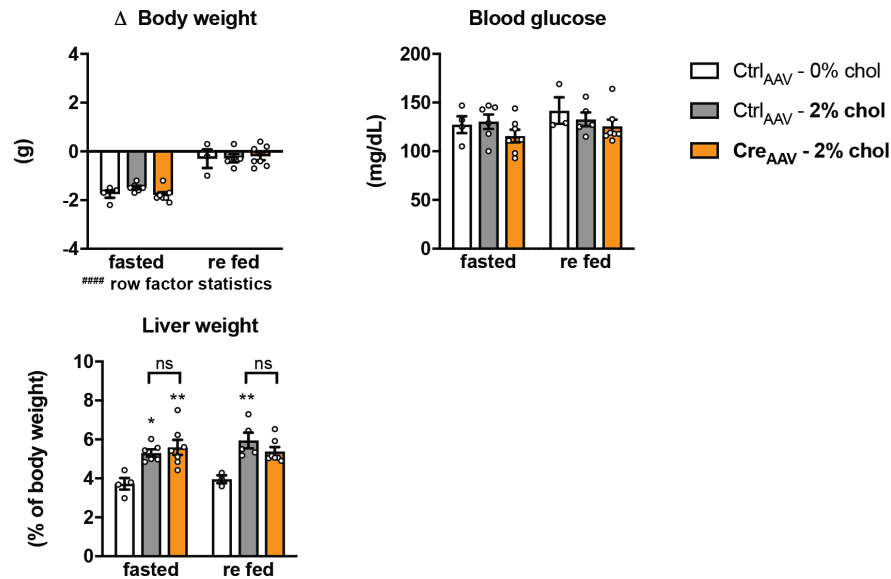
B) **Females**
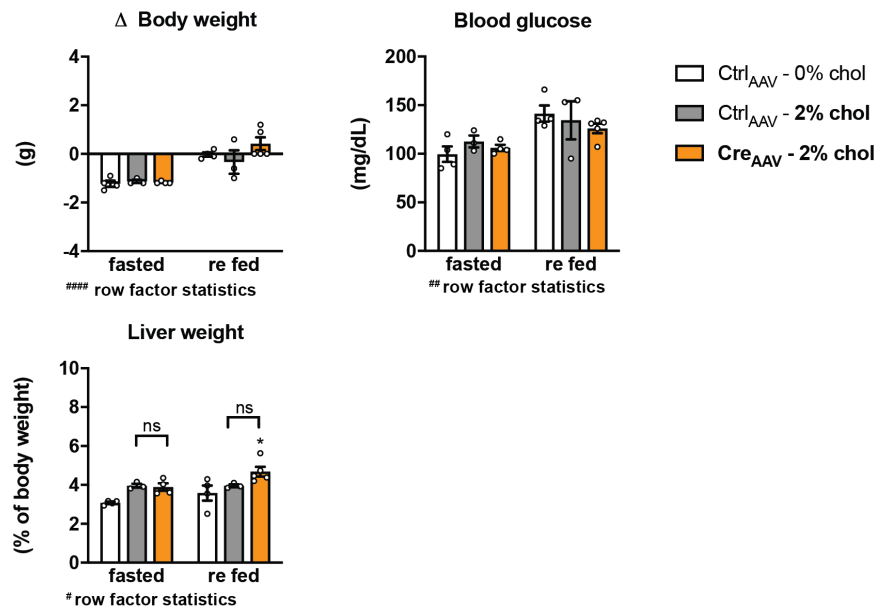
Figure 2.33: **High cholesterol challenge: Body/tissue weights and blood glucose levels**
8 weeks-old (f/f) mice were injected with a control AAV (Ctrl_AAV) or with an AAV to overexpress Cre recombinase (Cre_AAV) and placed on a high cholesterol (2 %) or control (0 %) diet. 14 weeks after the AAV injection and the diet start the study was terminated as described above. A) Male mice (n=4-7). B) Female mice (n=3-5). (A-B) Body weight change and blood glucose levels upon fasting and re feeding as well as the liver weight in (%) relative to the total body weight are shown. Every dot represents one individual mouse. Data: mean $\pm$ SEM. Significance was determined by two-way ANOVA with Tukey´s multiple comparison test between different conditions. * $P \leq 0.05$, ** $P \leq 0.01$. Row factor statistics: # $P \leq 0.05$, ## $P \leq 0.01$, #### $P \leq 0.0001$.
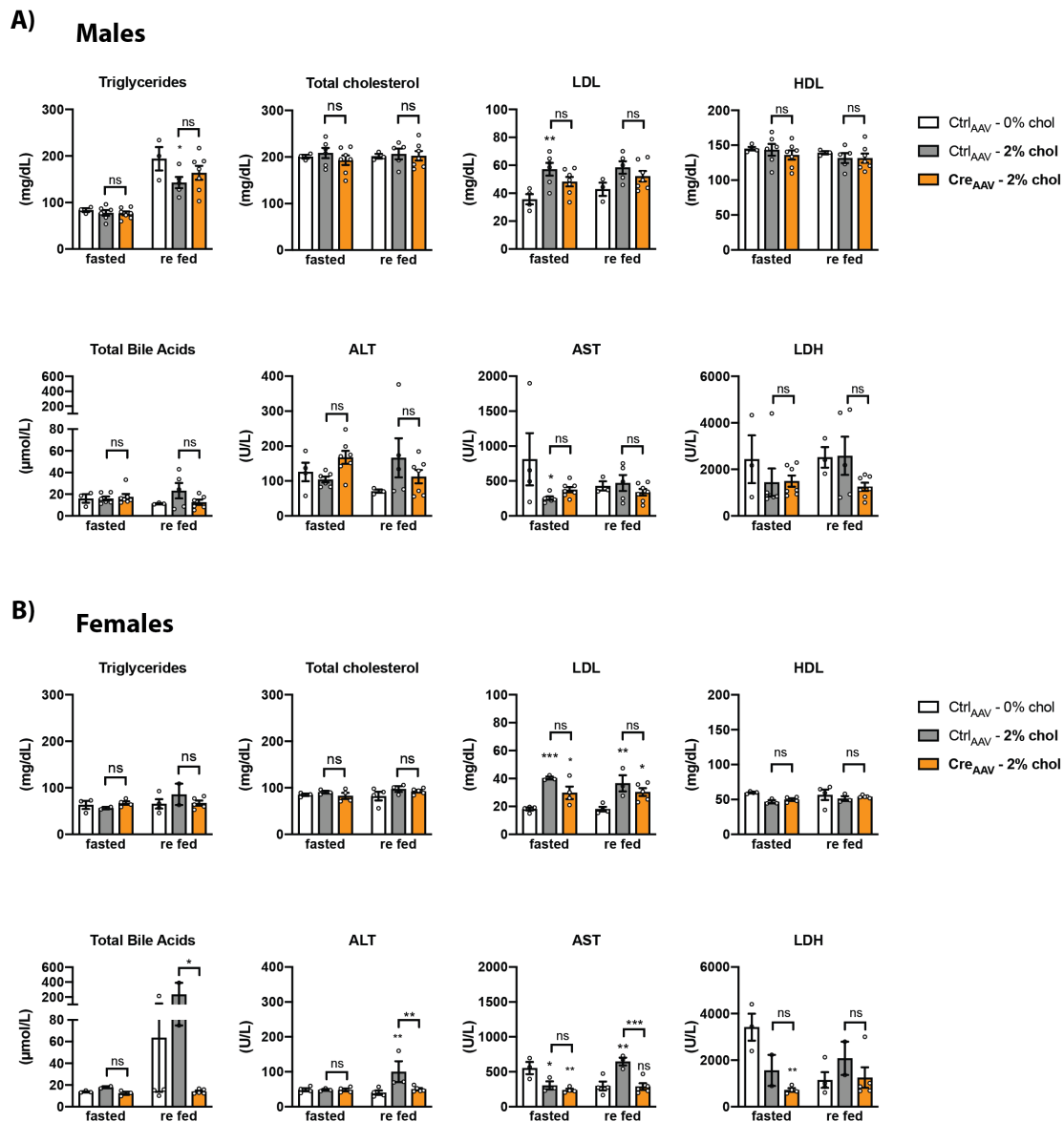
Figure 2.34: **High cholesterol challenge: Serum analysis**
Blood was collected by decapitation and processed for serum analysis using a colorimetric-based serum analyzer. Fasted: 8 hrs (ZT 7 to 15). Re fed: fasted for 8 hrs (ZT 4 to 12) and re fed for 4-5 hrs (ZT 12 to 16-17). A) Male mice (n=4-7). B) Female mice (n=3-5). (A-B) Levels of triglycerides, total cholesterol, low density lipoprotein (LDL), high density lipoprotein (HDL), total bile acids, alanine aminotransferase (ALT), aspartate aminotransferase (AST) and lactate dehydrogenase (LDH) are shown. Every dot represents one individual mouse. Data: mean $\pm$ SEM. Significance was determined by two-way ANOVA with Tukey´s multiple comparison test between different conditions. * P $\leq$ 0.05, ** P $\leq$ 0.01, *** P $\leq$ 0.001.

The serum lipoprotein profile of the SUMO-deficient Prox1(liver) mice was investigated further in collaboration with Prof. Dr. Susanna Hofmann. The fast phase liquid chromatography (FPLC) was done by Sebastian Cucuruz. Given the large amount of serum required for this analysis, it was performed using a serum pool from 4-5 different male mice per group; not enough material was left to analyze the serum from the female animals. An increase in the VLDL- and HDL-associated cholesterol was detected in response to the high cholesterol diet in the controls and the SUMO-deficient Prox1(liver) mice (Fig.2.35). A shift from LDL-associated cholesterol towards bigger particles was also detected in the groups fed the high cholesterol diet. A trend towards higher VLDL-, LDL- and HDL-associated cholesterol was observed in the SUMO-deficient Prox1(liver) mice in the re fed condition (Fig.2.35). These results contradict the colorimetric measurements obtained with our serum analyzer (Fig.2.34.A).

FPLC lipoprotein profile - 14 weeks after AAV injection and diet start

Males
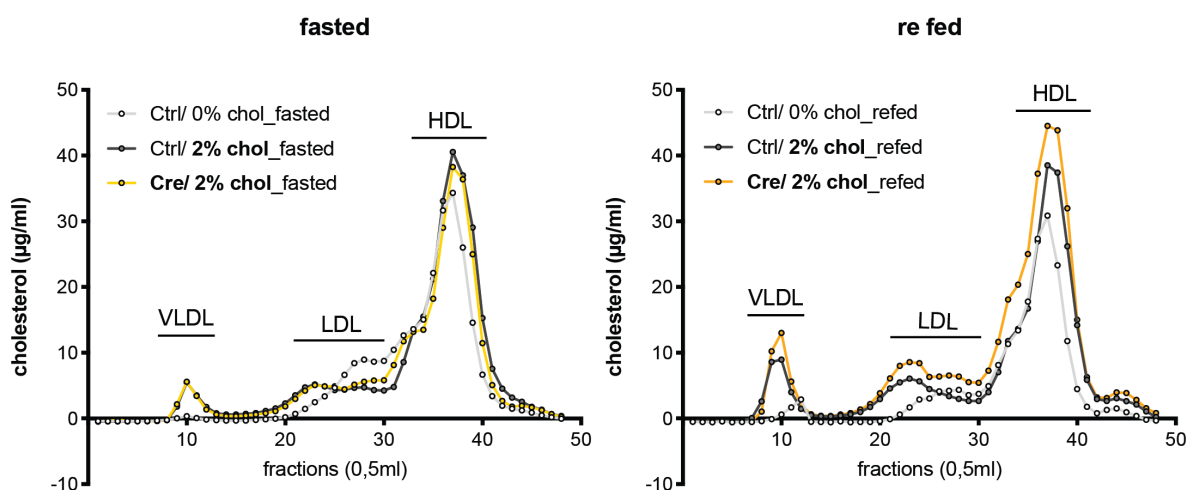
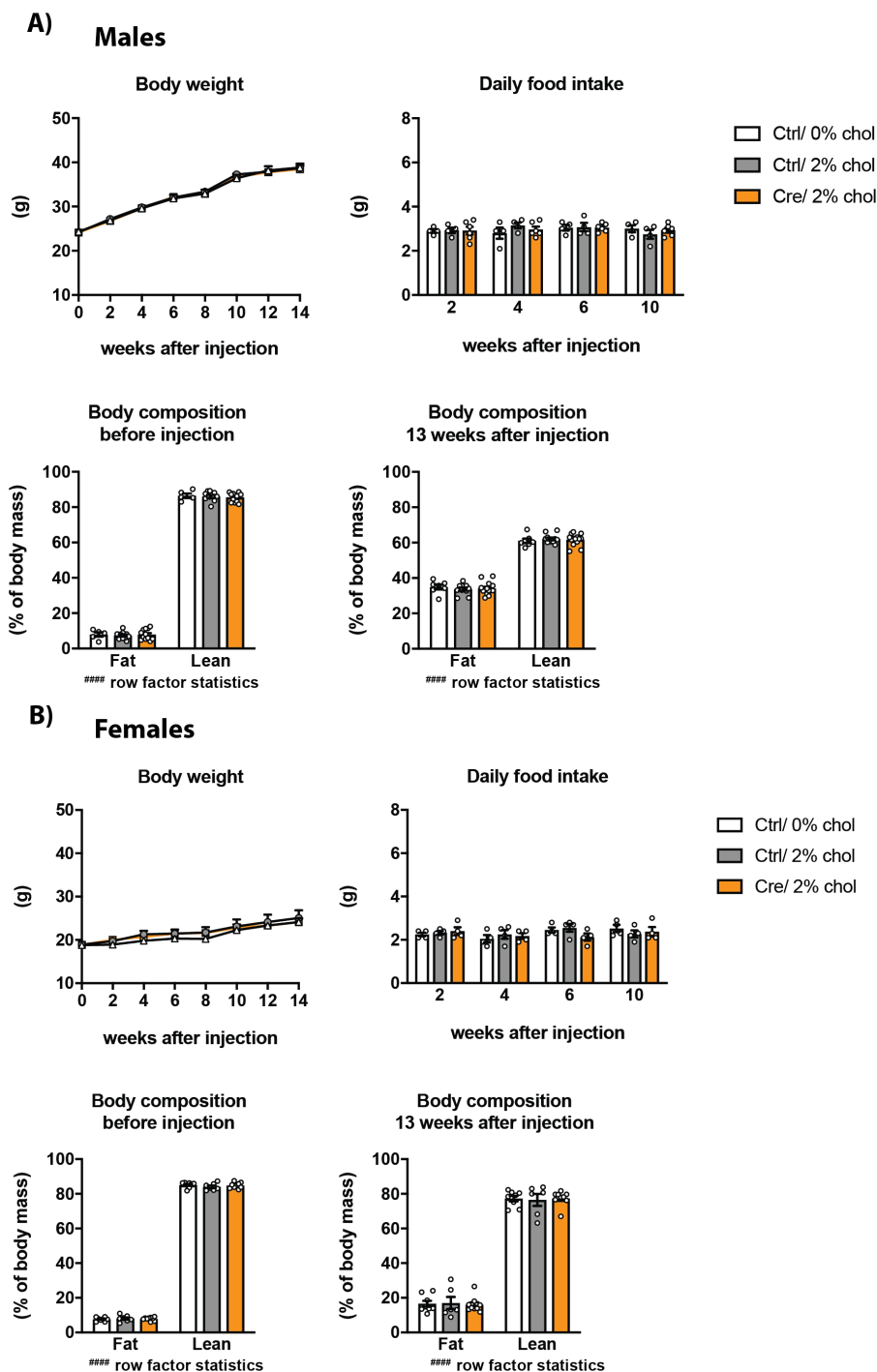Figure 2.35: **High cholesterol challenge: FPLC lipoprotein profile**
8 weeks-old (f/f) mice were injected with a control AAV (Ctrl_AAV) or with an AAV to overexpress Cre recombinase (Cre_AAV) and placed on a high cholesterol (2 %) or control (0 %) diet. 14 weeks after the AAV injection and the diet start the study was terminated. Fasted: 8 hrs (ZT 7 to 15). Re fed: fasted for 8 hrs (ZT 4 to 12) and re fed for 4-5 hrs (ZT 12 to 16-17). Blood was collected by decapitation, equal amounts of serum were pooled and analyzed by FPLC (male mice: n=4-5). Serum lipoprotein cholesterol profiles are shown.

After a discussion with Prof. Dr. Susanna Hofmann we concluded that the discrepancies between the serum analyzer and the FPLC profile are likely due to the preparation of the blood samples. For a proper FPLC analysis the blood serum should be centrifuged and handle according to a special protocol that was not implemented in this study. Thus, the impacts of Prox1 SUMOylation

on lipoprotein metabolism will be investigated further. The SUMO-deficient Prox1(liver) mice will be challenged with a high fat (45 %)/ high fructose (30 % w/v) diet to manipulate both fatty acid utilization and *de novo* synthesis; a standard chow diet will be used as control. The required protocols for a proper analysis of lipoprotein metabolism have been integrated. Due to limited time this study will be performed outside the scope of this thesis.

To further investigate the metabolism of the SUMO-deficient Prox1(liver) mice upon a high cholesterol challenge, the accumulation of triglycerides and cholesterol within the liver was analyzed. The triglyceride content in the liver was comparable between all groups, in both males and females (Fig.2.36.A-B). There was a remarkable accumulation of cholesterol in the control and the SUMO-deficient Prox1(liver) mice fed the high cholesterol diet as compared to the control animals fed the control diet, in both males and females (Fig.2.36.A-B). These results show that the animals retained the cholesterol overload within the liver. There were no differences in the accumulation of cholesterol between the control and the SUMO-deficient Prox1(liver) mice, in both males and females (Fig.2.36.A-B).
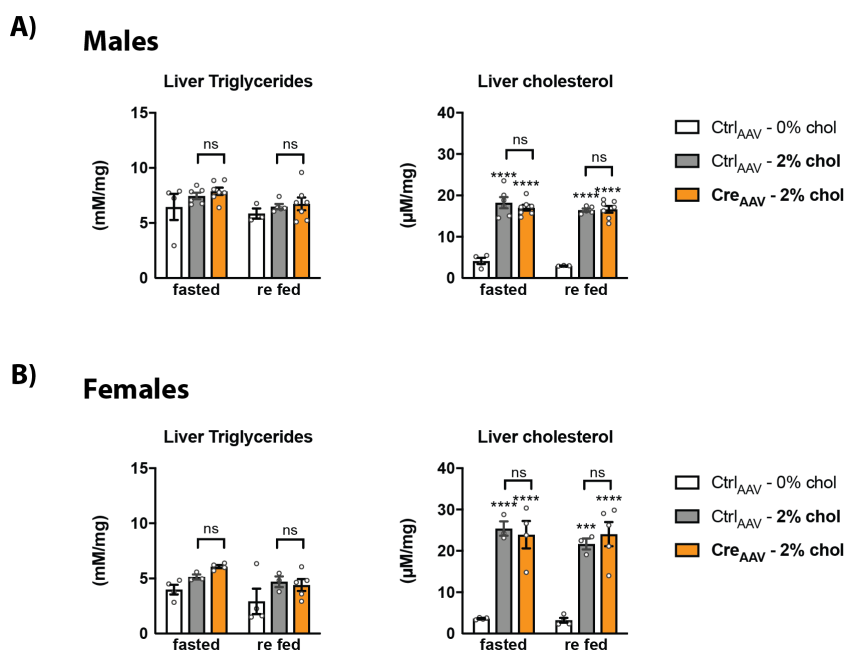
Figure 2.36: **High cholesterol challenge: Liver metabolites**
8 weeks-old (f/f) mice were injected with a control AAV (Ctrl_AAV) or with an AAV to overexpress Cre recombinase (Cre_AAV) and placed on a high cholesterol (2 %) or control (0 %) diet. A) Male mice (n=4-7). B) Female mice (n=3-5). (A-B) Colorimetric measurement of triglycerides and total cholesterol content within the liver. Every dot represents one individual mouse. Data: mean ± SEM. Significance was determined by two-way ANOVA with Tukey´s multiple comparison test between different conditions. *** $P \leq 0.001$, **** $P \leq 0.0001$.

The liver morphology was analyzed at the pathology core facility of our research center. No major morphological changes were observed between the control and the SUMO-deficient Prox1(liver) mice, in both males and females (Fig.2.37.A-B). The levels of lipid accumulation were higher in male mice fed the high cholesterol diet than compared to mice fed the control diet; no differences were detected between the control and the SUMO-deficient Prox1(liver) male mice (Fig.2.37.A). The levels of lipid accumulation were comparable between all groups in the female cohort (Fig.2.37.B).
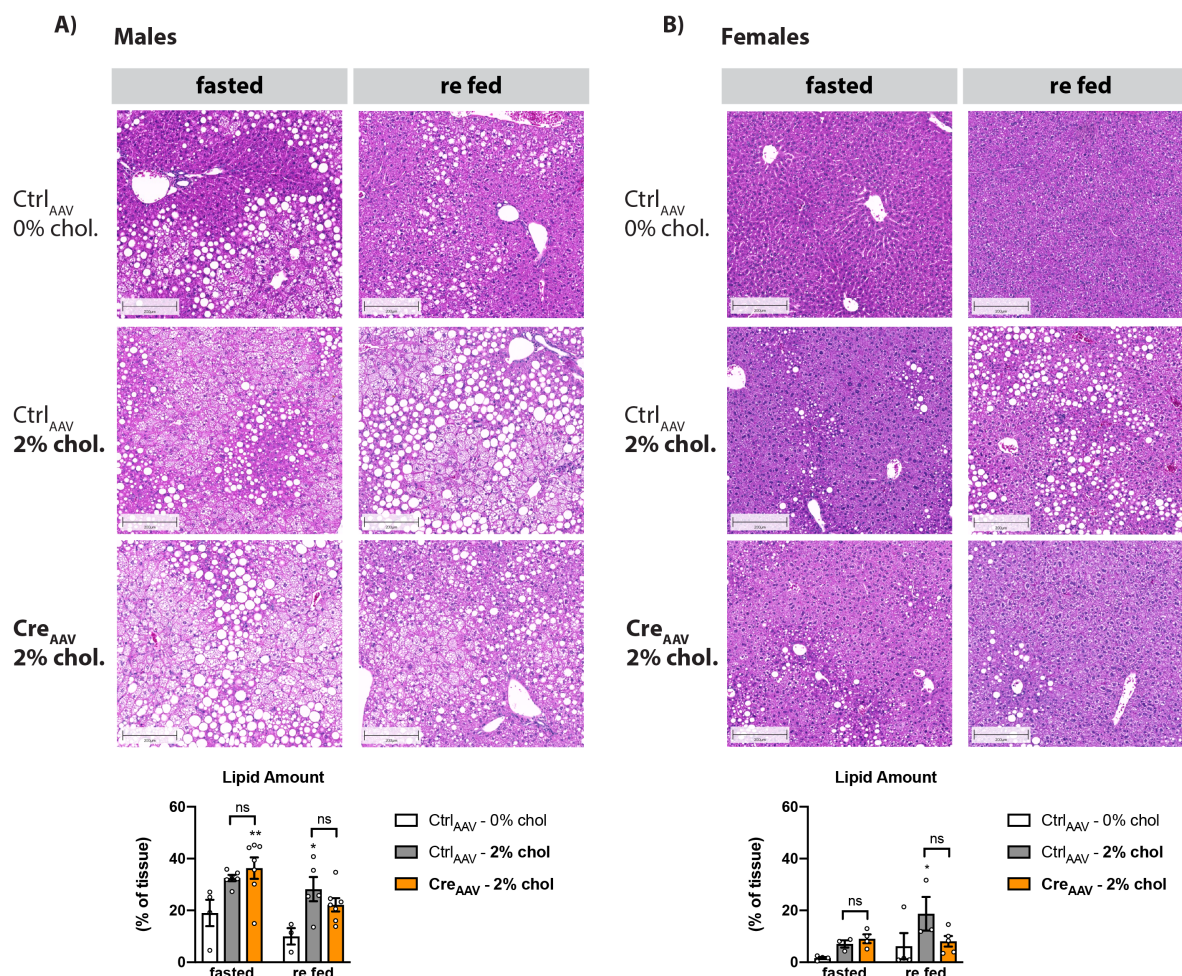
Figure 2.37: **High cholesterol challenge: Liver morphology**
8 weeks-old (f/f) mice were injected with a control AAV (Ctrl_AAV) or with an AAV to overexpress Cre recombinase (Cre_AAV) and placed on a high cholesterol (2 %) or control (0 %) diet. 14 weeks after the AAV injection and the diet start the study was terminated. Fasted: 8 hrs (ZT 7 to 15). Re fed: fasted for 8 hrs (ZT 4 to 12) and re fed for 4-5 hrs (ZT 12 to 16-17). A) Male mice (n=4-7). B) Female mice (n=3-5). (A-B) Liver morphology analyzed via hematoxylin and eosin staining. Representative images and quantification of lipid content are shown. Every dot represents one individual mouse. Data: mean $\pm$ SEM. Significance was determined by two-way ANOVA with Tukey´s multiple comparison test between different conditions. * $P \leq 0.05$, ** $P \leq 0.01$.

The results obtained with this work suggest that blocking Prox1 SUMOylation in hepatocytes has little effect on systemic metabolism even under a high cholesterol challenge. It appears that male and female SUMO-deficient Prox1(liver) mice coped with the high cholesterol diet to the same degree to the control animals. To make a final conclusion, it is necessary to assess the impact of blocking hepatic Prox1 SUMOylation at the transcriptional level under these experimental conditions. Thus, representative RNA samples from the male cohort will be sequenced by Novogene Europe and analyzed as described above. Due to limited time the RNA sequencing analysis will be performed outside the scope of this thesis.

It is clear that more research is required to clarify the function of Prox1 SUMOylation in the liver. Thus, a follow-up study designed to manipulate several aspects of lipid metabolism will be performed with the SUMO-deficient Prox1(liver) mice.

2.6 Prox1 SUMOylation in mouse models of fatty liver and NASH

Prox1 SUMOylation in diet induced obesity

As stated above, Prox1 has been identified as a regulator of lipid metabolism by us and others (Dufour et al., 2011), (Dittner, 2016) and (Armour et al., 2017). Knock-down of hepatic Prox1 results in higher lipid accumulation in the liver upon a high fat diet challenge when compared to control animals (Dittner, 2016). Thus, the behavior of Prox1 expression and SUMOylation upon a high fat diet challenge was investigated. Hopefully, a better comprehension of its regulation upon a metabolic burden will help us understand its regulatory function. For this, wild type C57BL/6N male mice were fed with a high fat (60 %) diet for eight weeks; a standard chow diet was used as a control. The animals were kept on a regular 12/12 hrs light/dark cycle. On the day of the study termination the liver samples were collected in the fasted and re fed state at ZT 15.

The levels of Prox1 SUMOylation were drastically decreased upon fasting in mice fed the chow diet but not in mice fed the high fat diet (Fig.2.38). The levels of Prox1 SUMOylation in the re fed state were comparable between both groups (Fig.2.38). The expression of Prox1 was not affected by the high fat diet (Fig.2.38). A blunted de-SUMOylation of Prox1 during fasting has previously been observed. Either when the fasting blood glucose levels are abnormally high (Fig.2.4) or when the circadian rhythm is not in concordance with the nutrient signaling (Fig.2.2). Mice fed the high fat diet showed higher fasting blood glucose levels as compared to the controls (Fig.2.38.B) The expression of BMAL1 was altered in mice fed the high fat diet, but only in the fasted state (Fig.2.38.C). The expression of CYP7a1 upon fasting was also affected in mice fed the high fat diet (Fig.2.38.C).

Glucose metabolism and the molecular oscillations driven by the circadian rhythm are disrupted by high fat diets (Hatori et al., 2012), (Chaix, Zarrinpar, et al., 2014) and (Chaix, T. Lin, et

al., 2019). The impacts of the high fat diet observed on metabolism and circadian rhythm could also be reflected on the Prox1 SUMO-switch. These results motivate us to further investigate the metabolic consequences of a high fat diet challenge in mice lacking Prox1 SUMOylation in hepatocytes.
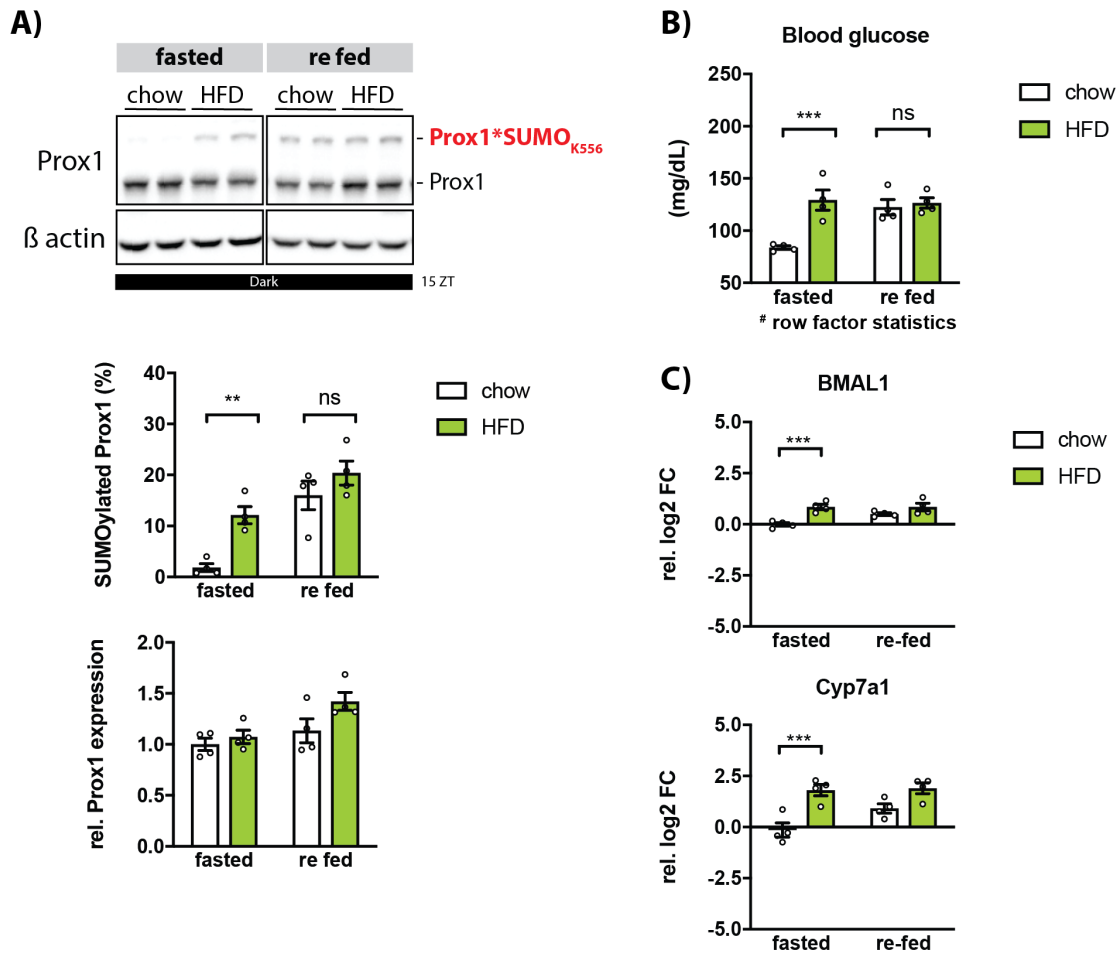
Figure 2.38: **The Prox1 SUMO-switch is affected by a high fat diet**
6 weeks-old C57BL/6N male mice were fed either a high fat (60 %) diet (HFD) or a standard chow diet for 8 weeks. Fasted: Food was removed at ZT 7, tissues were collected 8 hrs later at ZT 15. Re fed: Mice were fasted for 8 hrs (ZT 4-12) for synchronization. Food was re-introduced at ZT 12, tissues were collected at ZT 15 (n=4). A) Liver lysates were analyzed by immunoblotting using an anti-Prox1 antibody; β actin was detected for input control. The quantification of SUMOylated Prox1 (%) and relative Prox1 expression are shown. B) Blood glucose levels. C) Expression analysis at the mRNA level by qPCR of BMAL1 and CYP7a1 in the liver, data presented as relative log2 fold change (FC) normalized to the housekeeping gene TBP. (A-C) Every dot represents one individual mouse. Data: mean $\pm$ SEM. Significance was determined by two-way ANOVA with Sidak´s multiple comparison test between different conditions. ** $P \leq 0.01$, *** $P \leq 0.001$. Row factor statistics: # $P \leq 0.05$.

Prox1 SUMOylation in mouse models for NASH

Loss of hepatic Prox1 promotes the accumulation of lipids in the liver (Dittner, 2016) and (Armour et al., 2017). In addition, Prox1 has been characterized as a master regulator of hepatocyte proliferation and migration during liver development and liver injury (Sosa-Pineda, Wigle, and Oliver, 2000), (Dudas et al., 2006) and (Kamiya et al., 2008). Thus, I hypothesize that hepatic Prox1 could also have a regulatory function in the context of liver damage and regeneration. Furthermore, I wonder whether the regulatory aspect of SUMO conjugation could be relevant in the development of liver fibrosis. To get a first line of evidence, the status of Prox1 SUMOylation was investigated in different mouse models for NASH, a condition where the steatotic liver is accompanied by the presence of inflammation and fibrosis.

First, a NASH model that relies on a choline and L-amino acid deficient (0.1% methionine) high fat (60%) diet (CDA-HFD) was analyzed. Choline is a precursor for *de novo* phosphatidylcholine synthesis and is required for triglyceride export via VLDL. Thus, the CDA-HFD results in an impaired lipid export from the liver to peripheral tissues, making the hepatocytes susceptible to oxidative stress and inflammation (Caballero et al., 2010). The CDA-HFD treatment is known to trigger a rapid progression of steatosis, fibrosis and impaired liver function; six weeks of treatment is enough to induce a strong NASH phenotype (Matsumoto et al., 2013). It is important to mention that the CDA-HFD model causes severe systemic effects and impaired body weight gain. A CDA-HFD study was conducted as part of a different project lead by Dr. Anne Loft. For this, six weeks-old C57BL/6N male mice were fed a CDA-HFD for eight weeks, a custom made diet was used as a control. The day of the study termination liver samples were collected in the *ad libitum* state; liver fibrosis (Fig.39.B), steatosis as well as increased levels of liver damage markers were confirmed (data not shown). The levels of Prox1 SUMOylation were drastically reduced in the mice fed the CDA-HFD as compared to the control animals; the expression of Prox1 at the protein level was mildly but significantly reduced in the fibrotic livers (Fig.2.39.A). Note the loss of body weight gain in the CDA-HFD fed mice (Fig.2.39.B).
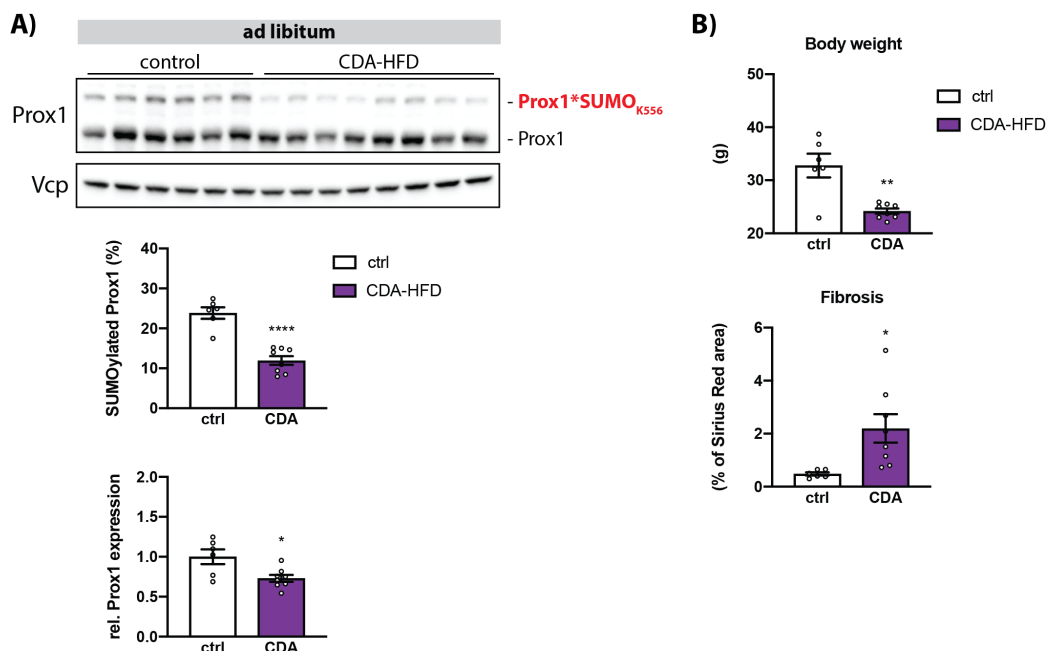
Figure 2.39: **Prox1 expression and SUMOylation is affected in the CDA-HFD NASH model**
6 weeks-old C57BL/6N male mice were fed either a choline and L-amino acid-defined deficient (0.1 % methionine) high fat (60 %) diet (CDA-HFD) or a control diet for 8 weeks. Liver samples were collected from mice fed *ad libitum* (n=6-8). The study was conducted by Dr. Anne Loft. A) Liver lysates were analyzed by immunoblotting using an anti-Prox1 antibody; Vcp was detected for input control. The quantification of SUMOylated Prox1 (%) and relative Prox1 expression are shown. B) Body weight and histochemical detection of fibrosis/collagen (% of Sirius Red area). (A-B) Every dot represents one individual mouse. Data: mean $\pm$ SEM. Significance was determined by two-tailed, unpaired t-test. * $P \leq 0.05$, ** $P \leq 0.01$, **** $P \leq 0.0001$.

Given that NASH develops most often in a scenario of insulin resistance and obesity, we next studied a mouse model that presents a high degree of liver fibrosis in the context of diet-induced obesity. For this, we relied on a high fructose, palmitate and cholesterol (FPC) diet. The FPC diet has been shown to induce liver steatosis and fibrosis accompanied by an increase in body weight gain, fasting blood glucose and plasma insulin (X. Wang et al., 2016). Dr. Anne Loft conducted a study where six weeks-old C57BL/6N male mice were fed the FPC diet for twenty weeks. The day of the study termination liver samples were collected in the *ad libitum* state; liver fibrosis, steatosis as well as increased levels of liver damage markers were confirmed (data not shown). In our hands, both the FCP and control diet fed mice had a comparable body weight gain (Fig.40.B). The levels of Prox1 SUMOylation were slightly but significantly decreased in the liver of the FPC diet fed mice (Fig.40.A). The loss of Prox1 SUMOylation showed a correlation with the degree of fibrosis (Fig.40.A). The expression of Prox1 at the protein level was significantly reduced in the FPC diet fed mice (Fig.40.A).

Figure 2.40: **Prox1 expression and SUMOylation is affected in the FPC NASH model**
6 weeks-old C57BL/6N male mice were fed either a high fructose (55 % glucose/45 % fructose solution), palmitate (4 % palmitic acid) and cholesterol (1.25 %) diet (FPC) or a standard chow diet for 20 weeks. Liver samples were collected from mice fed *ad libitum* (n=6-8). The study was conducted by Dr. Anne Loft. A) Liver lysates were analyzed by immunoblotting using an anti-Prox1 antibody; Vcp was detected for input control. The quantification of SUMOylated Prox1 (%), the correlation between SUMOylated Prox1 (%) and the degree of fibrosis (% of Sirius Red area) and relative Prox1 expression are shown. B) Body weight. (A-B) Every dot represents one individual mouse. Data: mean $\pm$ SEM. Significance was determined by two-tailed, unpaired t-test. Spearman correlation was computed with two-tailed P value. * $P \leq 0.05$, ** $P \leq 0.01$.

The status of Prox1 SUMOylation was also investigated in the STAM mouse model. In the STAM model streptozotocin (STZ) is administered to neonatal mice to induce pancreatic damage and consequent impairment of insulin secretion, which is then followed by a high fat diet challenge. As a result, mice develop liver steatosis and fibrosis accompanied by a state of insulin resistance after eight weeks. The STAM mouse model was engineered by SMC Laboratories Inc. (Fujii et al., 2013). Liver samples from ten weeks-old male STAM mice collected in the *ad libitum* state were obtained from SMC Laboratories Inc . The levels of Prox1 SUMOylation were drastically reduced in the STAM mice as compared to the control animals while the expression of Prox1 at the protein level was not affected (Fig.2.41.A).

Furthermore, Dr. Bilgen Ekim Üstünel from our laboratory division at the Heidelberg University Clinic performed a liver phospho-proteome analysis comparing the STAM mice vs control animals and high fat diet fed mice vs control animals hoping to identify changes in the phospho-proteome in the fibrotic and steatotic liver. Significant differences in the phosphorylation at four serine residues located inside and adjacent to the SUMO consensus motif at lysine 556 were identified (Fig.2.41.B; the SUMO consensus motif is marked in red). Phosphorylation of residues Ser539, Ser557 (within the SUMO consensus motif), Ser566 and Ser69 appear to be hyper-phosphorylated in the fibrotic liver as compared to the controls; no significant changes were detected in the steatotic liver (Fig.2.41.B).

A)

B)

Serine residue	Sequence Phospho	Fold Change		p-Value	
		STAM vs. Control	HFD vs. Control	STAM vs. Control	HFD vs. Control
539	MSSHHLSHHPC**S**PAHPPSTAEGLSLSL**IK**[12]Phospho	2.46	3.23	0.012	0.174
179	GMSH**S**PSVALRGNENER[5]Phospho	0.13	1.80	0.216	0.629
291/295	AQDSVGR**S**DNEMCELDPGQFIDR[4]Phospho[8]Phospho	0.77	0.43	0.457	0.061
557	**SE**CGDLQDMSDISPYSGSAMQEGLSPNHLK[1]Phospho	2.00	1.10	0.010	0.883
566	**SE**CGDLQDM**S**DISPYSGSAMQEGLSPNHLK[10]Phospho	2.00	1.10	0.010	0.883
569	**SE**CGDLQDMSDI**S**PYSGSAMQEGLSPNHLK[13]Phospho	1.90	1.09	0.011	0.876

Figure 2.41: **Prox1 SUMOylation is affected in the STAM NASH model**
Samples from 10 weeks-old STAM male mice fed *ad libitum* were obtained from SMC Laboratories Inc. (n=5). A) Liver lysates were analyzed by immunoblotting using an anti-Prox1 antibody; Vcp was detected for input control. The quantification of SUMOylated Prox1 (%) and relative Prox1 expression are shown. B) Liver phospho-proteome analysis from STAM or high fat diet (HFD) fed mice vs control performed by Dr. Bilgen Ekim Üstünel at the Heidelberg University Clinic; Prox1 SUMO consensus motif around lysine residue 556 is marked in red. (A) Every dot represents one individual mouse. Data: mean $\pm$ SEM. Significance was determined by two-tailed, unpaired t-test. *** P $\leq$ 0.001.

Considering these observations I propose that Prox1 could also be involved in some aspects of liver fibrosis and regeneration. It will be interesting to investigate whether Prox1 SUMOylation has an impact in the development and severity of liver damage. For this, the metabolism of the SUMO-deficient Prox1(liver) mice under a NASH inducing protocol could be analyzed. It is also possible that Prox1 SUMOylation participates in the regulation of hepatocyte proliferation after liver injury. Therefore, I suggest to investigate the regeneration rate in the SUMO-deficient Prox1(liver) mice upon liver injury.

2.7 Consequences of Prox1 SUMOylation

The conjugation of a SUMO moiety to a target protein can result in multiple and cell specific functional outcomes. By generating or disrupting binding sites for interacting partners, SUMOylation can affect the function of a protein. For example: it can influence changes in cellular localization, protein stability and modulate the interaction with functional binding partners. In a previous project lead by Prof. Dr. Frauke Melchior and conduced by myself, we identified that SUMOylation does not affect the nuclear localization of Prox1 nor its binding affinity to chromatin *in vitro* (Alfaro N., 2016). To further investigate the consequences of Prox1 SUMOylation at the molecular level we aim to identify SUMO-dependent partners of Prox1.

Tools to identifying SUMO-dependent interaction partners of Prox1

Prox1 seems to act as a transcriptional co-regulator in the liver. Whether SUMO conjugation influences the binding capacity of Prox1 is an open question. We had previously optimized a nuclear protein extraction protocol that allowed us to purify and maintain SUMOylated Prox1 from HEK293T cell lysates (Alfaro N., 2016). A similar protocol was applied to purify Prox1 from liver samples of control and SUMO-deficient Prox1(liver) male mice fed a standard chow diet (section 2.4). Three representative samples of mice injected with either the Ctrl_AAV or with the Cre_AAV, in both the fasted and re fed conditions, were subjected to a protein nuclear extraction protocol followed by a Prox1 immunoprecipitation. To assess the quality of the immunoprecipitation process, one representative sample from both the control (Ctrl_AAV) and the SUMO-deficient Prox1(liver) (Cre_AAV) mice in the re fed state were analyzed by immunoblotting.

Prox1 Immunoprecipitation: Ctrl_AAV vs Cre_AAV
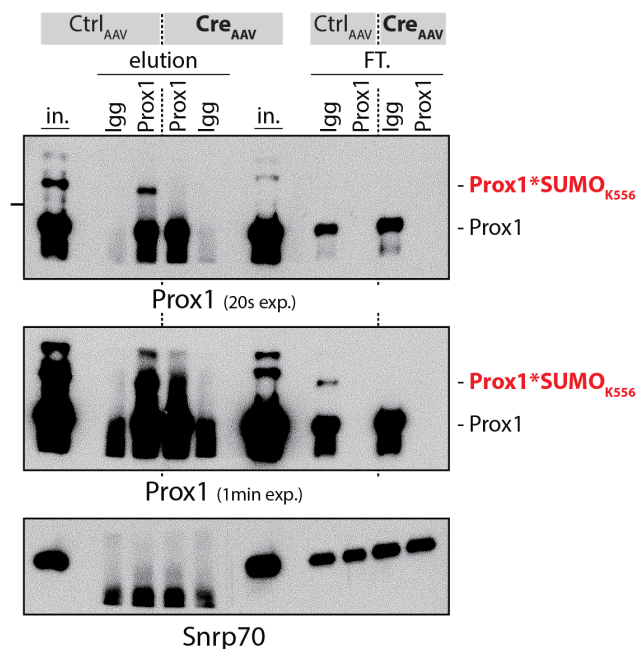
Figure 2.42: **Purification of Prox1 for the analysis of SUMO-dependent interaction partners**
Representative liver samples from control (Ctrl_AAV) and SUMO-deficient Prox1(liver) (Cre_AAV) mice in the fasted and re fed state were processed for nuclear protein extraction (n=3). The total nuclear protein concentration was determined using a BCA protocol and 50 µg total nuclear protein samples were used for the Prox1 immunoprecipitation. Samples were pre-cleared and incubated with either an anti-Prox1 (Millipore-07 537) or an anti-rabbit Igg (Cell Signaling Technology-2729) control antibody together with 20 µl Protein G Dynabeads. One sample of each group in the re fed state was analyzed by immunoblotting using an anti-Prox1 antibody; Snrp70 was detected for input control. in. = input (1 %); Elution (20 %); FT. = flow-through (0.4 %).

The Prox1 isolation protocol was successful; note that a portion the SUMOylated species of Prox1 running at 120 kDa was conserved in the control samples (Fig.2.42). These samples will be subjected to a mass spectrometry analysis in collaboration with Dr. Christina Ludwig at the Bavarian Center for Biomolecular Mass Spectrometry, with the aim of identifying SUMO-dependent interaction partners of Prox1. We will also assess whether the conjugation of Prox1 with SUMO is affecting other post-translational modifications on Prox1. Due to time restrictions, the results from this analysis will not be presented in this thesis.

2.8 Tools to identify SUMO-dependent transcription targets of Prox1

Prox1 is a highly efficient SUMO target in the mouse liver and has been identified as a key factor modulating hepatic lipid metabolism (Dittner, 2016) and (Armour et al., 2017). Nevertheless, the consequences of blocking Prox1 SUMOylation in the adult liver remain unknown. It is evident that this molecular switch is relevant for metabolism as it is tightly and rapidly regulated in response to nutrient availability. Therefore, the function of hepatic Prox1 SUMOylation will be investigated further in our laboratory.

Prox1 knock-down in the K556R Prox1 knock-in mouse model

One way to identify the regulatory function of SUMO conjugation on Prox1 is to compare the liver transcriptome of mice expressing the SUMO-deficient Prox1 variant vs mice lacking hepatic Prox1. Thus, it was investigated whether the AAV_LP1_Prox1-miRNA construct used previously in our laboratory to knock-down Prox1 in wild-type mice (Dittner, 2016) could also block the expression of Prox1 in our SUMO-deficient K556R Prox1 Knock-in animals. A pilot experiment was conducted where eight weeks-old male K556R Prox1 (f/f) mice were injected with either PBS, a non-specific miRNA control construct (NC-miRNA) or with the AAV_LP1_Prox1-miRNA (Prox1-miRNA) vector. The Prox1-miRNA construct was able to efficiently down-regulate the expression of Prox1 at the protein level in K556R Prox1 (f/f) mice. With this tool we will be able to take an integral approach to clarity the function of Prox1 and its regulation by SUMOylation in the liver.
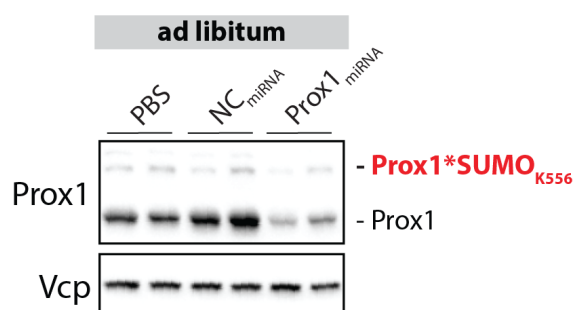
Figure 2.43: **Prox1 knock-down in the SUMO-deficient K556R Prox1 knock-in mouse model**
8 weeks-old K556R Prox1 (f/f) male mice were injected with PBS, a non-specific miRNA control AAV (NC-miRNA) or with an AAV coding for a miRNA targeting Prox1 (Prox1-miRNA). Liver tissue samples were taken 3 weeks later from mice fed *ad libitum* (n=4). Liver lysates were analyzed by immunoblotting using anti-Prox1 and anti-Cre antibodies; Vcp and β actin were detected for input control.

Discussion

Hepatocytes are extraordinary cells that are able to sense physiological cues and orchestrate metabolic programs to maintain energy homeostasis. The regulation of metabolic processes upon changes in nutrient availability is modulated by a network of signal transduction pathways. These signals are mediated in part by dynamic post-translational modifications that control the activity of participating enzymes and regulatory factors. This signaling system also translates into transcriptional changes for a long term adaptation of cellular metabolism. SUMOylation is an important mechanism for the regulation of transcription. For example, SUMO conjugation can influence the DNA binding affinity, the nuclear localization or the interaction partners of target transcription factors (Treuter and N. Venteclef, 2011) and (Talamillo et al., 2020).

To identify new components of the signal transduction pathway controlling hepatic metabolism, our laboratory analyzed the mouse liver SUMO-proteome during fasted and fed conditions (Becker, 2012) and (Becker et al., 2013). The transcription factor Prox1 was identified as a nutrition-dependent SUMO target (Becker, 2012). Hepatic Prox1 has been implicated in the control of energy homeostasis acting mainly as negative regulator of nuclear receptors modulating bile acid synthesis, reverse cholesterol transport, detoxification, glucose and lipid metabolism (Qin et al., 2004), (Stein et al., 2014), (Azuma et al., 2011), (Charest-Marcotte et al., 2010), (Ouyang et al., 2013), (Armour et al., 2017) and (Dittner, 2016). In addition, Prox1 has been identified as a member of the peripheral molecular clock in the liver (Dufour et al., 2011) and (Takeda and Jetten, 2013).

In the course of this work, the function of the SUMO-switch on hepatic Prox1 was investigated. We hypothesize that the transcriptional activity of Prox1 could be modulated by SUMOylation in response to changes in nutrient availability. It is possible that SUMO conjugation influences the interaction of Prox1 with co-regulators and/or transcription factors to promote an efficient energy metabolism in the liver. For a schematic representation of the project hypothesis see Fig.3.1.
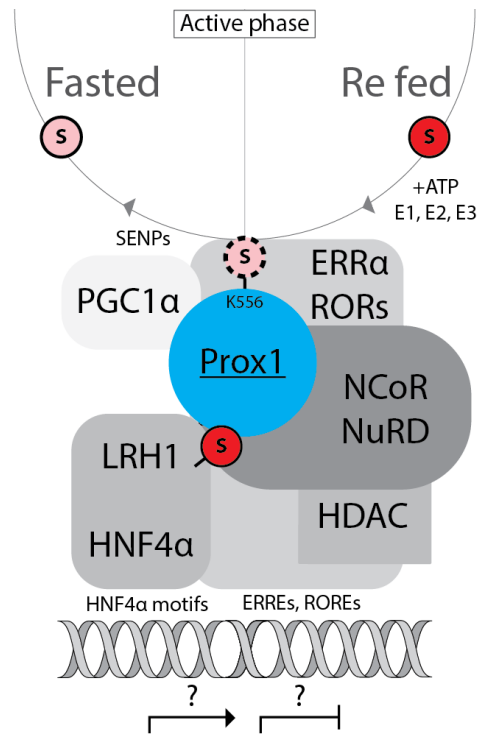
Figure 3.1: **Proposed model: The Prox1 SUMO-Switch**
The Prox1 SUMO-switch in hepatocytes could be modulated by nutrient availability in a diurnal manner. SUMO conjugation could influence the interaction of Prox1 with transcription factors and/or chromatin modifier complexes. The function of the Prox1 SUMO-switch in hepatocytes is currently unknown.

3.1 Prox1 SUMOylation is regulated by metabolic and diurnal signals in vivo

We have previously identified Prox1 as a highly efficient SUMO target in the mouse liver. In this work we demonstrated that its conjugation is influenced by food availability; Prox1 SUMOylation is blunted in the liver of fasted mice, but it is promoted during feeding. The nutrition-dependent SUMO-switch on Prox1 is highly responsive in the active phase of the mice, which comprises the dark phase. However, the conjugation of Prox1 with SUMO is not affected by the nutritional state of the animals during their rest (light) phase. These observations suggest that the regulation of Prox1 SUMOylation could be mediated not only by feeding and fasting signals but also by a factor that oscillates through the 12/12 hrs dark/light cycle. To investigate whether a diurnal component influences hepatic Prox1 SUMOylation, the peripheral clock driven by food was uncoupled from the central rhythm set by light. This was achieved by entraining mice to consume their food during the light phase using a time restricted feeding (TRF) protocol. The conjugation of Prox1 with SUMO was promoted by food intake while the levels of Prox1 SUMOylation were not affected upon fasting in the entrained animals.

The Prox1 SUMO-switch showed a similar behavior in mice entrained to eat during the active (dark) phase; the levels of Prox1 SUMOylation were promoted by food intake but not affected upon fasting.

In both studies, the conjugation of Prox1 with SUMO was induced by feeding signals independent of light, suggesting that Prox1 SUMOylation is influenced by the peripheral clock in the liver. The loss of Prox1 SUMOylation upon fasting was not detected in animals entrained to eat during the light or the dark phase. If the de-SUMOylation of Prox1 was solely dependent on fasting signals, the loss of Prox1 SUMOylation would be expected in fasted animals independently of the TRF protocol, at least during the dark phase. However, this is not the case.

Through the course of this work, I observed a correlation between loss of Prox1 SUMOylation and low fasting blood glucose levels. This effect was not observed after an overnight fasting period (Fig.2.2.B). Whether this is due to the length of the fasting period or due to the transition into the light phase remains to be elucidated. It is important to point out that the overnight fasted mice losing Prox1 SUMOylation also presented a strong S6K1 phosphorylation (Fig.2.2.B). The reason behind this observation also requires further investigation. In the same line, Prox1 SUMOylation is maintained in the liver of mice with high fasting blood glucose levels, as observed in mice entrained to eat during the dark phase. Mice on a TRF protocol have been shown to synchronize metabolic processes to anticipate and prepare for an optimal energy homeostasis (Hatori et al., 2012) and (Chaix, T. Lin, et al., 2019). It is probable that mice on the TRF protocol during the dark phase were able to maintain constant blood glucose levels even in the absence of food due to improved coordination of metabolic regulators.

Therefore, I suggest that the SUMO-switch on hepatic Prox1 is regulated by the integration of metabolic and diurnal cues. Further investigation on the function of hepatic Prox1 and its regulation by SUMOylation should be conducted in concordance with the circadian rhythm of the model organism in use.

3.2   Crosstalk between phosphorylation and SUMOylation on Prox1

According to our SUMO-proteome analysis, only few proteins changed their SUMOylation status upon changes in nutrient availability (Becker, 2012). Therefore, it is likely that the regulation of SUMO conjugation is mediated by alterations on Prox1 itself rather that changes in the SUMO-loading machinery. For example, it is well known that SUMO conjugation can be influenced by phosphorylation (X.-J. Yang and Grégoire, 2006), (Mohideen et al., 2009), (Desterro, Rodriguez, and Hay, 1998) and (J.-Y. Lin, Ohshima, and Shimotohno, 2004). A published phospho-proteome analysis of the mouse liver (Wilson-Grady, Haas, and Gygi, 2013) and data obtained in our laboratory (Dittner, 2016) indicate that Prox1 is indeed differentially phosphorylated in the fasted and re fed

state. For a schematic summary of these phosphorylation sites see Fig.3.2.A.

Furthermore, a circadian phospho-proteome of the mouse liver revealed that Prox1 is phosphory-lated in a circadian manner on serine residue 199 (S119) (Fig.3.2.B) (Robles, Humphrey, and Mann, 2017). Prox1 was also identified as a potential target of the Akt pathway which activity peaks during the active phase of the mice (Robles, Humphrey, and Mann, 2017).
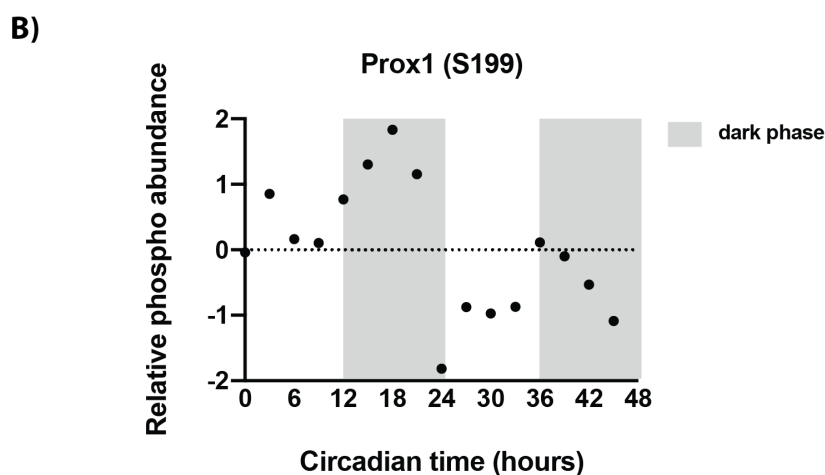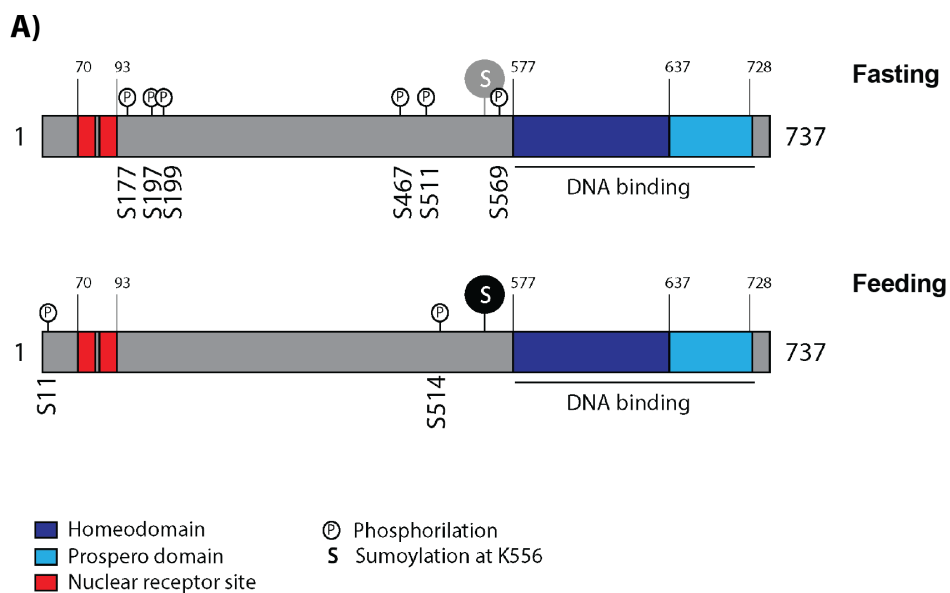
Figure 3.2: **Possible crosstalk between phosphorylation and SUMOylation on Prox1**
A) Schematic representation of Prox1 serine residues that are differentially phosphorylated during fasting (top) and feeding (bottom) according to (Wilson-Grady, Haas, and Gygi, 2013) and (Dittner, 2016). Functional domains are highlighted; S: SUMOylation at lysine residue 556 (K556). Figure adapted from (Elsir, Eriksson, et al., 2010). B) Circadian phosphorylation at serine residue 199 (S199) according to (Robles, Humphrey, and Mann, 2017).

It is possible that the phosphorylation of residues close to the SUMO consensus motif at lysine 556 blunt, directly or indirectly, the conjugation of Prox1 with SUMO in response to fasting cues. Furthermore, the oscillating phosphorylation of serine 199 could be an effect of the diurnal factor regulating Prox1 SUMOylation. I hypothesize that independent metabolic and diurnal signals converge on Prox1 as phosphorylation events to coordinate the activity of Prox1 via SUMOylation-mediated responses. Converging signals mediating signal transduction is a mechanism proposed and investigated for decades, for example (Roenneberg and Merrow, 1998) and (Robles, Humphrey, and Mann, 2017). The crosstalk between phosphorylation and SUMOylation on Prox1 is currently been investigated in our laboratory.

3.3 Upstream signals regulating Prox1 SUMOylation in vitro

We have identified a nutrition-dependent SUMO-switch on Prox1 in the mouse liver. The levels of hepatic Prox1 SUMOylation are drastically reduced when mice have no access to food. Thus, it appears that Prox1 is either actively de-SUMOylated or its conjugation with SUMO is blocked in response to fasting signals. There are multiple possible mechanisms for how the conjugation of Prox1 with SUMO could be mediated upon fasting cues: For example: A) A specific SENP may be activated and/or relocated. B) The interaction of Prox1 with a binding partner could be lost making the modified lysine residue accessible for SENPs. C) Its interaction with a binding partner blocking the main SUMOylation site could be induced. D) Its interaction with the SUMO-loading machinery could be impaired. Given all the possible scenarios, identifying the upstream regulatory signals represents a first step towards clarifying the mechanisms driving the regulation of Prox1 SUMOylation. Therefore, the response of the Prox1 SUMO-switch to an array of molecules mimicking key fasting signals was investigated in polarized primary hepatocytes.

The conjugation of Prox1 with SUMO was inhibited in a time dependent manner by AICAR, an AMPK activator. The loss of Prox1 SUMOylation upon AICAR treatment was proportional to the increase in AMPK activity. Thus, the regulatory role of AMPK on the Prox1 SUMO-switch was investigated further. Nevertheless, the conjugation of Prox1 with SUMO was not affected by a more selective and potent AMPK activator, the MK-8722 compound (Makhnevych et al., 2007). The status of the Prox1 SUMO-switch was also investigated in AMPK knock-out MEFs. Nevertheless, Prox1 is not equally modified in MEFs and hepatocytes.

Given the inconclusive results, more investigation is required to elucidate whether the regulation of Prox1 de-SUMOylation is mediated via the AMPK pathway.

The conjugation of Prox1 with SUMO was also inhibited by chenodeoxycholic acid (bile acid) in a time dependent manner. Prox1 has been identified as a transcriptional regulator of cholesterol and bile acid metabolism (Armour et al., 2017) and (Dittner, 2016). In addition, bile acids are the

mediators of the negative feedback loop controlling its own synthesis. Follow-up experiments are being conducted to investigate whether the Prox1 SUMO-switch is part of this regulatory feedback mechanism.

AMPK expression, nuclear localization and kinase activity are subjected to circadian regulation in the mouse liver: The expression of the AMPKβ2 sub-unit oscillates through the day with a maximal expression at the end of the light and beginning of the dark phase. In line, AMPK nuclear localization peaks during the transition from the light to the dark phase (Lamia et al., 2009). Bile acid synthesis is a process that is also subjected to circadian regulation. The expression of key enzymes, such as Cyp7a1, are under the control of core clock components; Cyp7a1 expression peaks in the mouse liver at the end of the light phase (Le Martelot et al., 2009). In addition, the activation of AMPK by chenodeoxycholic acid has been described (Noh et al., 2011). Thus, I hypothesize that the conjugation of Prox1 with SUMO could be regulated by the convergence of higher concentrations of bile acids and AMPK activation. If true, the Prox1 SUMO-switch could be a mechanism to maintain cholesterol and bile acid homeostasis in a fasting state where bile acids have accumulated in anticipation to food intake. This hypothesis would also fit with the unresponsive SUMO-switch observed during the light phase.

The status of Prox1 SUMOylation in response to key feeding signals was also investigated. Unexpectedly, Prox1 SUMOylation was rapidly impaired by insulin in polarized primary hepatocytes but not in liver slices. Thus, the influence of insulin in the regulation of the Prox1 SUMO-switch remains to be elucidated. To further investigate the potential mediators of the Prox1 SUMO-switch, the mTORC1 complex was inhibited with rapamycin. However, Prox1 SUMOylation was not affected upon an acute mTORC1 inhibition. The role of the mTORC1 complex in the regulation of Prox1 SUMOylation requires further investigation. It is important to mention that upon a prolonged rapamycin treatment of 24 hrs, the conjugation of Prox1 was lost and the total Prox1 protein levels were increased (Fig.2.14.B). It has been published that Prox1 is down-regulated at the protein level upon a $24 \geq$ hrs rapamycin treatment using similar concentrations in human hepatoma HepG2 cells (H. S. Kwon et al., 2004). This is not observed in polarized primary hepatocytes.

Giving the diurnal responsiveness of the Prox1 SUMO-switch, it is possible that glucocorticoid hormones participate in its regulation. Follow-up studies in multiple *in vitro* systems are been conducted to investigate this further.

Working with SUMO-modified proteins in vitro

Multiple studies have relayed on *in vitro* systems to investigate the function of Prox1 in hepatocytes (Qin et al., 2004), (Charest-Marcotte et al., 2010), (Dufour et al., 2011), (Azuma et al.,

2011), (Takeda and Jetten, 2013), (Ouyang et al., 2013) (S. Kwon et al., 2016) and (Alfaro N., 2016). However, the complex network regulating the conjugation of Prox1 with SUMO observed *in vivo* makes it clear that its function is tightly modulated in the liver. In line with these observations, the modification pattern of Prox1 detected in the mouse liver is not easily conserved *in vitro* (Fig.2.9.C). In the non-tumor cell line AML12, a dominant modified species of Prox1 was detected at 180 kDa. However, mono-SUMOylation of hepatic Prox1 at lysine residue 556 was detected at 120 kDa (Fig.2.16.A). The dynamic 120 kDa Prox1 species was also replaced by the 180 kDa variant in primary hepatocytes cultured as a monolayer, but restored in polarized primary hepatocytes. These results suggest that the conjugation of a single SUMO moiety at lysine residue 556 is me-diated intrinsically by hepatocytes, but requires a complex cellular system closely resembling the cellular state of hepatocytes within the liver.

Post-translational modifications generate a dynamic system to translate multiple signals into functional outcomes. This system is tightly controlled in living organisms and it is not surprising that signals get altered *in vitro*. The conjugation of Prox1 with SUMO in hepatocytes is a clear example. This technical challenge should be taken into consideration when investigating the regulation and function of post-translational modifications *in vitro*.

3.4   Blocking the conjugation of Prox1 with SUMO in the adult liver

The characterization of the conditional SUMO-deficient (K556R) Prox1 knock-in mouse model demonstrated that Prox1 is highly modified by a single SUMO moiety at lysine residue 556 in hepatocytes. Blocking the conjugation of Prox1 with SUMO in the liver of young male mice had no effects on systemic glucose and lipid metabolism. In line, the loss of Prox1 SUMOylation in hepatocytes had very subtle changes in the liver transcriptome of young male mice. According to a differential expression analysis, losing Prox1 SUMOylation affected the expression of sixteen genes during fasting and one gene during re feeding. The occupancy of Prox1 at the promoter of differentially expressed genes was analyzed using the Cistrome Data Browse (Mei et al., 2017) and (Zheng et al., 2019). Prox1 has been located at the promoter region of the following genes affected in the fasted state: Nt5e, Dpy19I3, Ces4a, Tbc1d30, Insig2, Hsb3b2 and Tubb2a (Armour et al., 2017). Prox1 was also detected at the promoter region of the only gene affected in the re fed state, Atxn1 (Armour et al., 2017). According to the literature some of these genes are contributing to hepatic lipid homeostasis. However, further research is required to clarify the relevance of these transcriptional changes on metabolism.

Considering that Prox1 is a highly efficient SUMO target in hepatocytes and that its conjugation is heavily influenced by food availability, it is reasonable to think that the Prox1 SUMO-switch participates in the regulation of hepatic metabolism. To investigate this further, young male and

female mice lacking Prox1 SUMOylation in hepatocytes were challenged with a high choles-
terol (2 %) diet. Blocking Prox1 SUMOylation had no impact on systemic glucose handling or
body composition. No significant changes in circulating triglycerides, cholesterol, LDL, HDL
or total bile acids were detected. Young male and female mice lacking Prox1 SUMOylation in
hepatocytes metabolized the cholesterol overload to the same degree as the control animals
and showed no signs of liver damage. These results suggest that hepatic Prox1 SUMOylation is
not essential for the maintenance of cholesterol homeostasis in young male and female mice.
Thus, the relevance of the Prox1 SUMO-switch is being investigated in alternative scenarios of
metabolic dysfunction.

It is clear that Prox1 regulates important aspects of lipid metabolism in the liver (Armour et al.,
2017) and (Dittner, 2016). In addition, an altered Prox1 SUMO-switch was detected in male mice
fed a high fat (60 %) diet where the conjugation of Prox1 with SUMO was not inhibited by food
deprivation. Therefore, the regulatory function of hepatic Prox1 SUMOylation will be addressed
at multiple control levels of lipid metabolism including *de novo* synthesis, absorption, storage,
metabolism and secretion. For this, the SUMO-deficient Prox1(liver) mice will be challenged
with a high fat (45 %) high fructose (30 % w/v) diet. Increasing both dietary fat content and
carbohydrate load will inflict pressure at multiple pathways regulating energy homeostasis.

3.5   Towards identifying SUMO-dependent interaction partners of Prox1

Studies have demonstrated that hepatic Prox1 interacts with multiple nuclear receptors to mod-
ulate their transcriptional activity. Prox1 has been identified as a recurrent member of the re-
pression complexes NuRD and NCoR. Prox1 mediates the recruitment of histone modifying en-
zymes such as the histone demethylase LSD1 and the histone deacetylases HDAC2 and HDAC3
to regulate transcription (Ouyang et al., 2013) and (Armour et al., 2017). Prox1 also shows a com-
petitive function with the co-activator PGC-1α (Charest-Marcotte et al., 2010). We hypothesize
that the interaction affinity of Prox1 with nuclear receptors and/or co-regulator complexes could
be modulated by SUMOylation in response to nutrient availability. We are currently investigat-
ing whether hepatic Prox1 has SUMO-dependent interaction partners under fasting and feeding
conditions. For this, the wild type and the SUMO-deficient K556R Prox1 variants were purified
from liver tissue samples of fasted and re fed mice collected in the dark phase. If the mass
spectrometry analysis is optimal we will also be able to assess whether the conjugation of Prox1
with SUMO is affecting other post-translational modifications on Prox1.

3.6 Research opportunities

Prox1 SUMOylation in liver fibrosis and regeneration

The activity of hepatic Prox1 is required for a proper lipid metabolism (Dittner, 2016) and (Armour et al., 2017). In addition, Prox1 is an essential regulator of hepatocyte proliferation and migration during liver development; hepatocytes lacking Prox1 fail to migrate from the liver bud (Sosa-Pineda, Wigle, and Oliver, 2000). Furthermore, in models of liver damage the expression of hepatic Prox1 is drastically reduced upon injury but normalized during the regeneration process; new Prox1 positive stem/progenitor cells appeared in the injured livers (Dudas et al., 2006). It has also been shown that Prox1 induces cell proliferation and migration of hepatic stem/progenitor cells isolated from the mouse liver (Kamiya et al., 2008). I propose that Prox1 could be a regulator of liver fibrosis and regeneration. The expression of Prox1 and its SUMOylation status were analyzed in 3 independent mouse models of non-alcoholic steatohepatitis (NASH), a state of liver steatosis, inflammation and fibrosis. The expression of Prox1 at the protein level was reduced in the CDA-HFD and the FPC NASH models. On the other hand the expression of Prox1 was not affected in the STAM mice. The conjugation of Prox1 with SUMO was significantly impaired in the fibrotic livers of all NASH models. In addition, a phospho-proteome analysis done in our laboratory indicates that Prox1 is differentially phosphorylated in the STAM mouse model. A schematic summary of the results is presented in Fig.3.3. The hyper-phosphorylated region detected in the fibrotic liver is in proximity to the SUMO consensus motif at lysine 556. It is possible that the Prox1 SUMO-switch is also influenced by signals activated upon liver damage and/or fibrosis.
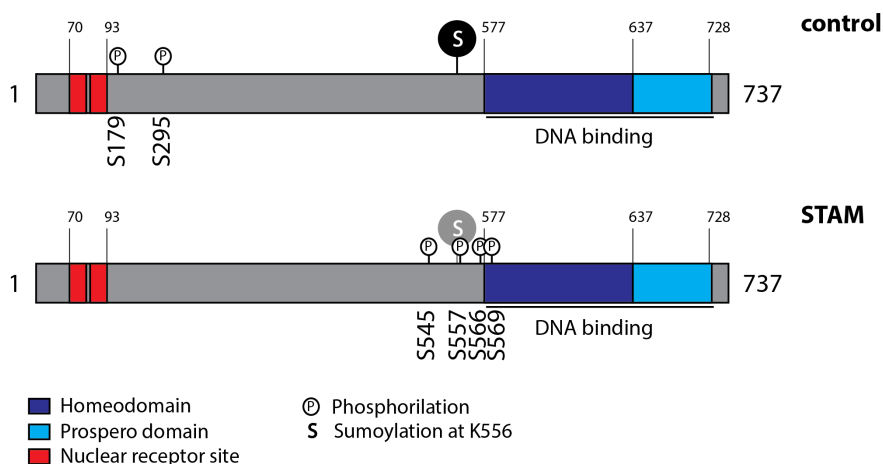
Figure 3.3: **Prox1 phosphorylation in the fibrotic liver**
Schematic representation of Prox1 showing serine residues that are differentially phosphorylated in the fibrotic liver of STAM mice vs control animals. The liver phospho-proteome analysis was conducted by Dr. Bilgen Ekim Üstünel at the Heidelberg University Clinic. Functional domains are highlighted. Figure adapted from (Elsir, Eriksson, et al., 2010)

Prox1 SUMOylation: a new molecular switch

A new molecular switch in the mouse liver has been identified. The conjugation of Prox1 with SUMO is drastically regulated by nutrient availability in hepatocytes. Moreover, the Prox1 SUMO-switch is only responsive during the active phase of the mice. The functional consequences of Prox1 SUMOylation have yet to be identified. Losing a single post-translational modification can have strong effects on the activity of a protein. To elucidate how these effects influence systemic metabolism we must overcome: 1) Timing discrepancies, as we can only speculate the time window where the Prox1 SUMO-switch becomes relevant. 2) Redundancy, as a mutation of lysine residue 556 could abolish not only SUMOylation, but also other lysine modifications. 3) Knowledge, because we developed our hypothesis using scientific observations as the core structure. Thus, it is possible that the SUMO-switch regulates aspects of metabolism where the participation of Prox1 has yet to be discovered.

The molecular switch described in this work could be an example of how organisms translate environmental cues into biological processes to maintain energy homeostasis. Although more data is required to confirm this idea, the pure observation opens questions at multiple levels, all worth exploring.

Figure 2.1: The formulation of ideas/hypothesis as well as generation of data and analysis was performed by myself. Dr. Adriano Maida and Dr. Anastasia Georgiadi contributed to the tissue collection.

Figure 2.2: The formulation of ideas/hypothesis as well as generation of data and analysis was performed by myself. Andrea Takas contributed to the tissue collection.

Figure 2.3 and 2.4: The formulation of ideas/hypothesis as well as generation of data and analysis was performed by myself. Dr. Phivos Tsokanos contributed to the tissue collection.

Figure 2.5: The formulation of ideas/hypothesis as well as generation of data and analysis was performed by myself. Dr. Adriano Maida contributed to the tissue collection.

Figure 2.6: The liver samples were kindly provided by Dr. Hermine Mohr. Generation of data and analysis was performed by myself.

Figure 2.7 and 2.8: The formulation of ideas/hypothesis as well as generation of data and analysis was performed by myself.

Figure 2.9 to 2.15: The formulation of ideas/hypothesis as well as generation of data and analysis was performed by myself. Sebastian Krämer and Dr. Revathi Sekar contributed to the isolation of primary hepatocytes. Dr. Adriano Maida contributed to the generation of liver slices.

Figure 2.16 and 17: The formulation of ideas/hypothesis as well as generation of data and analysis was performed by myself. Andrea Takas contributed to the AAV injection.

Figure 2.18 and 2.23: The formulation of ideas/hypothesis as well as generation of data and analysis was performed by myself. Andrea Takas contributed to the AAV injection. Dr. Phivos Tsokanos contributed to the tissue collection.

Figure 2.19 and 20: The formulation of ideas/hypothesis as well as generation of data and analysis was performed by myself. Dr. Phivos Tsokanos contributed to the first stages of the glucose and insulin tolerance tests.

Figure 2.21 and 22: The formulation of ideas/hypothesis as well as generation of data and analysis was performed by myself.

Figure 2.24: The formulation of ideas/hypothesis as well as data analysis was performed by myself. Sebastian Krämer contributed to the measurement of serum metabolites.

Figure 2.25: The formulation of ideas/hypothesis was performed by myself. Dr. Annette Feuchtinger and Dr. Andreas Parzefall as members of the pathology core facility contributed to the histology

data analysis and interpretation. Liver metabolites data generation and analysis was performed by myself.

Figure 2.26, 2.27 and 2.28: The formulation of ideas/hypothesis as well as data analysis was performed by myself. Elisabeth Graf as member of the Genome Sequencing facility contributed to the sequencing of RNA samples.

Figure 2.29 and 2.33: The formulation of ideas/hypothesis as well as generation of data and analysis was performed by myself. Elena Vogl contributed to the AAV injection. Dr. Katarina Klepac and Dr. Adriano Maida contributed to the tissue collection.

Figure 2.30: The formulation of ideas/hypothesis as well as generation of data and analysis was performed by myself. Dr. Phivos Tsokanos contributed to the first stages of the glucose tolerance tests.

Figure 2.31 and 2.32: The formulation of ideas/hypothesis as well as generation of data and analysis was performed by myself.

Figure 2.34: The formulation of ideas/hypothesis as well as data analysis was performed by myself. Dr. Adriano Maida contributed to the measurement of serum metabolites.

Figure 2.35: Prof. Dr. Susanna Hofmann and Sebastian Cucuruz contributed to the fast phase liquid chromatography (FPLC) data generation analysis and interpretation.

Figure 2.36: The formulation of ideas/hypothesis as well as generation of data and analysis was performed by myself.

Figure 2.37: The formulation of ideas/hypothesis was performed by myself. Dr. Annette Feuchtinger and Dr. Andreas Parzefall as members of the pathology core facility contributed to the histology data analysis and interpretation.

Figure 2.38: The formulation of ideas/hypothesis as well as generation of data and analysis was performed by myself. Valeria Lopez contributed to the tissue collection.

Figure 2.39 and 2.40: The formulation of ideas/hypothesis as well as the establishment of the NASH mouse models was performed by Dr. Anne Loft. The generation of data and analysis was performed by myself.

Figure 2.41: Liver samples were obtained from SMC Laboratories Inc. A) The formulation of ideas/hypothesis as well as generation of data and analysis was performed by myself. B) Dr. Bilgen Ekim Üstünel contributed to the liver phospho-proteome data generation.

Figure 2.42: The formulation of ideas/hypothesis as well as generation of data and analysis was performed by myself.

Figure 2.43: The formulation of ideas/hypothesis as well as generation of data and analysis was performed by myself. Elena Vogl contributed to the AAV injection.

5.1 Materials

Technical equipment

Table 5.1: Technical equipment

Equipment	Manufacturer
Bacterial Incubator HERAtherm	Thermo Scientific
Bioanalyzer 2100	Agilent
Biopsy punches 6 mm	Servoprax
Centrifuge Allegra X-15R	Beckman Coulter
Centrifuge ultra SORVALI LYNX 6000	Thermo Scientific
Centrifuge 5427R	Eppendorf
ChemiDoc TMi imager	BioRad
CO2 Incubator HERAcell 150i	Thermo Scientific
Concentrate plus	Eppendorf
Douncer Homogenizer	Kimble
Electrophoresis and blotting chambers	BioRad
Ice machine ZBE 110-35	Ziegra
Light Microscope MFA33500	Nikon
Live tissue slicer	Krumdieck (TSE Systems)
NanoDrop 2000	Thermo Scientific
Plate reader Varioscan Lux	Thermo Scientific
QIAxcel Advance	QIAGEN
Real-Time PCR-system QuantStudio 6 Flex	Thermo Scientific
Rotating-mixer	Benchmark
Serum Analyzer AU480	Beckman Coulter
Sonicator	BANDELIN SONOPULS
Thermoshaker Thermomixer C	Eppendorf
TissueLyser MM400	Retsch
Vortex Genie 2 G560E	Scientific Industries
Waterbath Aqualine AL 25	Lauda

Consumables

Table 5.2: Consumables

Item	Manufacturer	Reference Nr.
Cell strainer 100 µm	Thermo Scientific	11517532
Cell culture plates	Falcon	3530-43/46-47
Centrifugal filter units 3K	Amicon	UFC5003
Countess cell counting	Invitrogen	C10228
EconoSpin columns	Epochlife science	1920-250
Eppendorf Tubes	Eppendorf	0030119380
Falcon tubes 15 ml/50 ml	Corning	3520-96/-70
Filtertips TipOne	Starlabs	5001128-30/-48
Gloves Purple nitrile	Kimtech	90626
Glucometer ACCU-CHEK	Roche	70001889
Heparin-coated microvettes	Sarstedt	16.443
Histocasettes	Roth	XY28.1
Neubauer chamber	MARIENFELD	0650030
Nitrocellulose membrane 0.2 µm	BioRad	77012
Novex WedgeWell Tris-Glycine Gels	Thermo Scientific	XP00085BOX
Nunclon Delta plates	Thermo Scientific	142475
M ColorpHast indicator strips	VWR	1.09543.0001
Scalpels	BRAUN	5518083
Serum Z-gel tube	Sarstedt	41.1378.005

Mouse diets

Table 5.3: Media

Diet	Manufacturer	Reference Nr.
CDA-(10 %) fat control	Research Diets	A06071314
CDA-(60 %) fat high	Research Diets	A06071302
cholesterol (0 %) control	Research Diets	D11112225
cholesterol (2 %) high	Research Diets	D18101201
Chow regular	Altromin	1314
Fat (60 %) high	Research Diets	D12492
FPC	Research Diets	D17020104

Chemical, reagents, enzymes and kits

Table 5.4: Chemicals and reagents

Chemical or reagent	Manufacturer	Reference Nr.
Acetic acid	Sigma-Aldrichh	64-19-7
Agarose	Biozym	870088
AICAR	Sigma-Aldrichh	A9978
Ampicillin sodium salt	Sigma-Aldrichh	69-52-3
Bovine serum albumin (BSA) fatty acid free	Sigma-Aldrichh	9048-46-8
Calcium chloride (CaCl2)	Roth	CN93.1
Chenodeoxycholic acid	Sigma-Aldrichh	C9377
Chemiluminescent substrate Femto	Thermo Scientific	34094
Chloroform	VWR	22-711-290
Collagen rat tail	Roche	11 179 179 001
Collagenase	Sigma-Aldrichh	C5138
cOmplete Mini, EDTA-free protease inhibitor	Roche	42484600
Distilled water Nuclease free	Invitrogen	10977035
Dexamethasone	Sigma-Aldrichh	D4902
Dimethyl sulfoxide (DMSO)	Sigma	D4540
Dithiothreitol (DTT)	Roth	6908-2
DreamTag PCR MasterMix	Thermo Scientific	K1082
Dynabeads Protein G	Invitrogen	10004D
Ethanol absolut	VWR	20821.330
EDTA	Sigma-Aldrichh	E5134
EGTA	Sigma-Aldrichh	E4378
Formalin		
Forskolin	Sigma-Aldrichh	F6886
D-(-)- Fructose	Sigma-Aldrichh	F0127
GeneRuler DNA Ladder Mix	Thermo Scientific	11873963
Glucagon	Sigma-Aldrichh	G2044
D-(+)-Glucose	Sigma-Aldrichh	G8270
Glycine	Sigma-Aldrichh	G7126
Glycerol	Sigma-Aldrichh	15523
HEPES	Roth	9105.3
Insulin	Eli Lilly	2526396
Igepal CA-630	Sigma-Aldrichh	56741
Isopropanol	Sigma-Aldrich	33539
L-Alanine	Sigma-Aldrich	A7627
L-Aspartic acid	Sigma-Aldrich	A9256

L-Cysteine	Sigma-Aldrich	W326305
L-Glutamic acid	Sigma-Aldrich	G1251
L-Histidine	Sigma-Aldrich	H8000
L-Isoleucine	Sigma-Aldrich	I2752
L-Leucine	Sigma-Aldrich	L8000
L-Lysine	Sigma-Aldrich	L5501
L-Methionine	Sigma-Aldrich	M9625
L-Ornithine	Sigma-Aldrich	O6503
L-Phenylalanine	Sigma-Aldrich	P2126
L-Proline	Sigma-Aldrich	P0380
L-Serine	Sigma-Aldrich	S4500
L-Threonine	Sigma-Aldrich	T8625
L-Thryptophan	Sigma-Aldrich	T0254
L-Tyrosine	Sigma-Aldrich	T3754
L-Valine	Sigma-Aldrich	V0500
Magnesium chloride	Sigma-Aldrich	M8266
2-Mercaptoethanol	Roth	4227.2
Milk powder skim	Fluka	70166
MK-8722	MERCK	(Makhnevych et al., 2007)
N-Ethylmaleimide (NEM)	Sigma-Aldrichh	E3876
PageRuler Prestained Protein Ladder	BioRad	1610375
Penicillin/Streptomycin	Gibco	5000956
PhosSTOP phosphatase inhibitor	Roche	4906845001
Ponceau S solution	Sigma-Aldrichh	P7170
Potassium chloride (KCl)	Roth	6781.1
Potassium phosphate (KH2PO4)	Roth	3904.1
PowerUp SYBR Green Master Mix	Thermo Scientific	K1082
Sodium chloride (NaCl)	Roth	3957.1
Sodium deoxycholate	Sigma-Aldrichh	D6750
Sodium dodecyl sulfate (SDS)	Sigma-Aldrichh	75746
Sucrose	Sigma-Aldrichh	1888
TaqMan Gene Expression Master Mix	Thermo Scientific	4369016
Tris base	Roth	5429.1
Triton X-100	Roth	3051.4
Trizol	Thermo Scientific	15596018
Tween 20	Sigma-Aldrichh	P9416

Table 5.5: Enzymes

Enzymes	Manufacturer
BamHI	Thermo Scientific
BssHII	Thermo Scientific
HindII	Thermo Scientific
KpnI	Thermo Scientific
MscI	Thermo Scientific
NotI	Thermo Scientific
PstI	Thermo Scientific
PvuI	Thermo Scientific
SmaI	Thermo Scientific
T4 Ligase	Thermo Scientific
XbaI	Thermo Scientific

Table 5.6: Commercial Kits

Kit	Manufacturer	Reference Nr.
cDNA QuantiTect Reverse Transcription Kit	QIAGEN	205314
Cholesterol total Kit	Cell Biolabs	STA-384
DC Protein Assay Kit	BioRad	500-0116
EndoFree Plasmid Mega Kit	QUIAGEN	12381
Glycogen Assay Kit	Sigma-Aldrichh	MAK016
Mouse Insulin ELISA	ALPCO	80-INSMS-E10
Pierce BCA Protein Assay Kit	Thermo Scientific	23225
Trans-Blot Turbo Kit	BioRad	170-4270
Triglycerides Determination Kit	Sigma-Aldrichh	TR0100
RNA 6000 Nano Kit	Agilent	5067-1511

Buffers, standard solutions and media

Table 5.7: Buffers and standard solutions

Solution	Composition
5x SDS sample buffer	250 mM Tris pH 6.8, 10 % (w/v) SDS, 0.25 % (w/v) bromphenol blue, 30 % (v/v) glycerol, 500 mM DTT
Blocking buffer	5 % w/v skim milk in TBST buffer
Cell lysis buffer	20 mM Tris pH 7.5, 1 mM EDTA, 1 mM EGTA, 150 mM NaCl, 1 % SDS, 1 % Igepal and 100 mM NEM; supplemented with protease and phosphatase inhibitors (tablets)
High sucrose buffer	15 mM Tris pH 7.5, 25 mM KCl, 5 mM Mg2Cl and 2 M sucrose; supplemented with protease and phosphatase inhibitors (tablets)
IP buffer	Nuclear lysis buffer without glycerol and 150 mM KCl
Liver lysis buffer	50 mM Tris pH 6.8, 1 mM EDTA, 150 mM NaCl, 1 % Igepal and 100 mM NEM; supplemented with protease and phosphatase inhibitors (tablets)
Low sucrose buffer	15 mM Tris pH 7.5, 25 mM KCl, 5 mM Mg2Cl and 250 mM sucrose; supplemented with protease and phosphatase inhibitors (tablets)
Nuclear lysis buffer	20 mM Tris pH 8, 100 mM KCl, 5 mM Mg2Cl, 0.1 % Igepal, 10 % glycerol and 100 mM NEM; supplemented with protease and phosphatase inhibitors (tablets)
SDS running buffer	25 mM Tris, 192 mM glycine and 0.1 % w/v SDS
TBST buffer	TBS supplemented with 0.1 % v/v Tween 20
Tissue lysis buffer	50 mM Tris pH 6.8, 1 mM EDTA, 150 mM NaCl, 1 % Igepal, 1.5 mM Mg2Cl, 1 % glycerol, 0.1 % SDS, 0.5 % sodium deoxycholate and 100 mM NEM; supplemented with protease and phosphatase inhibitors (tablets)
Tris buffered saline (TBS)	20 mM Tris (pH 7.6) and 150 mM NaCl
Wash buffer	High sucrose buffer supplemented with 0.4 % Igepal

Table 5.8: Media

Media	Manufacturer	Reference Nr.
D-glucose	Thermo Scientific	A2494001
Dulbecco's phosphate-buffered saline (DPBS)	Thermo Scientific	14190250
Dulbecco's Modified Eagle Medium (DMEM)	Thermo Scientific	A1443001
DMEM Nutrient Mixture F-12	Thermo Scientific	21331020
Fetal bovine serum (Sera Plus)	Pan Biotech	P30-3702
L-Glutamine	Thermo Scientific	25030081
Williams Medium E	Biochrom	F1125
Trypsin-EDTA (0.05 %), phenol red	Thermo Scientific	25300054

Antibodies

Table 5.9: Primary antibodies

Antibody	Host species	Dilution	Source
anti-β Actin	mouse	1:10000	Sigma-Aldrichh (A5441)
anti-Cre Recombinase	rabbit	1:1000	Cell Signaling (15036)
anti-GAPDH	rabbit	1:10000	Sigma-Aldrichh (G8795)
anti-P_ACC(Ser79)	rabbit	1:1000	Cell Signaling (3661)
anti-P_Akt(Ser473)	rabbit	1:1000	Cell Signaling (9271)
anti-P_CREB(Ser113)	rabbit	1:1000	Cell Signaling (9198)
anti-P_S6K(Thr389)	rabbit	1:1000	Cell Signaling (9234)
anti-Prox1	rabbit	1:2000	Millipore (07-537)
anti-Vcp	mouse	1:10000	Abcam (ab11433)

Horseradish peroxidase-conjugated antibodies were obtained from Cell signaling and used for immunoblotting analysis in a 1:10000 dilution.

DNA oligonucleotides

Table 5.10: DNA oligonucleotides for sequencing and genotyping

Primer	Sequence 5'- 3'
Cre sequencing	AGCCGAAATTGCCAGGATC
LP1 promoter sequencing	AATACGGACGAGGACAGG
Prox1 sequencing	CCCCGAGAAAGTTACAGAGA
Prox1 genotyping_1	CTAGTTTGCATACAAAGAAGCTACC
Prox1 genotyping_2	CAGTCCATTATTGAACCAGGC

Table 5.11: DNA oligonucleotides for cloning

Primer	Sequence 5'- 3'
Cre stop codon 1	CCCGGTACCACCTAGCCCAAGAAGAAGAGGAA
Cre stop codon 1 and 2	CCCGGTACCACCTAGCCCAAGTAAAAGAGGAA
KpnI-Cre	CCCGGTACCACCATGCCCAAGAAGAAGAGGAA
Cre-NotI	CTGCTGGAAGATGGCGATTAGCGGCCGCCCC

Plasmids

Table 5.12: Plasmids

Plasmid	Features	Source
pdsAAV_LP1_Cre(mut)	coding for an un-translatable Cre recombinase under the LP1 promoter	this work
pdsAAV_LP1_Cre(wt)	coding for Cre recombinase under the LP1 promoter	this work
pdsAAV_LP1_GFPmut-miNC	AAV with the LP1 promoter	IDC (294)
dsAAV_Prox1-miRNA	coding for a miRNA against Prox1	(Dittner, 2016))
dsAAV_NC-miRNA	coding for a negative control miRNA	(Dittner, 2016))

Cell lines

Table 5.13: Microbial strains

Microbial strain	Manufacturer
One Shot Top10 competent Cells	Thermo Scientific (C404006)
SURE 2 Super competent Cells	Stratagene (200152)

Table 5.14: Cell lines

Cell line	Features	Source
AML12 cells	like alpha mouse liver 12	IDC stock
AMPK (-/-) MEFs	AMPK knock-out MEFs	Marcos R. Garcia (IDC)

Software

Table 5.15: Software

Software	Source
Adobe Illustrator CC 2017	Adobe Systems
Adobe Photoshop CC 2017	Adobe Systems
Image Lab	BioRad
Microsoft Office	Microsoft Corporation
Prism 8	GraphPad Software Inc.
RStudio	RStudio Inc.
SnapGene 5	Insightful Science

5.2 Molecular biological methods

Standard procedures in molecular biology were performed according to Molecular Cloning, A Laboratory Manual by Maniatis, T., Fritsch, E.F. & Sambrook, J. (Cold Spring Harbor Laboratory, New York, 1982).

Culturing and transformation of bacteria

Escherichia Coli strains One Shot Top10 or SURE 2 were propagated at 37° C in medium supplemented with antibiotics as required. Liquid cultures were grown under constant shaking at 120-180 rpm. For transformation, usually 100 µl cells were thawed and incubated with 50 ng plasmid DNA or 5 µl of the ligation reaction on ice for 30 min. A heat-shock was performed at 42° C for 42 sec to enhance DNA uptake. The cells were cooled on ice for 1 min then allowed to recover at 37° C for 1 hr while shaking at 800 rpm. The cells were finally platted or inoculated in medium containing the required antibiotic for selection.

Agarose gel electrophoresis and DNA extraction

For analysis and purification of DNA restrictions and PCR reactions, DNA fragments were separated by agarose gel electrophoresis using 1-2 % (w/v) agarose gels dependent on the fragment size at 90 V for 1.5 hrs. Desired DNA fragments were purified from the gel using the QIAquick Gel Extraction Kit (QUIAGEN) according to the manufacturer's protocol.

Plasmid DNA preparation

DNA plasmids were purified from transformed bacteria cultures using the EndoFree Plasmid Mega Kit (QUIAGEN) according to the manufacturer's protocol. For sequencing, 20 µl of of 20 ng/µl plasmid DNA were sent to GATC Biotech. Constructs were sequenced using forward and reverse primers from GATC Biotech. In addition, Cre and LP1 specific primers were used to sequence the

LP1_Cre region completely.

Measurement of nucleic acid concentration and purity

A NanoDrop 2000 spectrophotometer (Thermo Scientific) was used to measure absorption at 260 and 280 nm to determine the concentration and purity of DNA and RNA samples.

The integrity of total RNA samples chosen for sequencing was controlled by gel electrophoresis using a RNA 6000 Nano Kit (Agilent) according to the manufacturer's protocol using a 2100 Bioanalyzer (Agilent).

Restriction digestion of DNA by endonucleases and DNA ligation

Enzymes and buffer systems from Thermo Scientific were used for the restriction of plasmids and DNA fragments. Reaction conditions and buffers were chosen according to the manufacturer's protocol. Ligation reactions were performed using T4 DNA Ligase (Thermo Scientific) in a total volume of 20 µl.

Generation of AAV constructs

The pdsAAV_LP1_GFPmut-miNC vector was digested with KnpI and NotI to remove the GFPmut-miNC control sequence. The sequence coding for Cre recombinase was amplified from a bacterial expression construct from St. Judes Children's Research Hospital, Memphis, TN, USA. Primers were designed to introduce a KnpI restriction site before the Cre recombinase sequence and a NotI restriction site directly after. Parallel amplification reactions were performed to introduce two point mutations and generate two stop codons right after the Kozak sequence. After ligation and endotoxin-free plasmid purification, the LP1_Cre(wt) and LP1_Cre(mut) sequence integrity and orientation were confirmed by sequencing. To corroborate the integrity of the inverted terminal repeats (ITRs) the plasmids were subjected to a test digestion and the band pattern was controlled by comparison with previous results. The AAV_LP1_Cre(wt) and AAV_LP1_Cre(mut) were used for a large scale AAV stereotype 8 packaging and purification done by Vigene Biosciences Rockville, MD, USA; pDGdelta-helper and p5E18-RC plasmids were provided by our laboratory.

5.3 Cell biological techniques

Cell culture

AML12 cells were cultured in regular DMEM F 12 containing 5.5 mM D-glucose, 2 Mm L-glutamine and 55 ml/L pyruvate supplemented with 10 % (v/v) fetal bovine serum (FBS), 1 % (v/v) penicillin-streptomycin, 100 nM dexamethasone and 1x Insulin-Transferrin-Sodium Selenite at 37° C and 5 % CO_2.

Primary hepatocytes were cultured in Williams Medium E containing 11 mM D-glucose, 2 Mm L-glutamine and 25 ml/L pyruvate supplemented with 10 % (v/v) FBS and 1 % (v/v) penicillin-streptomycin at 37° C and 5 % CO_2.

Prior to simulations, cells were incubated in DMEM containing 5 mM D-glucose, 2 Mm L-glutamine, 0.5 % (v/v) FBS and 1 % (v/v) penicillin-streptomycin. Simulations with hormones and chemicals were performed using this medium.

5.4 Biochemical techniques

Preparation of cell lysates for immunoblotting analysis

AML12 cells and primary hepatocytes cultured as monolayer were washed with 1 ml ice-cold PBS, supplemented with 100 mM N-Ethylmaleimide (NEM), an isopeptidase inhibitor, and lysed with 100 µl ice-cold cell lysis buffer. After a 10 min incubation on ice, the samples were sonicated at a 20 % amplitude for 5 pulses (1 sec pulse and 1 sec break). Lysates were clarified by centrifugation at 15000 rpm for 10 min at 4° C.

Primary hepatocytes cultured in the collagen sandwich were lysed as described above with an extra incubation step rotating 30 min at 4° C prior to the lysate clarification. Due to liquid retention by the collagen matrix, the samples were concentrated form a 500 µl to a 100 µl volume using centrifugal filter units with a 3 kDa cut-off.

Protein lysates were snap-frozen in liquid nitrogen and stored at -80° C.

Determination of protein concentration

Protein concentration from lysates was determined according to the method described by (Bradford, 1976). Cell lysates were quantified using a DC Protein assay kit (BioRad) while liver lysates were quantified using a BCA protein assay kit (Thermo Scientific) according to the manufacturer's protocol. The protein concentration was determined against a standard curved prepared using a Quick bovine serum albumin (BSA) Standard Set (BioRad).

Protein separation by SDS-PAGE

Proteins were separated according to their molecular weight by sodium dodecyl sulfate polyacrylamide electrophoresis (SDS-PAGE) as described by (Laemmli, 1970). 8 % Novex Tris-Glycine gels were used. Protein samples were supplemented with 5x SDS sample buffer, boiled at 95° C for 5 min then loaded into the gel wells. Proteins were separated at 90-120 V for 2 hrs using SDS running buffer.

Immunoblotting analysis

For immunoblotting analysis, proteins were transfected to a nitrocellulose membrane using a transfer kit (BioRad) according to the manufacturer's protocol. The membranes were stained with Ponceau S to control the transfer efficiency, 1% acetic acid was used to wash the background staining.

To block unspecific binding sites, membranes were incubated for 1 hr in blocking buffer. Membranes were then incubated overnight with the primary antibody in blocking buffer at 4° C; for phospho_antibodies the blocking buffer was prepared with BSA instead of skim milk. Membranes were washed in TBST and incubated with the secondary antibody in blocking buffer for 1 hr. Membranes were washed with TBST and analyzed by enhanced chemiluminescence which was detected using the ChemiDoc TMi imager (BioRad) and the Image Lab software (BioRad). For an optimal detection of Prox1 the Femto ECL substrate was diluted 1:1 with distilled water.

Purification of Prox1 from frozen liver tissue

Liver tissue samples were pulverized with a tissue lyser. Around 0.25 g of pulverized tissue were resuspended in ice-cold PBS supplemented with 100 nM NEM and centrifuged at 2000 g for 3 min at 4° C. The pellet was homogenized in a low sucrose buffer using a douncer with a loose pestle for ten passes. The samples were supplemented with Igepal to a 5% concentration, homogenized with a tight pestle for five passes and filtered through a 100 μm filter.

Samples were centrifuged at 1500 rpm for 10 min at 4° C. The pellet was resuspended in a high sucrose buffer, centrifuged at 15000 rpm and washed in high sucrose buffer supplemented with 0.4% Igepal (wash buffer). The nuclei were lysed in nuclear lysis buffer and sonicated at a 20% amplitude for 5 pulses. Nuclear extracts were clarified by centrifugation at 20000 rpm for 30 min at 4° C.

The total nuclear protein concentration was determined as described above. 50 μg total nuclear protein samples in a 500 μl volume were prepared for the immunoprecipitation protocol. Samples were pre-cleared for 1 hr at 4° C then incubated with either 5 μl of the anti-Prox1 antibody (Millipore-07 537) or 2 μg of the anti-rabbit Igg control antibody (Cell Signaling Technology-2729) together with 20 μl Protein G Dynabeads overnight (18 hrs) at 4° C. The beads were washed twice in IP buffer by mixing (end-to-end rotation) for 10 min at 4° C. Finally, the beads were washed with 20 mM Tris-HCL (pH=8) and 150 mM KCl to remove the detergent and glycerol. The purified proteins were eluted in a buffer with 100 mM Tris-HCL (pH=8), 1% SDS and 0.5% β-mercaptoethanol at 70° C in a 30 μl volume.

Samples were snap-frozen in liquid nitrogen and stored at -80° C.

RNA isolation from frozen liver tissue

Around 5 mg of liver tissue were homogenized in 1 ml Trizol with a tissue lyser. The samples were mixed with 0.2 ml chloroform, the aqueous phase was collected and mixed with 0.6x volumes of 100 % ethanol. The samples were loaded on a EconoSpin column and the RNA was washed 3x with RPE buffer (QIAGEN). The RNA was eluted with distilled nuclease free water. The RNA purity and concentration was determined as described above; samples were diluted to a 100 ng/µl concentration and stored at -80° C.

cDNA synthesis and quantitative RT-PCR

The QuantiTect Reverse Transcription Kit (QIAGEN) was used to transcribe 1 µg of RNA into cDNA according to the manufacturer's protocol.

RT-qPCR was performed using either the TaqMan Gene Expression system (Thermo Scientific) or the SYBR Green qPCR technology (Thermo Scientific) according to the manufacturer's protocol using the QuantStudio 6 Flex Real-Time PCR system (Thermo Scientific).

Glycogen determination from frozen liver tissue

Liver tissue pieces were weighted (45-55 mg) and homogenized in 0.5 ml of a 30 % KOH solution with a tissue lyser. Samples were mixed at 1000 rpm for 1 hr at 95° C then centrifuged at 500 g for 5 min at room temperature. The supernatant was collected and mixed with 1.4 ml ice-cold 95 % ethanol, incubated for 30 min at -20° C and centrifuged at 3000 g for 20 min at room temperature. The pellets were washed with 95 % ethanol, dried for 10 min at 60° C and dissolved in 0.25 ml distilled water at 37° C.

Glycogen content was measured using a glycogen assay kit (Sigma-Aldrichh) according to the manufacturer's protocol.

Lipid extraction from frozen liver tissue

Liver tissue pieces were weighted (60-80 mg) and homogenized in 1.5 ml of a chloroform:methanol (2:1) solution with a tissue lyser. Samples were mixed at 1400 rpm for 20 min at room temperature then centrifuged at 13000 rpm for 30 min at room temperature. The liquid phase was collected and mixed with 0.2 ml NaCl (150 mM) and centrifuged at 2000 rpm for 5 min. 0.2 ml of the organic phase was mixed with 40 µl of a chloroform:Triton-X (1:1) solution and dried overnight with the speed-vac V-AL program in the Concentrate plus (Eppendorf). The Triton-X lipid solution was diluted (1.125x) in 0.2 ml distilled water by mixing (end-to-end rotation) for 1 hr at room temperature. Samples were stored at -80° C.

Triglycerides and total cholesterol colorimetric measurements

Triglycerides were measured using a Triglycerides determination kit (Sigma-Aldrichh) according to the manufacturer's protocol. Plasma samples (2 µl) and liver lipids samples (2 µl) were analyzed in duplicate.

Total cholesterol levels were measured using a total cholesterol assay kit (Cell Biolabs INC.) according to the manufacturer's protocol. Plasma samples (1 µl) and liver lipids samples (2 µl) were analyzed in duplicate.

5.5 Mouse work

All animal studies were performed in accordance with German animal welfare legislation and in specific pathogen-free conditions in the animal facility of the Helmholtz Center, Munich, Germany. Protocols were approved by the Institutional Animal Welfare Officer (Tierschutzbeauftragter), and necessary licenses were obtained from the state ethics committee and government of Upper Bavaria (ROB-55.2-2532.Vet_02-17-49 and ROB-55.2-2532.Vet_02-15-164).

Mouse husbandry

Male C57BL/6N mice purchased from Charles River laboratories were maintained on in a 12/12 hrs light/dark cycle and were fed a regular chow diet *ad libitum* unless indicated otherwise.

The K556R Prox1 mouse line was generated by Taconic Biosciences and expanded in the animal facility of the Helmholtz Center Munich. Mice were maintained on in a 12/12 hrs light/dark cycle and were fed a regular chow diet *ad libitum* unless indicated otherwise. The K556R Prox1 mice were genotype by gel electrophoresis using the QIAxcel (QIAGEN) following the protocol provided by Taconic Biosciences.

Glucose and Insulin tolerance tests

For the GTT, K556R Prox1 mice fed a regular chow diet were fasted for 5 to 6 hrs (ZT 2-8) then challenged with 1.5 g/kg glucose via an intraperitoneal injection. Blood samples were collected in heparin coated tubes at time points: 0 and 15 min from the tail vein; the blood glucose levels were recorded with a glucometer at time points: 0, 15, 30, 60 and 120 min. Blood samples were centrifuged at 2000 g for 5 min at 4° C; the plasma was collected, snap-frozen in liquid nitrogen and stored at -80° C. The plasma insulin content was measured with a mouse insulin ELISA (ALPCO).

K556R Prox1 mice fed a high cholesterol (2 %) or a control (0 %) diet were fasted for 6 hrs (ZT 4-10) then challenged with 2 g/kg glucose via an intraperitoneal injection. The GTT was performed as described above.

For the ITT, K556R Prox1 mice fed a regular chow diet were fasted for 5 hrs (ZT 2-7) then challenged with 1.2 U/kg insulin via an intraperitoneal injection. Blood glucose levels were recorded with a glucometer at time points: 0, 15, 30, 60 and 120 min from the tail vein. A 1-week recovery period was given after the tests.

Blood sampling

Blood samples of 20-60 µl volume were collected in heparin coated tubes by piercing the tail vein. Blood samples were centrifuged at 2000 g for 5 min at 4° C; the plasma was collected, snap-frozen in liquid nitrogen and stored at -80° C. A 1-week recovery period was given after sampling.

Tissue collection

The body weight and the blood glucose levels were recorded in every study prior to tissue collection. Mice were sacrificed by cervical dislocation and decapitated immediately. The blood was collected in serum gel tubes, incubated at room temperature for 5-10 min and store at 4° C until further processing. The tissues were collected, weighted, washed in PBS and snap-frozen in liquid nitrogen. A sample from the medial liver lobe was placed on a histocasette and incubated in formalin for fixation. Once all tissues were collected the blood samples were centrifuged at 2000 g for 10 min at 4° C; the serum was collected and snap-frozen in liquid nitrogen. Tissue and serum samples were stored at -80° C.

5.6   Statistical analysis

Statistical analyses were performed using a 1- or 2-way analysis of variance (ANOVA) with Dunnett´s multiple comparisons test, or Sidak´s multiple comparisons test, respectively. Correlation was determined using Pearson's correlation coefficient. $P \leq 0.05$ was considered statistically significant. * $P \leq 0.05$, ** $P \leq 0.01$, *** $P \leq 0.001$, **** $P \leq 0.0001$. Done.

BIBLIOGRAPHY

Abdel-Misih, Sherif R Z and Mark Bloomston (Aug. 2010). "Liver Anatomy". In: *Surgical Clinics of North America* 90.4, pp. 643–653.

Accad, M and R V Farese (Aug. 1998). "Cholesterol homeostasis: a role for oxysterols." In: *Current biology : CB* 8.17, R601–4.

Alegre, Kamela O and David Reverter (Oct. 2011). "Swapping small ubiquitin-like modifier (SUMO) isoform specificity of SUMO proteases SENP6 and SENP7." In: *The Journal of biological chemistry* 286.41, pp. 36142–36151.

Alfaro N., Ana Jimena (Mar. 2016). "Molecular mechanisms of Prox1 SUMOylation". In: *unpublished, MA thesis, Heidelberg University, Heidelberg*.

Altarejos, Judith Y and Marc Montminy (Mar. 2011). "CREB and the CRTC co-activators: sensors for hormonal and metabolic signals". In: *Nature Reviews Molecular Cell Biology* 12.3, pp. 141–151.

Armour, Sean M et al. (Sept. 2017). "An HDAC3-PROX1 corepressor module acts on HNF4α to control hepatic triglycerides". In: *Nature communications* 8.1, p. 549.

Asher, Gad et al. (July 2008). "SIRT1 regulates circadian clock gene expression through PER2 deacetylation." In: *Cell* 134.2, pp. 317–328.

Avruch, Joseph (1998). "Insulin signal transduction through protein kinase cascades". In: *Insulin Action*. Boston, MA: Springer US, pp. 31–48.

Azuma, Kotaro et al. (Nov. 2011). "PROX1 suppresses vitamin K-induced transcriptional activity of Steroid and Xenobiotic Receptor." In: *Genes to cells : devoted to molecular & cellular mechanisms* 16.11, pp. 1063–1070.

Bechmann, Lars P et al. (Apr. 2012). "The interaction of hepatic lipid and glucose metabolism in liver diseases". In: *Journal of Hepatology* 56.4, pp. 952–964.

Becker, Janina (June 2012). "Endogenous SUMOylation in cells and tissues". In: *unpublished, MA thesis, Heidelberg University, Heidelberg*.

Becker, Janina et al. (Mar. 2013). "Detecting endogenous SUMO targets in mammalian cells and tissues". In: *Nature Structural & Molecular Biology* 20.4, pp. 525–531.

Birkenfeld, Andreas L and Gerald I Shulman (Feb. 2014). "Nonalcoholic fatty liver disease, hepatic insulin resistance, and type 2 diabetes." In: *Hepatology* 59.2, pp. 713–723.

Bouskila, Michale et al. (Nov. 2010). "Allosteric regulation of glycogen synthase controls glycogen synthesis in muscle." In: *Cell Metabolism* 12.5, pp. 456–466.

Bradford, M (May 1976). "A Rapid and Sensitive Method for the Quantitation of Microgram Quantities of Protein Utilizing the Principle of Protein-Dye Binding". In: *Analytical Biochemistry* 72.1-2, pp. 248–254.

Browning, Jeffrey D and Jay D Horton (July 2004). "Molecular mediators of hepatic steatosis and liver injury." In: *Journal of Clinical Investigation* 114.2, pp. 147–152.

Brubaker, P L and D J Drucker (May 2002). "Structure-Function of the Glucagon Receptor Family of G Protein-Coupled Receptors: The Glucagon, GIP, GLP-1, and GLP-2 Receptors". In: *Receptors and Channels* 8, pp. 179–188.

Bugianesi, Elisabetta, Arthur J McCullough, and Giulio Marchesini (Nov. 2005). "Insulin resistance: A metabolic pathway to chronic liver disease". In: *Hepatology* 42.5, pp. 987–1000.

Burke, Zoë and Guillermo Oliver (Oct. 2002). "Prox1 is an early specific marker for the developing liver and pancreas in the mammalian foregut endoderm". In: *Mechanisms of Development* 118.1-2, pp. 147–155.

Caballero, Francisco et al. (June 2010). "Specific contribution of methionine and choline in nutritional nonalcoholic steatohepatitis: impact on mitochondrial S-adenosyl-L-methionine and glutathione." In: *The Journal of biological chemistry* 285.24, pp. 18528–18536.

Cain, Derek W and John A Cidlowski (Apr. 2017). "Immune regulation by glucocorticoids." In: *Nature Reviews Immunology* 17.4, pp. 233–247.

Cantó, Carles and Johan Auwerx (Apr. 2009). "PGC-1α, SIRT1 and AMPK, an energy sensing network that controls energy expenditure". In: *Current Opinion in Lipidology* 20.2, pp. 98–105.

Chaix, Amandine, Terry Lin, et al. (Feb. 2019). "Time-Restricted Feeding Prevents Obesity and Metabolic Syndrome in Mice Lacking a Circadian Clock." In: *Cell Metabolism* 29.2, 303–319.e4.

Chaix, Amandine, Amir Zarrinpar, et al. (Dec. 2014). "Time-restricted feeding is a preventative and therapeutic intervention against diverse nutritional challenges." In: *Cell Metabolism* 20.6, pp. 991–1005.

Chang, Che-Chang et al. (Apr. 2011). "Structural and functional roles of Daxx SIM phosphorylation in SUMO paralog-selective binding and apoptosis modulation." In: *Molecular Cell* 42.1, pp. 62–74.

Charest-Marcotte, A et al. (Mar. 2010). "The homeobox protein Prox1 is a negative modulator of ERR /PGC-1 bioenergetic functions". In: *Genes & Development* 24.6, pp. 537–542.

Clarke, P R and D G Hardie (Aug. 1990). "Regulation of HMG-CoA reductase: identification of the site phosphorylated by the AMP-activated protein kinase in vitro and in intact rat liver." In: *The EMBO Journal* 9.8, pp. 2439–2446.

Cossec, Jack-Christophe et al. (Nov. 2018). "SUMO Safeguards Somatic and Pluripotent Cell Identities by Enforcing Distinct Chromatin States." In: *Cell stem cell* 23.5, 742–757.e8.

Damiola, F et al. (Dec. 2000). "Restricted feeding uncouples circadian oscillators in peripheral tissues from the central pacemaker in the suprachiasmatic nucleus." In: *Genes & Development* 14.23, pp. 2950–2961.

Dang, Fabin et al. (Aug. 2016). "Insulin post-transcriptionally modulates Bmal1 protein to affect the hepatic circadian clock." In: *Nature communications* 7.1, pp. 12696–12.

Day, Christopher P and Oliver F W James (Apr. 1998). "Steatohepatitis: A tale of two right?" In: *Gastroenterology* 114.4, pp. 842–845.

Desterro, Joana M P, Manuel S Rodriguez, and Ronald T Hay (Aug. 1998). "SUMO-1 Modification of IκBα Inhibits NF-κB Activation". In: *Molecular Cell* 2.2, pp. 233–239.

Di Bacco, Alessandra et al. (June 2006). "The SUMO-specific protease SENP5 is required for cell division." In: *Molecular and cellular biology* 26.12, pp. 4489–4498.

Dibble, Christian C and Lewis C Cantley (Sept. 2015). "Regulation of mTORC1 by PI3K signaling." In: *Trends in cell biology* 25.9, pp. 545–555.

Dibner, Charna, Ueli Schibler, and Urs Albrecht (2010). "The mammalian circadian timing system: organization and coordination of central and peripheral clocks." In: *Annual review of physiology* 72.1, pp. 517–549.

Dittner, Claudia (July 2016). "Prox1 regulates hepatic lipid homeostasis". In: *unpublished PhD thesis, Heidelberg University, Heidelberg*.

Dudas, Jozsef et al. (June 2006). "Prospero-related homeobox 1 (Prox1) is a stable hepatocyte marker during liver development, injury and regeneration, and is absent from "oval cells"". In: *Histochemistry and Cell Biology* 126.5, pp. 549–562.

Dufour, Catherine R et al. (June 2011). "Genomic Convergence among ERRα, PROX1, and BMAL1 in the Control of Metabolic Clock Outputs". In: *PLoS Genetics* 7.6, e1002143.

Edwards, Peter A, Matthew A Kennedy, and Puiying A Mak (Apr. 2002). "LXRs; oxysterol-activated nuclear receptors that regulate genes controlling lipid homeostasis." In: *Vascular pharmacology* 38.4, pp. 249–256.

Egli, Martin (Mar. 2017). "Architecture and mechanism of the central gear in an ancient molecular timer." In: *Journal of the Royal Society, Interface* 14.128.

Elkouris, Maximilianos et al. (Jan. 2011). "Sox1 Maintains the Undifferentiated State of Cortical Neural Progenitor Cells via the Suppression of Prox1-Mediated Cell Cycle Exit and Neurogenesis". In: *STEM CELLS* 29.1, pp. 89–98.

Elsir, Tamador, Anna Eriksson, et al. (Feb. 2010). "Expression of PROX1 Is a common feature of high-grade malignant astrocytic gliomas." In: *Journal of Neuropathology & Experimental Neurology* 69.2, pp. 129–138.

Elsir, Tamador, Anja Smits, et al. (June 2012). "Transcription factor PROX1: its role in development and cancer". In: *Cancer and Metastasis Reviews* 31.3-4, pp. 793–805.

Fernández-Alvarez, Ana et al. (Apr. 2010). "Characterization of the human insulin-induced gene 2 (INSIG2) promoter: the role of Ets-binding motifs." In: *The Journal of biological chemistry* 285.16, pp. 11765–11774.

Flotho, Annette and Frauke Melchior (2013). "Sumoylation: a regulatory protein modification in health and disease." In: *Annual review of biochemistry* 82.1, pp. 357–385.

Francis, Gordon A et al. (2003). "Nuclear receptors and the control of metabolism." In: *Annual review of physiology* 65.1, pp. 261–311.

Fu, Chuanhai et al. (Aug. 2005). "Stabilization of PML nuclear localization by conjugation and oligomerization of SUMO-3." In: *Oncogene* 24.35, pp. 5401–5413.

Fujii, Masato et al. (Sept. 2013). "A murine model for non-alcoholic steatohepatitis showing evidence of association between diabetes and hepatocellular carcinoma." In: *Medical molecular morphology* 46.3, pp. 141–152.

Gareau, Jaclyn R and Christopher D Lima (Dec. 2010). "The SUMO pathway: emerging mechanisms that shape specificity, conjugation and recognition". In: *Nature Publishing Group* 11.12, pp. 861–871.

Geiss-Friedlander, Ruth and Frauke Melchior (Dec. 2007). "Concepts in sumoylation: a decade on". In: *Nature Reviews Molecular Cell Biology* 8.12, pp. 947–956.

Giguère, Vincent (Oct. 2008). "Transcriptional Control of Energy Homeostasis by the Estrogen-Related Receptors". In: *Endocrine Reviews* 29.6, pp. 677–696.

Goto, Toshihiko et al. (Jan. 2017). "Liver specific Prox1 inactivation causes hepatic injury and glucose intolerance in mice." In: *FEBS Letters*.

Grant, D M (July 1991). "Detoxification pathways in the liver". In: *Journal of Inherited Metabolic Disease* 14.4, pp. 421–430.

Guo, Dehuang et al. (July 2004). "A functional variant of SUMO4, a new IκBα modifier, is associated with type 1 diabetes". In: *Nature Genetics* 36.8, pp. 837–841.

Harmer, S L, S Panda, and S A Kay (2001). "Molecular bases of circadian rhythms." In: *Annual Review of Cell and Developmental Biology* 17.1, pp. 215–253.

Harvey, Natasha L et al. (Sept. 2005). "Lymphatic vascular defects promoted by Prox1 haploinsufficiency cause adult-onset obesity". In: *Nature Genetics* 37.10, pp. 1072–1081.

Hatori, Megumi et al. (June 2012). "Time-Restricted Feeding without Reducing Caloric Intake Prevents Metabolic Diseases in Mice Fed a High-Fat Diet". In: *Cell Metabolism* 15.6, pp. 848–860.

Heath, Richard B et al. (Nov. 2003). "Selective partitioning of dietary fatty acids into the VLDL TG pool in the early postprandial period." In: *The Journal of Lipid Research* 44.11, pp. 2065–2072.

Hecker, Christina-Maria et al. (June 2006). "Specification of SUMO1- and SUMO2-interacting motifs." In: *Journal of Biological Chemistry* 281.23, pp. 16117–16127.

Herzig, Stephan et al. (Oct. 2001). "correction: CREB regulates hepatic gluconeogenesis through the coactivator PGC-1". In: *Nature* 413.6856, pp. 652–652.

Ishibashi, Koutaro et al. (Jan. 2009). "Identification and characterization of a novel Tre-2/Bub2/Cdc16 (TBC) protein that possesses Rab3A-GAP activity." In: *Genes to cells : devoted to molecular & cellular mechanisms* 14.1, pp. 41–52.

Johnson, Erica S (2004). "Protein modification by SUMO." In: *Annual review of biochemistry* 73.1, pp. 355–382.

Johnson, Nicole C et al. (Dec. 2008). "Lymphatic endothelial cell identity is reversible and its maintenance requires Prox1 activity." In: *Genes & Development* 22.23, pp. 3282–3291.

Juza, Ryan M and Eric M Pauli (Jan. 2014). "Clinical and surgical anatomy of the liver: A review for clinicians". In: *Clinical Anatomy* 27.5, pp. 764–769.

Kaltezioti, Valeria et al. (Dec. 2010). "Prox1 Regulates the Notch1-Mediated Inhibition of Neurogenesis". In: *PLoS Biology* 8.12, e1000565.

Kamiya, Akihide et al. (July 2008). "Prospero-related homeobox 1 and liver receptor homolog 1 coordinately regulate long-term proliferation of murine fetal hepatoblasts." In: *Hepatology* 48.1, pp. 252–264.

Karalay, O et al. (Apr. 2011). "Prospero-related homeobox 1 gene (Prox1) is regulated by canonical Wnt signaling and has a stage-specific role in adult hippocampal neurogenesis". In: *Proceedings of the National Academy of Sciences* 108.14, pp. 5807–5812.

Kerscher, Oliver (June 2007). "SUMO junction-what's your function? New insights through SUMO-interacting motifs." In: *EMBO reports* 8.6, pp. 550–555.

Kerscher, Oliver, Rachael Felberbaum, and Mark Hochstrasser (Nov. 2006). "Modification of Proteins by Ubiquitin and Ubiquitin-Like Proteins". In: *Annual Review of Cell and Developmental Biology* 22.1, pp. 159–180.

Kido, Y (Mar. 2001). "The Insulin Receptor and Its Cellular Targets". In: *Journal of Clinical Endocrinology & Metabolism* 86.3, pp. 972–979.

Kim, Dong-Hyun et al. (Jan. 2015). "A dysregulated acetyl/SUMO switch of FXR promotes hepatic inflammation in obesity." In: *The EMBO Journal* 34.2, pp. 184–199.

Kretowski, Adam et al. (Jan. 2015). "The rs340874 PROX1 type 2 diabetes mellitus risk variant is associated with visceral fat accumulation and alterations in postprandial glucose and lipid metabolism". In: *Genes & Nutrition* 10.2, pp. 4–7.

Krycer, James R et al. (May 2010). "The Akt–SREBP nexus: cell signaling meets lipid metabolism". In: *Trends in Endocrinology & Metabolism* 21.5, pp. 268–276.

Kwon, H S et al. (Mar. 2004). "Protein Kinase B- Inhibits Human Pyruvate Dehydrogenase Kinase-4 Gene Induction by Dexamethasone Through Inactivation of FOXO Transcription Factors". In: *Diabetes* 53.4, pp. 899–910.

Kwon, Sora et al. (Feb. 2016). "Rapamycin up-regulates triglycerides in hepatocytes by down-regulating Prox1." In: *Lipids in health and disease* 15.1, p. 41.

Laemmli, U K (Aug. 1970). "Cleavage of Structural Proteins during the Assembly of the Head of Bacteriophage T4". In: *Nature* 227.5259, pp. 680–685.

Lamia, Katja A et al. (Oct. 2009). "AMPK regulates the circadian clock by cryptochrome phosphorylation and degradation." In: *Science* 326.5951, pp. 437–440.

Le Martelot, Gwendal et al. (Sept. 2009). "REV-ERBalpha participates in circadian SREBP signaling and bile acid homeostasis." In: *PLoS Biology* 7.9, e1000181.

Lee, Gha Young et al. (Mar. 2014). "PIASy-mediated sumoylation of SREBP1c regulates hepatic lipid metabolism upon fasting signaling." In: *Molecular and cellular biology* 34.6, pp. 926–938.

Li, Xiaoling et al. (Oct. 2007). "SIRT1 deacetylates and positively regulates the nuclear receptor LXR." In: *Molecular Cell* 28.1, pp. 91–106.

Li, Yu et al. (Apr. 2011). "AMPK phosphorylates and inhibits SREBP activity to attenuate hepatic steatosis and atherosclerosis in diet-induced insulin-resistant mice." In: *Cell Metabolism* 13.4, pp. 376–388.

Lian, Jihong, Randal Nelson, and Richard Lehner (Feb. 2018). "Carboxylesterases in lipid metabolism: from mouse to human." In: *Protein & cell* 9.2, pp. 178–195.

Lian, Jihong, Enhui Wei, et al. (Dec. 2012). "Liver specific inactivation of carboxylesterase 3/triacylglycerol hydrolase decreases blood lipids without causing severe steatosis in mice." In: *Hepatology* 56.6, pp. 2154–2162.

Lin, Hua et al. (Feb. 2017). "Differential proteomics analysis of liver failure in peripheral blood mononuclear cells using isobaric tags for relative and absolute quantitation." In: *Biomedical reports* 6.2, pp. 167–174.

Lin, Jye-Yee, Takayuki Ohshima, and Kunitada Shimotohno (Aug. 2004). "Association of Ubc9, an E2 ligase for SUMO conjugation, with p53 is regulated by phosphorylation of p53". In: *FEBS Letters* 573.1-3, pp. 15–18.

Liu, Chang et al. (May 2007). "Transcriptional coactivator PGC-1alpha integrates the mammalian clock and energy metabolism." In: *Nature* 447.7143, pp. 477–481.

Liu, Yuhan et al. (Nov. 2016). "SUMO-specific protease 3 is a key regulator for hepatic lipid metabolism in non-alcoholic fatty liver disease." In: *Scientific reports* 6.1, pp. 37351–11.

Love, Michael I, Wolfgang Huber, and Simon Anders (2014). "Moderated estimation of fold change and dispersion for RNA-seq data with DESeq2." In: *Genome biology* 15.12, pp. 550–21.

Luo, Jie, Hongyuan Yang, and Bao-Liang Song (Apr. 2020). "Mechanisms and regulation of cholesterol homeostasis." In: *Nature Publishing Group* 21.4, pp. 225–245.

Mahajan, Rohit et al. (Jan. 1997). "A Small Ubiquitin-Related Polypeptide Involved in Targeting RanGAP1 to Nuclear Pore Complex Protein RanBP2". In: *Cell* 88.1, pp. 97–107.

Makhnevych, Taras et al. (Apr. 2007). "The role of karyopherins in the regulated sumoylation of septins." In: *The Journal of cell biology* 177.1, pp. 39–49.

Makishima, M et al. (May 1999). "Identification of a nuclear receptor for bile acids." In: *Science* 284.5418, pp. 1362–1365.

Matsumoto, Masahiko et al. (Apr. 2013). "An improved mouse model that rapidly develops fibrosis in non-alcoholic steatohepatitis." In: *International journal of experimental pathology* 94.2, pp. 93–103.

Matunis, M J, E Coutavas, and G Blobel (Dec. 1996). "A novel ubiquitin-like modification modulates the partitioning of the Ran-GTPase-activating protein RanGAP1 between the cytosol and the nuclear pore complex." In: *The Journal of cell biology* 135.6 Pt 1, pp. 1457–1470.

Mei, Shenglin et al. (Jan. 2017). "Cistrome Data Browser: a data portal for ChIP-Seq and chromatin accessibility data in human and mouse." In: *Nucleic Acids Research* 45.D1, pp. D658–D662.

Mendoza-Viveros, Lucia et al. (Mar. 2017). "Molecular modulators of the circadian clock: lessons from flies and mice." In: *Cellular and molecular life sciences : CMLS* 74.6, pp. 1035–1059.

Meulmeester, Erik et al. (June 2008). "Mechanism and Consequences for Paralog-Specific Sumoylation of Ubiquitin-Specific Protease 25". In: *Molecular Cell* 30.5, pp. 610–619.

Min, Hae-Ki et al. (May 2012). "Increased hepatic synthesis and dysregulation of cholesterol metabolism is associated with the severity of nonalcoholic fatty liver disease." In: *Cell Metabolism* 15.5, pp. 665–674.

Mohideen, Firaz et al. (Aug. 2009). "A molecular basis for phosphorylation-dependent SUMO conjugation by the E2 UBC9". In: *Nature Structural & Molecular Biology* 16.9, pp. 945–952.

Munday, M R et al. (Aug. 1988). "Identification by amino acid sequencing of three major regulatory phosphorylation sites on rat acetyl-CoA carboxylase." In: *European Journal of Biochemistry* 175.2, pp. 331–338.

Mure, Ludovic S et al. (Mar. 2018). "Diurnal transcriptome atlas of a primate across major neural and peripheral tissues." In: *Science* 359.6381, eaao0318.

Musso, Giovanni, Maurizio Cassader, and Roberto Gambino (Apr. 2016). "Non-alcoholic steatohepatitis: emerging molecular targets and therapeutic strategies." In: *Nature reviews. Drug discovery* 15.4, pp. 249–274.

Musso, Giovanni, Roberto Gambino, and Maurizio Cassader (Jan. 2013). "Cholesterol metabolism and the pathogenesis of non-alcoholic steatohepatitis." In: *Progress in lipid research* 52.1, pp. 175–191.

Newman, John C and Eric Verdin (Jan. 2014). "Ketone bodies as signaling metabolites". In: *Trends in Endocrinology & Metabolism* 25.1, pp. 42–52.

Niwa, Yuki et al. (Mar. 2016). "Identification of DPY19L3 as the C-mannosyltransferase of R-spondin1 in human cells." In: *Molecular biology of the cell* 27.5, pp. 744–756.

Noh, Kyoung et al. (Aug. 2011). "Farnesoid X receptor activation by chenodeoxycholic acid induces detoxifying enzymes through AMP-activated protein kinase and extracellular signal-regulated kinase 1/2-mediated phosphorylation of CCAAT/enhancer binding protein β." In: *Drug metabolism and disposition: the biological fate of chemicals* 39.8, pp. 1451–1459.

Nuttall, Frank Q, Angela Ngo, and Mary C Gannon (Sept. 2008). "Regulation of hepatic glucose production and the role of gluconeogenesis in humans: is the rate of gluconeogenesis constant?" In: *Diabetes/Metabolism Research and Reviews* 24.6, pp. 438–458.

Ouimet, Mireille, Tessa J Barrett, and Edward A Fisher (May 2019). "HDL and Reverse Cholesterol Transport." In: *Circulation research* 124.10, pp. 1505–1518.

Ouyang, Huafang et al. (Apr. 2013). "Prox1 Directly Interacts with LSD1 and Recruits the LSD1/NuRD Complex to Epigenetically Co-Repress CYP7A1 Transcription". In: *PLoS ONE* 8.4, e62192.

Owerbach, David et al. (Nov. 2005). "A proline-90 residue unique to SUMO-4 prevents maturation and sumoylation". In: *Biochemical and Biophysical Research Communications* 337.2, pp. 517–520.

Pan, Mei-Ren et al. (Sept. 2009). "Sumoylation of Prox1 controls its ability to induce VEGFR3 expression and lymphatic phenotypes in endothelial cells." In: *Journal of Cell Science* 122.Pt 18, pp. 3358–3364.

Panda, Satchidananda et al. (May 2002). "Coordinated transcription of key pathways in the mouse by the circadian clock." In: *Cell* 109.3, pp. 307–320.

Parks, D J et al. (May 1999). "Bile acids: natural ligands for an orphan nuclear receptor." In: *Science* 284.5418, pp. 1365–1368.

Peng, Zhongsheng et al. (July 2008). "Ecto-5'-nucleotidase (CD73)-mediated extracellular adenosine production plays a critical role in hepatic fibrosis." In: *FASEB journal : official publication of the Federation of American Societies for Experimental Biology* 22.7, pp. 2263–2272.

Petrova, Tatiana V et al. (May 2008). "Transcription factor PROX1 induces colon cancer progression by promoting the transition from benign to highly dysplastic phenotype." In: *Cancer cell* 13.5, pp. 407–419.

Qin, Jun et al. (Oct. 2004). "Prospero-Related Homeobox (Prox1) Is a Corepressor of Human Liver Receptor Homolog-1 and Suppresses the Transcription of the Cholesterol 7-α-Hydroxylase Gene". In: *Molecular Endocrinology* 18.10, pp. 2424–2439.

Reif, Raymond et al. (Oct. 2015). "Bile canalicular dynamics in hepatocyte sandwich cultures." In: *Archives of toxicology* 89.10, pp. 1861–1870.

Robles, Maria S, Sean J Humphrey, and Matthias Mann (Jan. 2017). "Phosphorylation Is a Central Mechanism for Circadian Control of Metabolism and Physiology." In: *Cell Metabolism* 25.1, pp. 118–127.

Roenneberg, T and M Merrow (Apr. 1998). "Molecular circadian oscillators: an alternative hypothesis." In: *Journal of biological rhythms* 13.2, pp. 167–179.

Rogers, Maximillian A et al. (July 2015). "Acyl-CoA:cholesterol acyltransferases (ACATs/SOATs): Enzymes with multiple sterols as substrates and as activators." In: *The Journal of Steroid Biochemistry and Molecular Biology* 151, pp. 102–107.

Rosas-Acosta, Germán et al. (Jan. 2005). "A universal strategy for proteomic studies of SUMO and other ubiquitin-like modifiers." In: *Molecular & Cellular Proteomics* 4.1, pp. 56–72.

Ryter, Jodi M, Chris Q Doe, and Brian W Matthews (Nov. 2002). "Structure of the DNA Binding Region of Prospero Reveals a Novel Homeo-Prospero Domain". In: *Structure (London, England : 1993)* 10.11, pp. 1541–1549.

Saitoh, H (Feb. 2000). "Functional Heterogeneity of Small Ubiquitin-related Protein Modifiers SUMO-1 versus SUMO-2/3". In: *Journal of Biological Chemistry* 275.9, pp. 6252–6258.

Saxton, Robert A and David M Sabatini (Mar. 2017). "mTOR Signaling in Growth, Metabolism, and Disease." In: *Cell* 168.6, pp. 960–976.

Schoonjans, Kristina et al. (Dec. 2002). "Liver receptor homolog 1 controls the expression of the scavenger receptor class B type I." In: *EMBO reports* 3.12, pp. 1181–1187.

Shan, Shi-fang et al. (Nov. 2008). "Modulation of transcriptional corepressor activity of prospero-related homeobox protein (Prox1) by SUMO modification". In: *FEBS Letters* 582.27, pp. 3723–3728.

Shimoda, M et al. (Oct. 2006). "A Homeobox Protein, Prox1, Is Involved in the Differentiation, Proliferation, and Prognosis in Hepatocellular Carcinoma". In: *Clinical Cancer Research* 12.20, pp. 6005–6011.

Simard, Jacques et al. (June 2005). "Molecular biology of the 3beta-hydroxysteroid dehydrogenase/delta5-delta4 isomerase gene family." In: *Endocrine Reviews* 26.4, pp. 525–582.

Song, Kwang-Hoon, Tiangang Li, and John Y L Chiang (Apr. 2006). "A Prospero-related homeodomain protein is a novel co-regulator of hepatocyte nuclear factor 4alpha that regulates the cholesterol 7alpha-hydroxylase gene." In: *Journal of Biological Chemistry* 281.15, pp. 10081–10088.

Sosa-Pineda, B, J T Wigle, and G Oliver (July 2000). "Hepatocyte migration during liver development requires Prox1." In: *Nature Genetics* 25.3, pp. 254–255.

Staels, Bart and Vivian A Fonseca (Nov. 2009). "Bile acids and metabolic regulation: mechanisms and clinical responses to bile acid sequestration." In: *Diabetes Care* 32 Suppl 2.suppl 2, S237–45.

Steffensen, Knut R et al. (June 2004). "Functional conservation of interactions between a homeodomain cofactor and a mammalian FTZ-F1 homologue." In: *EMBO reports* 5.6, pp. 613–619.

Stein, Sokrates et al. (Oct. 2014). "SUMOylation-Dependent LRH-1/PROX1 Interaction Promotes Atherosclerosis by Decreasing Hepatic Reverse Cholesterol Transport". In: *Cell Metabolism* 20.4, pp. 603–613.

Steinberg, Gregory R and David Carling (July 2019). "AMP-activated protein kinase: the current landscape for drug development." In: *Nature reviews. Drug discovery* 18.7, pp. 527–551.

Stokkan, K A (Jan. 2001). "Entrainment of the Circadian Clock in the Liver by Feeding". In: *Science* 291.5503, pp. 490–493.

Sun, Xiujie et al. (Jan. 2015). "Glucagon-CREB/CRTC2 signaling cascade regulates hepatic BMAL1 protein." In: *The Journal of biological chemistry* 290.4, pp. 2189–2197.

Takeda, Yukimasa and Anton M Jetten (Aug. 2013). "Prospero-related homeobox 1 (Prox1) functions as a novel modulator of retinoic acid-related orphan receptors α- and γ-mediated transactivation." In: *Nucleic Acids Research* 41.14, pp. 6992–7008.

Talamillo, Ana et al. (May 2020). "SUMOylation in the control of cholesterol homeostasis." In: *Open biology* 10.5, p. 200054.

Tatham, M H et al. (Sept. 2001). "Polymeric Chains of SUMO-2 and SUMO-3 Are Conjugated to Protein Substrates by SAE1/SAE2 and Ubc9". In: *Journal of Biological Chemistry* 276.38, pp. 35368–35374.

Si-Tayeb, Karim, Frédéric P Lemaigre, and Stephen A Duncan (Feb. 2010). "Organogenesis and Development of the Liver". In: *Developmental Cell* 18.2, pp. 175–189.

Tong, Xin et al. (May 2011). "Ataxin-1 and Brother of ataxin-1 are components of the Notch signalling pathway." In: *EMBO reports* 12.5, pp. 428–435.

Tran, Hien et al. (Mar. 2003). "The many forks in FOXO's road." In: *Science's STKE : signal transduction knowledge environment* 2003.172, RE5–re5.

Treuter, Eckardt and Nicolas Venteclef (Aug. 2011). "Transcriptional control of metabolic and inflammatory pathways by nuclear receptor SUMOylation." In: *Biochimica et biophysica acta* 1812.8, pp. 909–918.

Venteclef et al. (Feb. 2010). "GPS2-dependent corepressor/SUMO pathways govern anti-inflammatory actions of LRH-1 and LXR in the hepatic acute phase response". In: *Genes & Development* 24.4, pp. 381–395.

Vertegaal, Alfred C O et al. (Dec. 2006). "Distinct and overlapping sets of SUMO-1 and SUMO-2 target proteins revealed by quantitative proteomics." In: *Molecular & Cellular Proteomics* 5.12, pp. 2298–2310.

Wan, Min et al. (Oct. 2011). "Postprandial hepatic lipid metabolism requires signaling through Akt2 independent of the transcription factors FoxA2, FoxO1, and SREBP1c." In: *Cell Metabolism* 14.4, pp. 516–527.

Wang, H and R H Eckel (July 2009). "Lipoprotein lipase: from gene to obesity". In: *American Journal of Physiology-Endocrinology And Metabolism* 297.2, E271–E288.

Wang, Su et al. (Dec. 2013). "Target analysis by integration of transcriptome and ChIP-seq data with BETA." In: *Nature protocols* 8.12, pp. 2502–2515.

Wang, Xiaobo et al. (Dec. 2016). "Hepatocyte TAZ/WWTR1 Promotes Inflammation and Fibrosis in Nonalcoholic Steatohepatitis." In: *Cell Metabolism* 24.6, pp. 848–862.

Wigle, J T, K Chowdhury, et al. (Mar. 1999). "Prox1 function is crucial for mouse lens-fibre elongation." In: *Nature Genetics* 21.3, pp. 318–322.

Wigle, J T and Oliver (Sept. 1999). "Prox1 function is required for the development of the murine lymphatic system." In: *Cell* 98.6, pp. 769–778.

Wilson-Grady, Joshua T, Wilhelm Haas, and Steven P Gygi (June 2013). "Quantitative comparison of the fasted and re-fed mouse liver phosphoproteomes using lower pH reductive dimethylation." In: *Methods (San Diego, Calif.)* 61.3, pp. 277–286.

Woerle, Hans J et al. (Apr. 2003). "Pathways for glucose disposal after meal ingestion in humans". In: *American Journal of Physiology - Endocrinology And Metabolism* 284.4, E716–E725.

Woods, Conor P, Jonathon M Hazlehurst, and Jeremy W Tomlinson (Nov. 2015). "Glucocorticoids and non-alcoholic fatty liver disease". In: *The Journal of Steroid Biochemistry and Molecular Biology* 154, pp. 94–103.

Wu, Lizhen et al. (Aug. 2014). "Rab8a-AS160-MSS4 regulatory circuit controls lipid droplet fusion and growth." In: *Developmental Cell* 30.4, pp. 378–393.

Yabe, Daisuke, Michael S Brown, and Joseph L Goldstein (Oct. 2002). "Insig-2, a second endoplasmic reticulum protein that binds SCAP and blocks export of sterol regulatory element-binding proteins." In: *Proceedings of the National Academy of Sciences* 99.20, pp. 12753–12758.

Yang, Xiang-Jiao and Serge Grégoire (Nov. 2006). "A Recurrent Phospho-Sumoyl Switch in Transcriptional Repression and Beyond". In: *Molecular Cell* 24.4, p. 635.

Yousef, Mohammad S and Brian W Matthews (Apr. 2005). "Structural basis of Prospero-DNA interaction: implications for transcription regulation in developing cells." In: *Structure (London, England : 1993)* 13.4, pp. 601–607.

Yunus, Ali A and Christopher D Lima (Sept. 2009). "Structure of the Siz/PIAS SUMO E3 ligase Siz1 and determinants required for SUMO modification of PCNA." In: *Molecular Cell* 35.5, pp. 669–682.

Zeigerer, Anja et al. (Jan. 2017). "Functional properties of hepatocytes in vitro are correlated with cell polarity maintenance." In: *Experimental cell research* 350.1, pp. 242–252.

Zheng, Rongbin et al. (Jan. 2019). "Cistrome Data Browser: expanded datasets and new tools for gene regulatory analysis." In: *Nucleic Acids Research* 47.D1, pp. D729–D735.

Zhu, Rongtao et al. (Apr. 2012). "Role of liver X receptors in cholesterol efflux and inflammatory signaling (review)." In: *Molecular medicine reports* 5.4, pp. 895–900.

Zhu, Shanshan et al. (Mar. 2009). "Protection from Isopeptidase-Mediated Deconjugation Regulates Paralog-Selective Sumoylation of RanGAP1". In: *Molecular Cell* 33.5, pp. 570–580.

Zinovieva, Rina D et al. (Aug. 1996). "Structure and Chromosomal Localization of the Human Homeobox Gene Prox 1". In: *Genomics* 35.3, pp. 517–522.

Zoncu, Roberto, Alejo Efeyan, and David M Sabatini (Dec. 2010). "mTOR: from growth signal integration to cancer, diabetes and ageing". In: *Nature Reviews Molecular Cell Biology* 12.1, pp. 21–35.